

# Tests of non-standard electroweak couplings of right-handed quarks

To cite this article: Véronique Bernard *et al* JHEP01(2008)015

View the [article online](#) for updates and enhancements.

## You may also like

- [The minimal seesaw and leptogenesis models](#)  
Zhi-zhong Xing and Zhen-hua Zhao
- [Scalar triplet leptogenesis in the presence of right-handed neutrinos with  \$S\_3\$  symmetry](#)  
Subhasmita Mishra and Anjan Giri
- [Has a coupling of right-handed quarks to  \$W\$  been observed?](#)  
M Oertel

# Tests of non-standard electroweak couplings of right-handed quarks

**Véronique Bernard**

*Université Louis Pasteur, Laboratoire de Physique Théorique,  
3-5 rue de l'Université, 67084 Strasbourg, France  
E-mail: [bernard@lpt6.u-strasbg.fr](mailto:bernard@lpt6.u-strasbg.fr)*

**Micaela Oertel**

*LUTH, CNRS, Observatoire de Paris, Université Paris Diderot  
5 place Jules Janssen, 92195 Meudon, France  
E-mail: [micaela.oertel@obspm.fr](mailto:micaela.oertel@obspm.fr)*

**Emilie Passemar\* and Jan Stern**

*Groupe de Physique Théorique, IPN, CNRS,  
Université de Paris Sud-XI, 91406 Orsay, France  
E-mail: [passemar@ipno.in2p3.fr](mailto:passemar@ipno.in2p3.fr), [stern@ipno.in2p3.fr](mailto:stern@ipno.in2p3.fr)*

**ABSTRACT:** The standard model can be interpreted as the leading order of a Low-Energy Effective Theory (LEET) invariant under a higher non linearly realized symmetry  $S_{\text{nat}} \supset \text{SU}(2)_W \times \text{U}(1)_Y$  equipped with a systematic power counting. Within the minimal version of this “not quite decoupling” LEET, the dominant non-standard effect appears at next-to-leading order (NLO) and is a modification of the couplings of fermions to  $W$  and  $Z$ . In particular, the coupling of right-handed quarks to  $Z$  is modified and a direct coupling of right-handed quarks to  $W$  emerges. Charged right-handed lepton currents are forbidden by an additional discrete symmetry in the lepton sector originally designed to suppress Dirac neutrino masses. A complete NLO analysis of experimental constraints on these modified couplings is presented. Concerning couplings of light quarks, the interface of the electroweak tests with QCD aspects is discussed in detail.

**KEYWORDS:** Beyond Standard Model, Kaon Physics, Chiral Lagrangians.

---

\*Present Address: Institute for theoretical physics, University of Bern, Sidlerstr. 5, CH-3012 Bern, Switzerland

---

## Contents

|   |           |
|---|-----------|
| <b>1. Introduction</b>  | <b>2</b>  |
| <b>2. Minimal not quite decoupling EW effective theory</b>            | <b>3</b>  |
| 2.1 Symmetry and particle content                                     | 6         |
| 2.2 Bottom-up reconstruction of the symmetry $S_{nat}$                | 7         |
| 2.3 The coset space $S_{nat}/S_{ew}$ and spurions                     | 10        |
| 2.3.1 The left-handed sector  | 10        |
| 2.3.2 The right-handed sector   | 11        |
| 2.3.3 Lepton number violation   | 12        |
| 2.4 The standard gauge  | 12        |
| 2.5 Fermion masses  | 13        |
| 2.5.1 Majorana mass terms and the unbearable lightness of neutrinos   | 14        |
| 2.6 Beyond the leading order  | 15        |
| <b>3. Next-to leading order (NLO)</b>                                 | <b>16</b> |
| 3.1 Formulary   | 17        |
| 3.2 Right-handed couplings and chiral flavor mixing                   | 18        |
| 3.3 $G_F, M_W^2$  | 19        |
| <b>4. Couplings to <math>Z</math></b>                                 | <b>20</b> |
| 4.1 Fit to $Z$ pole observables                                       | 21        |
| 4.2 Low energy observables  | 26        |
| 4.2.1 Atomic parity violation   | 26        |
| 4.2.2 Parity violation in $e^-e^-$ (Møller) scattering                | 27        |
| <b>5. Couplings of light quarks to <math>W</math></b>                 | <b>28</b> |
| 5.1 Exclusive low-energy tests of couplings of right-handed quarks    | 28        |
| 5.1.1 Chiral flavor mixing for light quarks                           | 28        |
| 5.1.2 Interface of effective electroweak and low-energy QCD couplings | 31        |
| 5.1.3 Neutron $\beta$ -decay and Adler-Weisberger sum rule            | 32        |
| 5.1.4 How to measure $F_\pi$ in non-EW processes?                     | 33        |
| 5.2 The gold plated test: $K_{\mu 3}^L$ decays                        | 34        |
| 5.3 Inclusive OPE based tests   | 36        |
| 5.3.1 Inelastic neutrino scattering                                   | 36        |
| 5.3.2 $W$ boson (semi-) inclusive decays                              | 38        |
| 5.3.3 Hadronic tau decays   | 39        |
| <b>6. Discussion</b>  | <b>47</b> |

|  |           |
|--|-----------|
| <b>7. Other possible tests</b>   | <b>50</b> |
| 7.1 NLO analysis: hyperon decays and heavy quark sector                      | 50        |
| 7.2 Loop effects: flavor changing neutral current processes and CP violation | 51        |
| <b>8. Summary and conclusion</b>   | <b>52</b> |
| <b>A. Expressions for the Z-pole observables</b>                             | <b>54</b> |
| <b>B. Hadronic tau decays: description of the perturbative part</b>          | <b>55</b> |

---

## 1. Introduction

In parallel to the direct searches of New Physics aiming at production of new heavy particles at LHC and other colliders it is important to further develop precision low-energy searches of small modifications of Electroweak (EW) couplings of known light particles that could not be explained within the Standard Model (SM). A combination of these two complementary approaches could help to correctly interpret forthcoming experimental results. Indirect low-energy tests may be based on a particular model of a high-energy completion of the SM and predict its observable low-energy signatures. This traditional “top - down” approach has the advantage of being well defined from the onset and the disadvantage of representing just one possibility among many others. This latter point becomes more relevant to the extent that a larger variety of high energy Models become theoretically conceivable. Indeed, during the last years many Models have appeared (and disappeared - both without any deeper experimental motivation) ranging from SUSY standard models with variable degree of minimality (see for example [1]), passing through variants of Technicolor [2] and even including non renormalizable models such as Little Higgs [3] and extradimensional models with or without Higgs particle(s) [4].

This landscape of open possibilities calls for an alternative “bottom - up” approach in which one starts with the experimentally established features of the SM viewed as the leading order of a non-decoupling Low Energy Effective Theory (LEET) and one asks what the higher orders may be without assuming any specific high energy completion of the LEET. This model independence is conceivable provided one respects two requirements:

- (i) The LEET is formulated as a consistent Quantum Field Theory renormalized and unitarized order by order in momentum expansion following the well elaborated example of Chiral Perturbation Theory [5–8]. The lack of renormalizability in the traditional sense (i.e, order by order in powers of coupling constant(s)) does not mean the lack of consistency but a limitation of predictivity at all scales.
- (ii) The second requirement concerns “naturalness”: At each order the LEET should contain all operators that are allowed by its symmetries. This principle stating that everything that is not forbidden by a symmetry is allowed and should be effectively

there, partially restores predictivity. First, the actual (non linear) symmetries of the LEET can be essentially inferred asking that no non-standard operators appear at Leading Order (LO). Furthermore, the power counting of the LEET provides a natural classification of effects beyond the SM according to their importance at low energies. In this respect, our results appear as non trivial and not quite expected: The first non-standard effects arise already at next-to-leading order (NLO) and resume to non-standard universal couplings of fermions to  $W$  and  $Z$ . They mainly concern right-handed quarks. The intensively studied oblique corrections, universality breaking effects and flavor changing neutral currents (FCNC) only appear at NNLO together with loops and are much more suppressed.

A detailed analysis of the NLO of our LEET and its confrontation with experiment is the main subject of this paper. The paper is organized as follows: section 2 reviews, comments and completes the theoretical framework of the “minimal not-quite decoupling LEET” developed some time ago [9–11]. In section 3, the physical content of the NLO is described and the notation is settled. Section 4 is devoted to the analysis of couplings to  $Z$ . A full NLO fit to the standard EW precision  $Z$ -pole and atomic parity violation observables is performed and discussed. In section 4.2.1 the main prediction of the LEET - the occurrence of couplings of right-handed quarks to  $W$  at NLO is discussed in the light of recent experimental tests involving light quarks. The latter include  $K_{\mu 3}$  decays, as well as inclusive tests using hadronic tau decays, deep inelastic scattering (DIS) of (anti-) neutrinos, and the leptonic branching fraction of  $W$ . These results are further discussed in sections 6 and 7. Section 8 concludes the paper.

## 2. Minimal not quite decoupling EW effective theory

First, we present a concise overview of effective theory framework suitable for a bottom-up analysis of possible extensions of the SM. No new material is involved in this section that would not be already contained in refs. [9–11] (see also ref. [12]).

The theoretical framework is intended to encompass a large class of (renormalizable) models extending to energies much larger than the scale at which the effective description operates (typically  $E \ll \Lambda_W \sim 3 \text{ TeV}$ ). These models remain so far unspecified except for a common symmetry pattern and the common light particle content. The latter then form the basis of the common Low Energy Effective Theory (LEET). The LEET is required to define, at least in principle,<sup>1</sup> a consistent Quantum Theory (characterized, in particular, by a finite, unitary, analytic and crossing symmetric S-matrix) through a well defined low-energy expansion in powers of momenta and gauge couplings. The crucial ingredient of this expansion is *the infrared power counting* which allows one to classify bare vertices (operators) as well as loops according to their importance in the low-energy limit. This in turn allows one to define a systematic “order by order renormalization” as formulated and experienced in Chiral Perturbation Theory [5–8]. The UV behavior and the requirement of “renormalizability at all scales” are not essential here, they concern more particularly the

---

<sup>1</sup>I.e. regardless to global questions of convergence

models susceptible to provide the high energy completion of the LEET. Similarly, the mass (or UV) dimension of an operator is not necessarily the sole indication of its relevance at low energies: Instead of representing the effective Lagrangian as the familiar (decoupling) expansion

$$\mathcal{L}_{\text{eff}} = \mathcal{L}_{\text{ren}} + \sum_{D>4} \frac{\mathcal{O}_D}{\Lambda^{D-4}} \quad (2.1)$$

which adds to the *renormalizable* SM Lagrangian (irrelevant) operators with increasing mass dimension  $D$  suppressed by inverse powers of an unspecified scale  $\Lambda$ , it is more convenient to organize the low-energy expansion as

$$\mathcal{L}_{\text{eff}} = \sum_{d \geq 2} \mathcal{L}_d \quad (2.2)$$

where  $d$  denotes the chiral (or IR) dimension indicating the low-momentum behavior

$$\mathcal{L}_d = \mathcal{O}([p/\Lambda_W]^d). \quad (2.3)$$

Each term in the expansion, eq. (2.2), contains a finite number of operators with the same infrared dimension  $d$ . Similarly, the order by order renormalization makes use at each order  $d$  of a finite number of new counterterms of dimension  $d$ . This makes appear new low-energy constants which are not fixed by the LEET itself. They reflect the missing information hidden in the high-energy completion of the LEET by a so far unspecified (renormalizable) Model. Even in the absence of this information, the LEET framework allows one to identify the most important effects beyond the SM and to provide an efficient parametrization of their experimental signature at low energies. The present paper illustrates how this statement works in practice and how it compares with experiment.

Eqs. (2.1) and (2.2) are two complementary representations of the same effective Lagrangian and they are not necessarily in contradiction with each other. Their comparison calls for few comments:

- (i) Except for counting derivatives, *the chiral (IR) dimension  $d$  and the mass (UV) dimension  $D$  do not coincide*. For theories involving gauge fields, chiral fermions and Goldstone bosons, the chiral dimension of a local operator is given by [5, 6, 13, 14]

$$d = n_\delta + n_g + n_f/2 \quad (2.4)$$

where  $n_\delta$ ,  $n_g$ , and  $n_f$  stand for the number of derivatives, number of gauge coupling constants and number of fermion fields, respectively.<sup>2</sup>

- (ii) *The importance of loops in the low-energy expansion* is given by a generalization of the Weinberg power counting formula originally established for Goldstone bosons [5] and subsequently extended to include gauge fields and chiral fermions [13–15]. The

---

<sup>2</sup>This concerns canonically normalized fields. For instance, a gauge field and GB fields have  $d = 0$ , whereas the gauge connection has  $d = 1$  so that this counting respects gauge invariance.

infrared dimension of a connected Feynman diagram made up from vertices of  $\mathcal{L}_{eff}$  labelled  $v = 1 \dots V$  and containing  $L$  loops should read

$$d = 2 + 2L + \sum_v (d_v - 2). \quad (2.5)$$

This provides a close link between momentum and loop expansions and it guarantees the renormalizability order by order, provided all vertices satisfy  $d_v \geq 2$ . This last condition means that the interaction must be suppressed in the low-energy limit as a consequence of the symmetry enjoyed by the effective theory. This may be viewed as a generalization of Adler's theorem stating that the interaction of GBs vanishes at  $E = 0$  due to chiral symmetry.

- (iii) The validity of the power counting formula, eq. (2.5), finally requires that all particles contained in the LEET should be *naturally light as a consequence of a symmetry*. Indeed, in order to guarantee the appropriate scaling of all propagators in the low - energy limit, the masses should scale as

$$\text{mass} = \mathcal{O}(p^n), \quad n \geq 1. \quad (2.6)$$

How this can happen is best illustrated by the example of the mass of a gauge field arising from the Higgs mechanism. Due to gauge symmetry such a mass takes the generic form  $M_W = \frac{1}{2}gF_W$ , where  $\Lambda_W = 4\pi F_W$  is an *intrinsic scale of the LEET*. The power counting, eq. (2.4), then implies  $M_W = \mathcal{O}(p)$ . Fermion masses protected by a chiral symmetry will be discussed shortly.

Let us stress, however, that no example of a low-energy symmetry except SUSY is known that would protect masses of scalar particles which are not Goldstone bosons. In this way the well known difficulty to construct a non SUSY *renormalizable model* with naturally light Higgs particles reappears within the LEET framework.

- (iv) It is worth stressing the difference between the starting points of the expansions, eq. (2.1) and (2.2),  $\mathcal{L}_{ren}$  and  $\mathcal{L}_2$ , respectively. In the decoupling case (cf. eq. (2.1)), the scale  $\Lambda$  is not fixed by the low-energy dynamics. The effective theory, eq. (2.1), should be internally consistent for an arbitrarily large  $\Lambda$  including in the decoupling limit  $\Lambda \rightarrow \infty$ . In this limit one should recover the full SM Lagrangian *including the Higgs sector as dictated by renormalizability*. In the alternative case, see eq. (2.2), the scale  $\Lambda_W$  is a fixed characteristic of the theory, cf.

$$\Lambda_W = 4\pi F_W \sim 3 \text{ TeV} \quad (2.7)$$

and there is no point in considering the limit of large  $\Lambda_W$ .  $\mathcal{L}_2$  is then the collection of all  $d = 2$  terms compatible with the symmetries of the LEET. In particular, whether a light Higgs particle should be included is no more dictated by the requirement of renormalizability but rather by symmetry considerations and last but not least by experiment.

- (v) The argument of dimensional suppression of operators with  $D > 4$  can very well coexist with the infrared power counting. Operators of higher mass dimension  $D$  and a lower chiral dimension  $d < D$  may still be dimensionally suppressed by  $\Lambda^{4-D}$ , where  $\Lambda \gg \Lambda_W$  is a scale exterior to the LEET. The best example is provided by the four fermion operators without derivatives and no insertion of gauge coupling  $g$  which have  $d = 2$  and  $D = 6$ . Even if one does not include these terms into  $\mathcal{L}_2$ , they will appear at the tree level proportional to the inverse squared of the LEET scale  $F_W$ . It is an assumption that extra four fermion operators with  $d = 2$  that are not generated within the LEET will be suppressed by a scale  $\Lambda \gg \Lambda_W = 4\pi F_W$  and can be disregarded. A similar reasoning can be developed for magnetic moment type operators with  $D = 5$ .

## 2.1 Symmetry and particle content

We do not know which new particles exist at scales much larger than  $\Lambda_W$  and which (local) symmetries beyond  $SU(2)_W \times U(1)_Y$  govern their interaction. If the energy decreases, particles above  $\Lambda_W$  will gradually decouple, meaning that the corresponding heavy degrees of freedom can be integrated out. This does, however, not imply that only symmetries acting linearly on light degrees of freedom will be relevant in the LEET. Heavy particles decouple whereas symmetries associated with them can reappear in the LEET and can become non-linearly realized. Such symmetries usually do not show up in the light particle spectrum but they can restrict the form of the effective interactions of light particles. In electroweak LEETs, this possibility was so far not enough exploited, despite the fact that it is realized and well understood in QCD below the chiral scale  $\Lambda_{ch} = 4\pi F_\pi$ .

The minimal version of the LEET just contains all observed particles:  $W, Z$ , photon and three generations of doublets of quarks and leptons, including right-handed neutrinos. They transform in the standard linear way under the EW group  $SU(2)_W \times U(1)_Y$ . Following the remark developed above, the latter may be embedded into a larger symmetry group

$$S_{nat} \supset S_{ew} = SU(2)_W \times U(1)_Y, \quad (2.8)$$

such that  $S_{nat}/S_{ew}$  is non-linearly realized.  $S_{nat}$  and its low-energy representation will be specified shortly. In addition, the theory must contain three real Goldstone bosons collected into an  $SU(2)$  matrix  $\Sigma(x)$  transforming under  $S_{ew}$  as

$$\Sigma(x) \longrightarrow G_L(x)\Sigma(x)G_R^{-1}(x), \quad (2.9)$$

where  $G_L$  represents the weak (left) isospin and the action of  $U(1)_Y$  is represented by the right multiplication by a  $SU(2)$  matrix  $G_R$  satisfying

$$G_R(x)\tau_3G_R^{-1}(x) = \tau_3. \quad (2.10)$$

Such  $G_R$  may be viewed as the right isospin pointing in the third direction. It is convenient to organize all right-handed fermions into right isospin doublets (presuming the existence of right-handed neutrinos). This is known to be strictly equivalent to the usual



SM assignment, provided the spectrum of hypercharges of right-handed fermions satisfies  $Y/2 = T_R^3 + (B - L)/2$ .

$\Sigma$  represents the three GBs contained in a complex doublet of Higgs fields that are needed to give masses to  $W$  and  $Z$  via the GB kinetic term<sup>3</sup>

$$\mathcal{L}_{\text{mass}} = \frac{1}{4} F_W^2 \langle D_\mu \Sigma^\dagger D^\mu \Sigma \rangle . \quad (2.11)$$

Notice that  $\mathcal{L}_{\text{mass}}$  has chiral dimension  $d = 2$  as well as kinetic terms of  $S_{ew}$  gauge fields and the usual gauge invariant fermion action.

Hence, among the  $SU(2)_W \times U(1)_Y$  invariants of the leading IR dimension  $d = 2$  one finds all the Higgsless vertices of the SM. The converse is, however, not true: As pointed out in ref. [9], there are several “unwanted”  $S_{ew}$  invariant operators with the leading chiral dimension  $d = 2$  that are absent in the SM and which are not observed. In the decoupling effective theory (cf. eq. (2.1)) such operators do not appear at the leading order because they carry the mass (UV) dimension  $D > 4$  and they are not renormalizable. In the not quite decoupling alternative the lack of renormalizability at low energies should be compensated by a higher symmetry  $S_{nat} \supset S_{ew}$ . The primary role of  $S_{nat}$  is to forbid all “unwanted operators” that appear at the leading order  $d = 2$ . In the “bottom - up” approach to the LEET it should be possible to infer the symmetry  $S_{nat}$  from the known SM interaction vertices below the scale  $\Lambda_W$ , before one identifies heavy states associated with a probable (linear) manifestation of  $S_{nat}$  in the spectrum of states above  $\Lambda_W$ .

## 2.2 Bottom-up reconstruction of the symmetry $S_{nat}$

Inspecting the list of  $d = 2$  “unwanted” operators [9, 11], the symmetry  $S_{nat}$  can be inferred in two steps: The first step involves the well known custodial symmetry [16, 17] protecting the standard model relation between gauge bosons mixing and masses,  $\rho = 1$ . It concerns operators that are invariant under  $S_{ew}$  thanks to the constraints, eq. (2.10) reducing the right isospin group  $G_R$  to its  $U(1)_{T_3}$  subgroup. A typical example is the  $\mathcal{O}(p^2)$  operator

$$\mathcal{O}_T = \langle \tau_3 \Sigma^\dagger D_\mu \Sigma \rangle^2 \quad (2.12)$$

which directly affects the GB kinetic term, eq. (2.11), inducing a potentially large modification of the SM gauge boson mixing. Unwanted operators of the type (2.12) are eliminated by the familiar left-right extension [18, 19]

$$S_{ew} \rightarrow S_{elem} = SU(2)_{G_L} \times SU(2)_{G_R} \times U(1)_{G_B}^{B-L} \subset S_{nat} \quad (2.13)$$

which is achieved by relaxing the condition (2.10) and allowing for a general  $G_R \in SU(2)_R$ . The same extension is operated for (RH) fermion doublets. The latter then transform under  $S_{elem}$  (2.13) as

$$\psi_L \in [1/2, 0; B - L], \psi_R \in [0, 1/2; B - L] \quad (2.14)$$

---

<sup>3</sup>We use the notation  $\langle A \rangle = \text{Tr}[A]$ .

where

$$\psi_{L/R} = \frac{1}{2}(1 \mp \gamma_5)\psi, \quad (2.15)$$

and  $\psi$  denotes a generic fermion doublet.

This first step is neither surprising nor new: as already mentioned, it is reminiscent of the custodial symmetry and of L-R extensions of the SM [18, 19]. The difference concerns the non linear realization of the right isospin in the LEET that does not necessarily require the existence of a light gauge particle  $W_R$  below the scale  $\Lambda_W$ . Before developing this point, it is worth stressing that the symmetry  $S_{elem}$  (2.13) does not eliminate all unwanted  $d = 2$  operators and that further extension of  $S_{nat}$  beyond (2.13) is necessary [9, 11].

Among the remaining  $d = 2$  unwanted operators invariant under  $S_{elem}$  (2.13) there is

$$\mathcal{O}_S = \langle G_{L,\mu\nu} \Sigma G_R^{\mu\nu} \Sigma^\dagger \rangle, \quad (2.16)$$

where  $G_{L,\mu\nu}$  and  $G_{R,\mu\nu}$  are the (canonically normalized) field strengths of  $SU(2)_{G_L} \times SU(2)_{G_R}$ . (They both carry the chiral dimension  $d = 1$ .) This operator represents an unsuppressed contribution to the parameter  $S$ . Then we turn to non-standard  $d = 2$  operators involving fermions:

$$\mathcal{O}_L = \bar{\psi}_L \gamma^\mu \Sigma D_\mu \Sigma^\dagger \psi_L, \quad (2.17)$$

$$\mathcal{O}_R = \bar{\psi}_R \gamma^\mu \Sigma^\dagger D_\mu \Sigma \psi_R. \quad (2.18)$$

These two operators represent potentially large (tree level) modifications of SM couplings of fermions to electroweak gauge bosons. They need to be suppressed, too. Finally, let us mention the unsuppressed Yukawa coupling

$$\mathcal{O}_{Yukawa} = \bar{\psi}_L \Sigma \psi_R \quad (2.19)$$

which is invariant under  $S_{elem}$  and carries the chiral dimension  $d = 1$ . Such an operator would naturally generate fermion masses of the order  $m_f \sim \Lambda_W$  contradicting the condition, eq. (2.6), for a fermion to belong to the LEET.

The problem with unsuppressed operators (2.16)–(2.19) concerns the origin and quantum numbers of GBs  $\Sigma(x) \in SU(2)$ , which were tacitly assumed to arise from the spontaneous breaking of the symmetry  $S_{elem}$ , i.e., to transform under the latter as the representation  $[1/2, 1/2; 0]$ . The alternative to this oversimplified scenario takes example in QCD and in Technicolor models without necessarily adopting all their (model dependent) consequences: The GBs that represent active agents of the Higgs mechanism need not be considered as “elementary” but rather as bound states of some so far unspecified Strong Dynamics (SD) operating at scales above  $\Lambda_W$  and involving new degrees of freedom. The GBs of the spontaneously broken chiral symmetry of the SD

$$S_{comp} = SU(2)_{\Gamma_L} \times SU(2)_{\Gamma_R} \quad (2.20)$$

then appear as the only manifestation of the SD much below the scale  $\Lambda_W$ . Such GBs now transform as

$$\Sigma(x) \rightarrow \Gamma_L(x) \Sigma(x) [\Gamma_R(x)]^{-1} \quad (2.21)$$

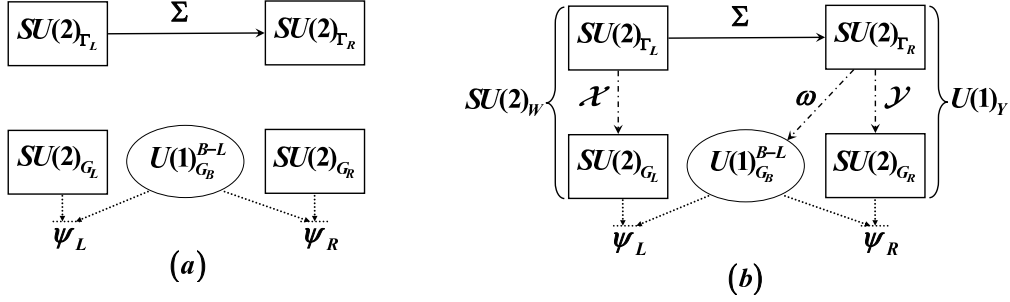


**Figure 1:** Moose diagram showing the structure of the LEET without spurions (left) and with spurions (right) connecting the elementary and the composite sector.

where  $\Gamma_{L/R}$  denote elements of  $S_{comp}$  (2.20). Accordingly, in the GB kinetic term, eq. (2.11), the covariant derivatives now involves the corresponding connections<sup>4</sup>

$$D_\mu \Sigma = \partial_\mu \Sigma - i \Gamma_{L,\mu} \Sigma + i \Sigma \Gamma_{R,\mu} . \quad (2.22)$$

On the other hand, the description of the “elementary sector” with the gauge group (2.13) and chiral fermion doublets transforming as

$$\psi_{L/R} \rightarrow G_{L/R} \exp \left[ -i \frac{B-L}{2} \alpha \right] \psi_{L/R} \quad (2.23)$$

remains as before. Consequently, the “unwanted operators” such as (2.16)–(2.19) are no more invariant and are suppressed.

The above picture combining elementary and composite sectors should be merely viewed as a possible physical motivation of the extension of the symmetry  $S_{nat}$  from  $S_{elem}$  to  $S_{elem} \times S_{comp}$ . This step is necessary within the class of LEETs considered here and it is not tied to any particular model. The result may be summarized as

$$S_{nat} = \left[ \text{SU}(2)_{G_L} \times \text{SU}(2)_{G_R} \times \text{U}(1)_{G_B}^{B-L} \right]_{elem} \times \left[ \text{SU}(2)_{\Gamma_L} \times \text{SU}(2)_{\Gamma_R} \right]_{comp} . \quad (2.24)$$

The corresponding transformation properties of GBs and elementary fermions are represented in figure 1a using the “Moose notation” [20]. At the leading order  $d = 2$ , the most general Lagrangian (see the comment (v) in section 2 about four fermion interactions) invariant under the linear action of  $S_{nat}$ , eq. (2.24), reads

$$\begin{aligned} \mathcal{L}(p^2) = & \frac{F_W^2}{4} \left\langle D_\mu \Sigma^\dagger D^\mu \Sigma \right\rangle + i \overline{\psi}_L \gamma^\mu D_\mu \psi_L + i \overline{\psi}_R \gamma^\mu D_\mu \psi_R \\ & - \frac{1}{2} \left\langle G_{L\mu\nu} G_L^{\mu\nu} + G_{R\mu\nu} G_R^{\mu\nu} \right\rangle - \frac{1}{4} G_{B\mu\nu} G_B^{\mu\nu} . \end{aligned} \quad (2.25)$$

It contains more gauge fields than actually observed at low energies. Most of them remain massless. The only hint of a mass term arises from the GB kinetic term. In the physical

<sup>4</sup>The composite gauge sector is entirely described by the connections  $\Gamma_{L/R,\mu}$  of chiral dimension  $d = 1$ . Unless one specifies the corresponding gauge field ( $d = 0$ ) and/or gauge coupling ( $d = 1$ ) there is no way to write a corresponding Yang-Mills action with  $d = 2$ . The square of the curvature  $\Gamma_{\mu\nu} = \partial_\mu \Gamma_\nu - \partial_\nu \Gamma_\mu - i [\Gamma_\mu, \Gamma_\nu]$  has  $d = 4$ .

gauge,  $\Sigma = 1$ , the latter reads

$$\mathcal{L}_{comp} = \frac{1}{4} F_W^2 \langle [\Gamma_{L,\mu} - \Gamma_{R,\mu}]^2 \rangle. \quad (2.26)$$

Since at this stage the composite and elementary sectors do not communicate, there is no link between the mass term (2.26) and the elementary gauge bosons  $G_{L/R,\mu}$  that couple to fermions. Furthermore, all fermions remain massless as a consequence of the symmetry  $S_{nat}$ .

In order to recover the SM Lagrangian hidden in eq. (2.25), one has to reduce the linear symmetry  $S_{nat}$  back to  $S_{ew}$ , imposing suitable  $S_{nat}$  invariant *constraints* that would eliminate the redundant degrees of freedom and provide the missing link between the elementary and composite sectors. We are now going to describe this reduction.

### 2.3 The coset space $S_{nat}/S_{ew}$ and spurions

The four SU(2) gauge fields  $G_{L/R,\mu}$  and  $\Gamma_{L/R,\mu}$  together with the U(1) gauge field  $G_{B,\mu}$  that appear in eq. (2.25) span the linear representation of the local symmetry group  $S_{nat}$ . It is conceivable that at ultrahigh energies such representation is actually realized, with nine among the thirteen involved fields acquiring a mass  $\gg \Lambda_W$ . As the energy decreases below  $\Lambda_W$ , the linearly realized subgroup is gradually reduced ending up with  $S_{ew} = \text{SU}(2)_W \times \text{U}(1)_Y$ , i.e., with four light EW gauge bosons. Since (by definition), all nine gauge fields from the coset  $S_{nat}/S_{ew}$  are very massive, they can be integrated out and, at low energies, there are no more gauge fields left in the coset  $S_{nat}/S_{ew}$ . It follows that any object that remains in the LEET and carries a local charge from  $S_{nat}/S_{ew}$  must necessarily be a *non propagating spurion*, since there is no way to write a corresponding gauge invariant kinetic term. One may anticipate that the reduction  $S_{nat} \rightarrow S_{ew}$  will yield three SU(2)-valued scalar spurions, reflecting the structure

$$S_{nat}/S_{ew} = [\text{SU}(2)]^3 \quad (2.27)$$

of the coset space. Following ref. [11], the reduction proceeds by pairwise identification of SU(2) factors from composite and elementary sectors. The precise alignment of gauge fields defining this identification is uniquely dictated by the requirement that one should end up with the couplings of the SM.

#### 2.3.1 The left-handed sector

One first identifies up to a gauge the “composite” and “elementary” SU(2)<sub>L</sub> imposing the *constraint*

$$\Gamma_{L,\mu} = \mathcal{X} g_L G_{L,\mu} \mathcal{X}^{-1} + i \mathcal{X} \partial_\mu \mathcal{X}^{-1} \quad (2.28)$$

where  $\mathcal{X}$  is a  $2 \times 2$  matrix field satisfying the reality condition

$$\mathcal{X} = \tau_2 \mathcal{X}^* \tau_2 \equiv \mathcal{X}^c. \quad (2.29)$$

This last condition is equivalent to the statement that  $\mathcal{X}$  is a real multiple of an SU(2) matrix

$$\mathcal{X}(x) = \xi \Omega_L(x), \quad \Omega_L(x) \in \text{SU}(2). \quad (2.30)$$

Taking the trace of eq. (2.28), it becomes obvious that  $\xi$  *must be a constant*. Furthermore, requiring that the constraint (2.28) should be invariant under  $S_{nat}$ , forces  $\mathcal{X}$  to transform as the bifundamental representation of the group  $\mathcal{G}_L = \text{SU}(2)_{\Gamma_L} \times \text{SU}(2)_{G_L}$ , cf.

$$\mathcal{X} \rightarrow \Gamma_L \mathcal{X} G_L^{-1}. \quad (2.31)$$

Given this transformation, the constraint (2.28) can be *equivalently rewritten* as

$$D_\mu \mathcal{X} = 0. \quad (2.32)$$

As anticipated above, the covariant reduction of the product  $\mathcal{G}_L = \text{SU}(2)_{\Gamma_L} \times \text{SU}(2)_{G_L}$  to the SM left isospin makes appear one *non propagating spurion*  $\mathcal{X}$ . The latter is a constant real multiple of a unitary unimodular matrix transforming as the representation  $[1/2, 1/2]$  of the product  $\mathcal{G}_L$ . There is a gauge (called standard gauge) in which the spurion becomes simply the  $\xi$  multiple of the unit matrix. This reduction procedure is represented on the left hand side of figure 1b, where the spurion  $\mathcal{X}$  and its transformation properties are shown.

### 2.3.2 The right-handed sector

The remaining reduction involves  $\mathcal{G}_R = \text{SU}(2)_{\Gamma_R} \times \text{SU}(2)_{G_R}$  together with the factor  $\text{U}(1)_{G_B}^{B-L}$ . It proceeds via a two-step identification ending up with  $\text{U}(1)_Y$  of the Standard Model

$$\mathcal{G}_R \times \text{U}(1)_{G_B}^{B-L} \rightarrow \text{U}(1)_Y \quad (2.33)$$

involving two  $\text{SU}(2)$ -valued spurions  $\mathcal{Y}$  and  $\omega$ , see the right hand side of Fig 1b.

In the first step one repeats what has been done in the left-handed sector. One imposes the constraint

$$\Gamma_{R,\mu} = \mathcal{Y} g_R G_{R,\mu} \mathcal{Y}^{-1} + i \mathcal{Y} \partial_\mu \mathcal{Y}^{-1} \quad (2.34)$$

where the spurion  $\mathcal{Y} = \mathcal{Y}^c$  is real implying

$$\mathcal{Y} = \eta \Omega_R, \quad \Omega_R \in \text{SU}(2). \quad (2.35)$$

$\eta$  is a constant parameter. Requiring the constraint (2.34) to be invariant under  $S_{nat}$  leads to the following transformation property of the spurion  $\mathcal{Y}$  (see also figure 1b)

$$\mathcal{Y} \rightarrow \Gamma_R \mathcal{Y} G_R^{-1}. \quad (2.36)$$

This means that the constraint (2.34) can equivalently be reexpressed as

$$D_\mu \mathcal{Y} = 0. \quad (2.37)$$

In the second step it is convenient to represent  $\text{U}(1)_{G_B}^{B-L}$  as a  $\text{SU}(2)$  matrix

$$G_B = \exp(-i\alpha\tau_3) \quad (2.38)$$

and to identify it with the right-handed isospin defined in the first step. (The parameter  $\alpha$  is the same as in eq. (2.23).) This amounts to orienting the right-handed isospin in the third direction, selecting a new (diagonal)  $\text{U}(1)_Y$ , where

$$\frac{Y}{2} = T_R^3 + \frac{B-L}{2}. \quad (2.39)$$

This procedure is equivalent to the constraint

$$\Gamma_{R,\mu} = \omega g_B G_{B,\mu} \frac{\tau_3}{2} \omega^{-1} + i\omega \partial_\mu \omega^{-1}, \quad (2.40)$$

where  $G_{B,\mu}$  is the  $U(1)_{G_B}^{B-L}$  gauge field and  $g_B$  stands for the corresponding gauge coupling. The covariance of the constraint, eq. (2.40), under  $S_{\text{nat}}$  is equivalent to the requirement that the spurion  $\omega$  transforms as

$$\omega \rightarrow \Gamma_R \omega G_B^{-1}, \quad (2.41)$$

as represented in figure 1b. As a consequence of the reality condition  $\omega = \omega^c$ , the spurion  $\omega$  is a real (constant) multiple of a  $SU(2)$  matrix:

$$\omega = \zeta \Omega_B, \quad \Omega_B \in SU(2). \quad (2.42)$$

### 2.3.3 Lepton number violation

The reduction (2.33) is necessary to make appear  $U(1)_Y$  as required by the Standard Model. It has two immediate consequences which follow from the existence of the spurion  $\omega$  and reflect the particular structure of the right-handed sector.

First, one can define the projection on up and down components of right-handed doublets that is covariant under the full symmetry  $S_{\text{nat}}$ . The real spurion  $\mathcal{Y}$  can be decomposed as

$$\mathcal{Y} = \mathcal{Y}_\uparrow + \mathcal{Y}_\downarrow, \quad \mathcal{Y}_{\uparrow,\downarrow} = \Pi_{\uparrow,\downarrow} \mathcal{Y} \rightarrow \Gamma_R \mathcal{Y}_{\uparrow,\downarrow} G_R^{-1} \quad (2.43)$$

where the covariant projectors  $\Pi_{\uparrow,\downarrow}$  are defined as

$$\Pi_{\uparrow,\downarrow} = \omega \frac{1 \pm \tau_3}{2} \omega^{-1} \rightarrow \Gamma_R \Pi_{\uparrow,\downarrow} \Gamma_R^{-1}. \quad (2.44)$$

Notice that a similar possibility to separate up and down components respecting the  $S_{\text{nat}}$  symmetry does not exist for left-handed doublets.

The second and most important consequence of the existence of the spurion  $\omega$  is the necessary appearance of *Lepton Number violating operators invariant under  $S_{\text{nat}}$* . Indeed, from  $\omega$  one can define the spurion  $\mathcal{Z}$  carrying two units of the  $B - L$  charge

$$\mathcal{Z} = \omega \tau_+ \omega^\dagger \rightarrow \exp(i\alpha) \Gamma_R \mathcal{Z} \Gamma_R^{-1} \quad (2.45)$$

which in turn allows to construct LNV operators which are invariant under  $S_{\text{nat}}$ . Such operators will be naturally suppressed by the parameter  $\zeta^2 \ll \xi, \eta$ . Hence, LNV is unavoidable though its strength cannot be predicted within the LEET alone. It can be consistently kept small. Consequences for the systematic LEET description of LNV processes have been discussed elsewhere [11].

## 2.4 The standard gauge

In order to make the emergence of the well known SM interaction vertices from the  $\mathcal{O}(p^2)$  Lagrangian (2.25) explicit, it is convenient to use the “standard gauge” in which

$$\Sigma = \Omega_L = \Omega_R = \Omega_B = 1. \quad (2.46)$$

The existence of this gauge has been shown in ref. [11]. The constraint (2.28) becomes in the standard gauge

$$\Gamma_{L,\mu}^i = g_L G_{L,\mu}^i, \quad i = 1, 2, 3, \quad (2.47)$$

representing the  $SU(2)_W$  group of the SM with  $g = g_L$ . In the right-handed sector the constraints (2.34), (2.40) reduce to

$$\Gamma_{R,\mu}^{1,2} = g_R G_{R,\mu}^{1,2} = 0 \quad (2.48)$$

and to

$$\Gamma_{R,\mu}^3 = g_R G_{R,\mu}^3 = g_B G_{B,\mu}. \quad (2.49)$$

Eq. (2.49) reflects the relation (2.39) between hypercharge,  $T_R^3$  and  $B - L$ , defining  $U(1)_Y$  of the SM. From the normalization of gauge field kinetic terms, one identifies the SM coupling  $g'$ :

$$g'^{-2} = g_R^{-2} + g_B^{-2}. \quad (2.50)$$

The three  $SU(2)$ -valued spurions reduce in the standard gauge to three constants  $\xi$ ,  $\eta$  and  $\zeta$ :

$$\mathcal{X} = \xi \times \mathbf{1}, \quad \mathcal{Y}_{\uparrow,\downarrow} = \eta \frac{1 \pm \tau_3}{2} \quad (2.51)$$

and the LNV spurion  $\mathcal{Z}$  reduces to

$$\mathcal{Z} = \zeta^2 \tau_+. \quad (2.52)$$

Inserting into the Lagrangian (2.25) the standard gauge expression of the constraints (2.28), (2.34), (2.40), one recovers the Higgsless part of the SM Lagrangian [9–11]. In particular

- $W$  and  $Z$  get standard masses and mixing through the GBs kinetic term (2.26).
- There are no physical scalars left: The three GBs  $\Sigma$  are absorbed by the longitudinal components of  $W$  and  $Z$ .
- Couplings of fermions to  $W, Z$  and photon are standard. There are no Yukawa couplings. At LO, the right-handed neutrino  $\nu_R$  decouples.
- Fermions stay massless as a consequence of the symmetry  $S_{\text{nat}}$ .
- There exists a huge accidental flavor symmetry acting in the family space.

## 2.5 Fermion masses

Fermion masses are suppressed with respect to the LEET scale  $\Lambda_W = 4\pi F_W \sim 3 \text{ TeV}$  by powers of spurions: Indeed, in order to write a *Dirac mass-term* invariant under the whole symmetry  $S_{\text{nat}}$ , one needs to insert at least one spurion  $\mathcal{X}$  and one spurion  $\mathcal{Y}_a$ . This can be seen from figure 1b: The shortest way from  $\Psi_R$  to  $\Psi_L$  necessarily meets both spurions. The resulting mass operator reads

$$\mathcal{M}_a = \bar{\Psi}_L \mathcal{X}^\dagger \Sigma \mathcal{Y}_a \Psi_R, \quad a \in \{\uparrow, \downarrow\}, \quad (2.53)$$

and it is of the order  $\mathcal{O}(p\xi\eta)$ . The natural size of the low-energy constant multiplying such operator is  $\sim \Lambda_W$ . The fact that the *highest* fermion mass (i.e. top mass) must be suppressed as  $\mathcal{O}(p)$ , suggests the following power counting of spurion factors  $\xi$  and  $\eta$ :

$$\xi\eta \sim m_{\text{top}}/\Lambda_W = \mathcal{O}(p) . \quad (2.54)$$

Adopting this power counting rule for spurions we define the total IR dimension

$$d^* = d + \frac{1}{2}(n_\xi + n_\eta) \quad (2.55)$$

where  $n_\xi$ ,  $n_\eta$  stand for the number of insertions of spurions  $\mathcal{X}$  and  $\mathcal{Y}$  respectively. The leading mass term in the Lagrangian has  $d^* = 2$  as well as the leading spurion-free Lagrangian (2.25). Together they constitute the *leading order of the LEET*. Notice that the formula (2.5) counting the chiral dimension of a Feynman graph holds if  $d$  is replaced by  $d^*$ .

Further suppression of Dirac fermion masses by additional powers of spurions is conceivable corresponding to running around the diagram (b) in Fig 1 several times. A similar description of fermion mass hierarchy has been proposed by Froggatt and Nielsen some time ago [22].

### 2.5.1 Majorana mass terms and the unbearable lightness of neutrinos

Majorana masses necessarily involve the spurion  $\mathcal{Z}$  and are further suppressed by the corresponding factor  $\zeta^2$  reflecting the scale of LNV. The corresponding mass operator involving the right-handed neutrino reads

$$\mathcal{M}_R = \bar{\Psi}_R \mathcal{Y}^\dagger \mathcal{Z} \mathcal{Y} \Psi_R^C = \mathcal{O}(p\zeta^2\eta^2) , \quad (2.56)$$

whereas the left-handed neutrino mass term reads

$$\mathcal{M}_L = \bar{\Psi}_L \mathcal{X}^\dagger \Sigma \mathcal{Z} \Sigma^\dagger \mathcal{X} \Psi_L^C = \mathcal{O}(p\zeta^2\xi^2) . \quad (2.57)$$

At this stage several conclusions can be drawn concerning the smallness of neutrino masses within the present LEET framework: First, there is no fundamental difficulty of keeping Majorana masses arbitrarily small, though their smallness can hardly be predicted within the LEET alone. Next, the Majorana masses of left-handed and right-handed neutrinos should be expected of the same order of magnitude unless the spurion parameters  $\xi$  and  $\eta$  are of essentially different size.<sup>5</sup> Finally, in order to accommodate the LEET with the smallness of neutrino masses it is necessary and sufficient to find the reason of *suppression of neutrino Dirac masses* compared to the observed masses of charged leptons and quarks.

In ref. [9, 11] it has been suggested that this suppression finds its origin in a discrete symmetry enjoyed by leptons and absent for quarks. This discrete symmetry is already

---

<sup>5</sup>The extreme such case, where  $\eta$  would be larger than  $\xi$  by several orders of magnitude, does not seem to be favored by the NLO fits discussed later within this article.



present at LO as a part of a huge accidental flavor symmetry: It is the  $Z_2$  *reflection symmetry* which can covariantly be defined as

$$\mathcal{Y}_\uparrow l_R \rightarrow -\mathcal{Y}_\uparrow l_R, \quad \mathcal{Y}_\downarrow l_R \rightarrow \mathcal{Y}_\downarrow l_R \quad (2.58)$$

where  $l_R$  stands for any lepton doublet. In the standard gauge this transformation simply becomes

$$\nu_R \longrightarrow -\nu_R. \quad (2.59)$$

Notice that the up-component of the RH lepton doublet, i.e.,  $\nu_R$  is the only fermion which does not carry any gauge charge and for which one may expect the reflection symmetry (2.59) to extend beyond the leading order.

The reflection symmetry does not prevent the right-handed neutrino to become massive through the Majorana mass term, eq. (2.56). It however forbids the Dirac mass term  $\bar{\nu}_L \nu_R$ . The further important consequence of this reflection symmetry is the *absence of charged right-handed lepton currents*  $\bar{e}_R \gamma \nu_R$  to all orders of the LEET. As will be seen shortly, this fact has its phenomenological relevance all over this article.

## 2.6 Beyond the leading order

In conclusion of this section we summarize the steps and rules to be followed in constructing order by order the whole effective Lagrangian.

- (i) Construct all local operators invariant under  $S_{\text{nat}}$  from the 13 gauge fields  $G_{L,\mu}, G_{R,\mu}, G_{B,\mu}, \Gamma_{L,\mu}, \Gamma_{R,\mu}$  from the Goldstone boson matrix  $\Sigma(x)$ , from the chiral fermion doublets, from spurions  $\mathcal{X}, \mathcal{Y}_{\uparrow,\downarrow}$ , as well as from the spurion  $\mathcal{Z}$  provided we wish to consider the LNV sector of the theory. Notice that the latter can be consistently omitted.

- (ii) Impose the constraints

$$D_\mu \mathcal{X} = D_\mu \mathcal{Y}_a = D_\mu \mathcal{Z} = 0, \quad a \in \{\uparrow, \downarrow\}, \quad (2.60)$$

go to the standard gauge, eliminate all redundant gauge degrees of freedom  $\Gamma_{L/R,\mu}, G_{R,\mu}^{1,2}, G_{B,\mu}$ , and trade the spurions for the constant factors  $\xi, \eta$ , and  $\zeta$ , cf. eqs. (2.51), (2.52).

- (iii) Collect all invariants with the same infrared dimension  $d^*$ , eq. (2.55), into  $\mathcal{L}_{d^*}$ ,  $d^* = 2, 3, \dots$ . Associate with each independent invariant a prefactor (Low Energy Constant (LEC)). The bare LECs are in general infinite, their divergent parts can be computed using dimensional regularization and they should cancel the divergences arising from loops at *the same order*  $d^*$  according to eq. (2.5). The renormalized LECs defined in this way depend on the renormalization scale  $\mu$ . The sum of all terms of a given  $d^*$  should be  $\mu$  independent.
- (iv) At the scale  $\mu \sim \Lambda_W$ , the renormalized LECs are expected to be of the order 1 (say,  $0.1 < \text{LEC} < 10$ ), unless the LEC carries an inverse power of the mass dimension. In the latter case an additional suppression may occur and additional physical input is needed to pin it down.

As already stated, the LO coincides with the Higgsless vertices of the SM and the fermion mass term, the latter being of spurionic origin. Loops, divergences, oblique corrections, corrections to universality, FCNC etc only start at NNLO ( $d^* \geq 4$ ) in agreement with their observed smallness. On the other hand, New Physics is predicted to start at NLO, i.e.  $d^* = 3$ . At this order there are *only two new operators*, describing non standard couplings of fermions to standard gauge bosons  $W$  and  $Z$ . They are suppressed by spurion factors: they are of order  $\mathcal{O}(p^2 \xi^2)$  and  $\mathcal{O}(p^2 \eta^2)$ , respectively. The observable effects of these non standard terms do not interfere with non leading (loop) effects present in the SM.

For years it has been believed that the most important effects beyond the SM should be searched among oblique corrections (parameters  $S$ ,  $T$ , and  $U \dots$ ) whereas the non standard vertex corrections should be tiny. The minimal not quite decoupling LEET does not bear out this wisdom and predicts NLO modifications of fermion couplings. In the sequel of this paper we discuss a systematic comparison of this prediction with experiment.

### 3. Next-to leading order (NLO)

Let us now specify the operators at next-to-leading order (NLO), i.e. at the order  $d^* = 3$ . These operators necessarily involve spurions. In contrast to the usual decoupling scenario, where there are 80 operators at NLO (mass dimension  $D = 6$ ) [21], only two operators appear at NLO.<sup>6</sup> They count as  $\mathcal{O}(p^2 \xi^2)$  and  $\mathcal{O}(p^2 \eta^2)$ , respectively, and represent non-standard couplings of fermions to gauge bosons. For left-handed fermions the unique such operator reads

$$\mathcal{O}_L = \bar{\psi}_L \mathcal{X}^\dagger \gamma^\mu \Sigma D_\mu \Sigma^\dagger \mathcal{X} \psi_L, \quad (3.1)$$

whereas in the right-handed sector the corresponding operator has four components ( $a, b \in \{\uparrow, \downarrow\}$ ) that are separately invariant under  $S_{nat}$

$$\mathcal{O}_R^{a,b} = \bar{\psi}_R \mathcal{Y}_a^\dagger \gamma^\mu \Sigma^\dagger D_\mu \Sigma \mathcal{Y}_b \psi_R. \quad (3.2)$$

Following the expansion scheme of the LEET, these two operators represent the most important effects of physics beyond the Standard Model. Oblique corrections only appear at NNLO ( $d^* = 4$ ) and so do loop corrections.

We will assume that, including LO and NLO effects, all flavor symmetry breaking effects can be transformed from vertices to the fermion mass matrix. It means that there exists a flavor symmetric basis in which the couplings of fermions to gauge bosons are proportional to the unit matrix in flavor space. This property is shared by many models with minimal flavor violation [23]. Within the LEET it can be motivated as follows. The LEET exhibits at LO an (accidental) flavor symmetry. At NNLO loop-induced effects can break this symmetry. It would appear rather unnatural to introduce tree-level flavor symmetry breaking effects via spurions at NLO (cf. the discussion on that point in ref. [11]).

---

<sup>6</sup>In principle, fermion mass terms counting as  $d = 1$ ,  $n_\xi + n_\eta = 4$  exist, too. Since a discussion of fermion mass hierarchy is beyond the scope of the present paper, we will not consider them here.

### 3.1 Formulary

The NLO Lagrangian reads:

$$\mathcal{L}_{\text{NLO}} = \rho_L \mathcal{O}_L(l) + \lambda_L \mathcal{O}_L(q) + \sum_{a,b} \rho_R^{a,b} \mathcal{O}_R^{a,b}(l) + \sum_{a,b} \lambda_R^{a,b} \mathcal{O}_R^{a,b}(q) \quad (3.3)$$

with  $l, q$  representing leptons and quarks, respectively. As discussed before,  $\rho_{L/R}$ , and  $\lambda_{L/R}$  are order one (unless suppressed by a symmetry) LECs.  $\rho_R^{e,\nu} = 0$  due to the presence of the discrete symmetry  $Z_2$  introduced in eqs. (2.58), (2.59) which forbids the Dirac mass of the neutrinos. In the standard gauge (*s.g.*), see section 2.4, we have (using the notation of [11])

$$i\Sigma^\dagger D_\mu \Sigma \stackrel{\text{s.g.}}{=} \frac{e}{2cs} \left\{ Z_\mu \tau^3 + \sqrt{2}c (W_\mu^+ \tau^+ + W_\mu^- \tau^-) \right\}, \quad (3.4)$$

where  $s$  and  $c$  are the sine and cosine of the Weinberg angle

$$s = \frac{g'}{\sqrt{g^2 + g'^2}}, \quad c = \frac{g}{\sqrt{g^2 + g'^2}}. \quad (3.5)$$

It is convenient to write the explicit form of the operators appearing in the Lagrangian in matrix notation with  $U = (u, c, t)^T$ ,  $D = (d, s, b)^T$ ,  $N = (\nu_e, \nu_\mu, \nu_\tau)^T$ ,  $L = (e, \mu, \tau)^T$ . We then have

$$\mathcal{O}_L(q) \stackrel{\text{s.g.}}{=} -\xi^2 \frac{e}{2cs} \left\{ \bar{U}_L \gamma^\mu Z_\mu U_L - \bar{D}_L \gamma^\mu Z_\mu D_L + \sqrt{2}c (\bar{U}_L \gamma^\mu W_\mu^+ D_L + \text{h.c.}) \right\}, \quad (3.6)$$

$$\mathcal{O}_R^{u,u}(q) \stackrel{\text{s.g.}}{=} \eta^2 \frac{e}{2cs} \bar{U}_R \gamma^\mu Z_\mu U_R, \quad (3.7)$$

$$\mathcal{O}_R^{d,d}(q) \stackrel{\text{s.g.}}{=} -\eta^2 \frac{e}{2cs} \bar{D}_R \gamma^\mu Z_\mu D_R, \quad (3.8)$$

$$\mathcal{O}_R^{u,d}(q) \stackrel{\text{s.g.}}{=} \eta^2 \frac{e}{\sqrt{2}s} (\bar{U}_R \gamma^\mu W_\mu^+ D_R + \text{h.c.}). \quad (3.9)$$

The operators for the leptons can be obtained by substituting  $U \mapsto N$ ,  $D \mapsto L$ .

For convenience, we will now rewrite the Lagrangian up to NLO directly in terms of effective couplings to the photon, to  $Z$  and to  $W$ . Since the symmetry  $U(1)_Q$  is unbroken, the coupling to the photon is unchanged with respect to the SM and is given by

$$\mathcal{L}_\gamma = e J^\mu A_\mu. \quad (3.10)$$

The Lagrangian describing neutral current interactions reads

$$\begin{aligned} \mathcal{L}_Z = \frac{e(1 - \xi^2 \rho_L)}{2cs} Z_\mu \bigg\{ & \bar{N}_L \gamma^\mu N_L + \epsilon^\nu \bar{N}_R \gamma^\mu N_R + (-1 + 2\tilde{s}^2) \bar{L}_L \gamma^\mu L_L + (-\epsilon^e + 2\tilde{s}^2) \bar{L}_R \gamma^\mu L_R \\ & + \left(1 + \delta - \frac{4}{3}\tilde{s}^2\right) \bar{U}_L \gamma^\mu U_L + \left(\epsilon^u - \frac{4}{3}\tilde{s}^2\right) \bar{U}_R \gamma^\mu U_R \\ & + \left(- (1 + \delta) + \frac{2}{3}\tilde{s}^2\right) \bar{D}_L \gamma^\mu D_L + \left(-\epsilon^d + \frac{2}{3}\tilde{s}^2\right) \bar{D}_R \gamma^\mu D_R \bigg\}, \end{aligned} \quad (3.11)$$

and for the charged current we have

$$\mathcal{L}_W = \frac{e(1 - \xi^2 \rho_L)}{\sqrt{2}s} \{ \bar{N}_L V_{\text{MNS}} \gamma^\mu L_L + (1 + \delta) \bar{U}_L V_L \gamma^\mu D_L + \epsilon \bar{U}_R V_R \gamma^\mu D_R \} W_\mu^+ + \text{h.c.} \quad (3.12)$$

$V_{\text{MNS}}$  is the mixing matrix in the lepton sector, and the two matrices  $V_L$  and  $V_R$  describe chiral quark flavor mixing. They arise from the diagonalisation of the quark mass matrices:

$$\begin{aligned} V_L &= \Omega_L^U \Omega_L^{D\dagger} \\ V_R &= \Omega_R^U \Omega_R^{D\dagger}, \end{aligned} \quad (3.13)$$

where  $\Omega_L^U$ ,  $\Omega_R^U$ ,  $\Omega_L^D$  and  $\Omega_R^D$  denote U(3) transformations of  $U_L$ ,  $U_R$ ,  $D_L$  and  $D_R$ , respectively, to the mass eigenstate basis. In this basis the mass matrices are diagonal and real. The two mixing matrices  $V_L$  and  $V_R$  are unitary by construction. Within the present framework, chiral flavor mixing is universal up to and including NLO. Note that in eqs. (3.11), (3.12) we have factorized  $1 - \xi^2 \rho_L$ , the factor describing the universal modification of the coupling of left-handed leptons. Defining

$$\tilde{s}^2 = \frac{s^2}{1 - \xi^2 \rho_L}, \quad (3.14)$$

allows to absorb the factor  $1 - \xi^2 \rho_L$  into the definition of  $G_F$ , see next section. The effective coupling parameters  $\epsilon^i, \delta$  defined above are then related to the spurion parameters and the LECs  $\rho_L, \rho_R, \lambda_L, \lambda_R$  in the following way:

$$(1 + \delta) = \frac{1 - \xi^2 \lambda_L}{1 - \xi^2 \rho_L}, \quad (3.15)$$

for the couplings of left-handed quarks and

$$\epsilon = \frac{\eta^2 \lambda_R^{u,d}}{1 - \xi^2 \rho_L}, \quad \epsilon^\nu = \frac{\eta^2 \rho_R^{\nu,\nu}}{1 - \xi^2 \rho_L}, \quad \epsilon^e = \frac{\eta^2 \rho_R^{e,e}}{1 - \xi^2 \rho_L}, \quad \epsilon^u = \frac{\eta^2 \lambda_R^{u,u}}{1 - \xi^2 \rho_L}, \quad \epsilon^d = \frac{\eta^2 \lambda_R^{d,d}}{1 - \xi^2 \rho_L}, \quad (3.16)$$

for the couplings of right-handed fermions to  $W$  (parameter  $\epsilon$ ) and  $Z$  (parameter  $\epsilon^\nu, \epsilon^e, \epsilon^d, \epsilon^u$ ).

### 3.2 Right-handed couplings and chiral flavor mixing

At NLO, one major effect is the appearance of direct couplings of right-handed quarks to  $W$ . We thus have to generalize flavor CKM mixing to include the mixing of right-handed quarks, too. Indeed, the charged current interaction (see eq. (3.12)) contains two mixing matrices,  $V_L$  and  $V_R$ . For  $n$  families,  $V_L$  and  $V_R$  are  $n \times n$  unitary matrices. Together they contain  $n(n - 1)$  angles and  $n(n + 1)$  phases. By a redefinition of the quark fields we can eliminate, as in the case of the SM,  $2n - 1$  phases. The total number of independent phases is thus  $n^2 - n + 1$ . Their assignment to  $V_L$  and  $V_R$  is somewhat arbitrary. A convenient choice is to use the freedom of redefining the quark fields to eliminate the maximum number of phases from  $V_L$ . Then  $V_L$  will have the same structure as the usual CKM mixing matrix

for left-handed quarks in the SM. The number of CP-violating phases  $N_{L/R}$  from  $V_L$  and  $V_R$ , respectively, is then

$$\begin{aligned} N_L &= \frac{(n-1)(n-2)}{2}, \\ N_R &= \frac{n(n+1)}{2}. \end{aligned} \quad (3.17)$$

For three generations, we will have six additional phases compared with the case without direct coupling of right-handed quarks to  $W$ . This generates new CP-violation effects as for instance in electric dipole moments. The determination of the CP-violating phases is a subject by itself and beyond the scope of this paper.

Even the analysis of CP-conserving charged current processes at NLO cannot be reduced to the genuine spurionic parameters  $\delta$  and  $\epsilon$ , see eqs. (3.15) and (3.16), but involves in addition unknown mixing angles for left-handed and right-handed quarks. For the comparison with experiment, it is convenient for the following analysis to introduce in eq. (3.12) effective vector and axial-vector couplings as:

$$\begin{aligned} \mathcal{V}_{eff}^{ij} &= (1 + \delta)V_L^{ij} + \epsilon V_R^{ij} + \text{NNLO}, \\ \mathcal{A}_{eff}^{ij} &= -(1 + \delta)V_L^{ij} + \epsilon V_R^{ij} + \text{NNLO}. \end{aligned} \quad (3.18)$$

It is obvious that at NLO, due to the direct coupling of right-handed quarks to  $W$ , we have  $\mathcal{V}_{eff} \neq -\mathcal{A}_{eff}$ . At this order, there is no reason for  $\mathcal{V}_{eff}$  or  $\mathcal{A}_{eff}$  to be unitary. We will return to this point in section 5.1.1. We should stress that  $V_L$  and  $V_R$  are completely general here. In particular, we do not assume, as is often the case in left-right symmetric models, a (pseudo)-manifest left-right symmetry which would suggest an alignment of  $V_L$  and  $V_R$ . It has already been pointed out in ref. [25] that allowing for a more general form of  $V_R$ , much of the stringent constraints on left-right symmetric models can be released.

### 3.3 $G_F, M_W^2$

As it is often done in the SM we will relate the fundamental couplings of the theory  $g$  and  $g'$  to the fine structure constant  $\alpha$  and the life time of the muon, two quantities which are measured to a very high degree of accuracy. One has

$$\alpha(0) = e^2/(4\pi). \quad (3.19)$$

At next to leading order the Fermi constant as determined by the muon life time is given by:

$$\frac{G_F}{\sqrt{2}} = \frac{4\pi\alpha(0)}{8m_Z^2 c^2 s^2 (1 - \Delta r)} (1 - \xi^2 \rho_L)^2. \quad (3.20)$$

Two remarks are in order concerning this equation. First, loop corrections are in principle appearing first at NNLO. However the LEET is essentially an expansion for the weak part of the theory. Consequently we have kept in eq. (3.20) the electromagnetic loop corrections,  $\Delta r = \Delta\alpha$  which describe the running of the electromagnetic coupling  $\alpha$ . Second, the spurion contribution and loop corrections modify the LO result in exactly the same way.

As already mentioned, see eq. (3.20), writing any observables in terms of the Fermi constant as it is done in the SM will absorb the factor  $1 - \xi^2 \rho_L$  appearing in eq. (3.12). It is thus not possible to determine this quantity from charged currents. However this quantity appears both in the coupling to  $Z$  through  $\tilde{s}^2$  and in the expression for  $G_F$ . Having fitted  $\tilde{s}^2$  to the available data as discussed in the next section one can solve a system of two equations with two unknowns. This leads to the relations

$$\frac{m_W^2}{m_Z^2} = \frac{h}{h + \tilde{s}^4}, \quad h = \frac{\pi\alpha(0)}{\sqrt{2}G_F m_Z^2(1 - \Delta r)} \quad (3.21)$$

and

$$1 - \xi^2 \rho_L = \frac{\tilde{s}^2}{h + \tilde{s}^4} \quad (3.22)$$

where use has been made of eq. (3.20) and (3.14) as well as of the on-shell relation

$$s^2 = 1 - m_W^2/m_Z^2. \quad (3.23)$$

Note that the expression for  $m_W$  is the same at tree level and at NLO. However its value differs since at LO  $\xi^2 \rho_L = 0$  which is not necessarily the case at NLO. In the following we will use  $G_F = 1.16637 \cdot 10^{-5} \text{ GeV}^{-2}$ , the canonical value  $\alpha(0) = 1/137.03599911$ ,  $m_Z = 91.1891 \text{ GeV}$  as given in the PDG [24] and  $\Delta r = 0.059$ . One thus gets  $h = 0.1776$  and one has at LO  $\tilde{s}^2 = 0.2309$  and  $m_W = 79.97 \text{ GeV}$ . We will come back to these values in section 4.

## 4. Couplings to $Z$

For the neutral current interaction, there are many accurate measurements available, in particular the huge amount of precise data from the experiments at LEP, LEP2 and SLC at energies around the  $Z$  resonance and even above. The latter data are parametrized in terms of effective observables (couplings, masses) including QED and QCD radiative effects, see ref. [26] for a thorough discussion of the definition of these effective “pseudo-observables”. It is understood that we will use these effective quantities throughout the following discussion. Following ref. [26] we denote these pseudo-observables by a superscript “0”.

Altogether six unknown parameters, defined in eq. (3.15) and eq. (3.16), appear in the couplings to  $Z$ :  $\epsilon^e$ ,  $\epsilon^\nu$ ,  $\epsilon^u$ ,  $\epsilon^d$ ,  $\tilde{s}^2$  and  $\delta$ . In contrast to the charged current where the additional  $Z_2$  symmetry of the LEET in the neutrino sector forbids a coupling of right-handed leptons to  $W$ , we have to consider here non-standard leptonic as well as non-standard quark couplings.

The parameter  $\epsilon^\nu$ , the coupling of right-handed neutrinos  $\nu_R$  to  $Z$ , cannot be determined at NLO from the asymmetry measurements. Since  $\nu_R$  are expected to be light enough to be pair-produced in  $Z$  decays,  $\epsilon^\nu$  enters the invisible width of  $Z$  [11]. But, as  $\nu_R$  have no  $SU(2)_L \times U(1)$  charge, their coupling to  $Z$  always contains powers of spurions. Therefore there is no interference with the SM contribution. This implies that  $\epsilon^\nu$  appears only quadratically in this invisible width, being thus additionally suppressed. The

|                              | Parameter  | Correlations                |                             |                             |                              |                         |
|------------------------------|------------|-----------------------------|-----------------------------|-----------------------------|------------------------------|-------------------------|
|                              |            | $(\epsilon^e)_{\text{NLO}}$ | $(\epsilon^u)_{\text{NLO}}$ | $(\epsilon^d)_{\text{NLO}}$ | $(\tilde{s}^2)_{\text{NLO}}$ | $(\delta)_{\text{NLO}}$ |
| $(\epsilon^e)_{\text{NLO}}$  | -0.0024(5) | 1.00                        |                             |                             |                              |                         |
| $(\epsilon^u)_{\text{NLO}}$  | -0.02(1)   | -0.07                       | 1.00                        |                             |                              |                         |
| $(\epsilon^d)_{\text{NLO}}$  | -0.03(2)   | -0.10                       | 0.60                        | 1.00                        |                              |                         |
| $(\tilde{s}^2)_{\text{NLO}}$ | 0.2309(3)  | 0.25                        | 0.44                        | 0.63                        | 1.00                         |                         |
| $(\delta)_{\text{NLO}}$      | -0.005(4)  | -0.16                       | 0.83                        | 0.94                        | 0.61                         | 1.00                    |
| $\chi^2/d.o.f$               | 3.1/5      |                             |                             |                             |                              |                         |

**Table 1:** Result of the restricted fit (see text) to  $Z$  pole data at NLO for  $\alpha_s(m_Z) = 0.1190$ .

experimental constraints are weak:  $\epsilon^\nu$  should be roughly of the order 0.1 or smaller for the contribution of  $\nu_R$  to the invisible width to become smaller than the experimental uncertainty [11]. At present we cannot determine its value more precisely.

In the next section we will discuss fits of the remaining five parameters to  $Z$  pole observables. In addition to the data at the  $Z$  resonance, there are several measurements at lower momentum transfer which are often included in precision tests of the standard model. We will comment on some of these measurements in section 4.2.

#### 4.1 Fit to $Z$ pole observables

In order to determine the unknown NLO parameters from the available data, we perform two different fits. For the “restricted fit” we take the following observables related to the  $Z$  (see ref. [26], table 8.4): the total width of the  $Z$ ,  $\Gamma_Z$ , the hadronic pole cross section  $\sigma_h^0$ , the ratios  $R_l^0 = \Gamma_h/\Gamma_l$ ,  $R_b^0 = \Gamma_b/\Gamma_h$ ,  $R_c^0 = \Gamma_c/\Gamma_h$ , the three asymmetries  $A_{FB}^{0,l}$ ,  $A_{FB}^{0,b}$ ,  $A_{FB}^{0,c}$ , and  $\mathcal{A}_l(P_\tau)$ . In the “full fit” we include in addition the direct measurement of  $\mathcal{A}_b$ ,  $\mathcal{A}_c$ , and  $\mathcal{A}_e$  from SLD. For the expression of these observables in terms of the effective couplings that appear at NLO, see appendix A. Note that, since we assume universal non-standard couplings, we have the following relation up to small radiative corrections  $3R_b^0 + 2R_c^0 = 1$ . The way this is obeyed in the fit merely tests the universality and the radiative corrections. As the parameter  $\delta$  appears both in the couplings to  $Z$  and to  $W$ , we included the leptonic branching fraction of the  $W$  into the fits [27]. It is sensitive to a correction induced by the parameter  $\delta$  to the hadronic width of  $W$ , see section 5.3.2. Alternatively, we could have considered the data for the total width of the  $W$ . However, the assigned experimental error induces a very large error on  $\delta$  and we did not consider the total width here.

We stated above that the main QED and QCD corrections are already included into the definition of pseudo-observables, such that the quantities assigned with a superscript “0” correspond to “bare” EW quantities. This is not entirely the case for the partial widths  $\Gamma_f$  for the  $Z$  decay into a fermion  $f\bar{f}$  pair. They have been defined in such a way that they add up to the total width. This means that they contain factors  $R_A^f, R_V^f$  describing the residual QED/QCD effects, see ref. [28]:

$$\Gamma_f = 4N_c^f \Gamma_0 \left( (g_V^f)^2 R_V^f + (g_A^f)^2 R_A^f \right). \quad (4.1)$$

|                              | Parameter  | Correlations                |                             |                             |                              |                         |
|------------------------------|------------|-----------------------------|-----------------------------|-----------------------------|------------------------------|-------------------------|
|                              |            | $(\epsilon^e)_{\text{NLO}}$ | $(\epsilon^u)_{\text{NLO}}$ | $(\epsilon^d)_{\text{NLO}}$ | $(\tilde{s}^2)_{\text{NLO}}$ | $(\delta)_{\text{NLO}}$ |
| $(\epsilon^e)_{\text{NLO}}$  | -0.0024(5) | 1.00                        |                             |                             |                              |                         |
| $(\epsilon^u)_{\text{NLO}}$  | -0.02(1)   | 0.0                         | 1.00                        |                             |                              |                         |
| $(\epsilon^d)_{\text{NLO}}$  | -0.03(1)   | -0.02                       | 0.35                        | 1.00                        |                              |                         |
| $(\tilde{s}^2)_{\text{NLO}}$ | 0.2307(2)  | 0.49                        | 0.19                        | 0.37                        | 1.00                         |                         |
| $(\delta)_{\text{NLO}}$      | -0.004(2)  | -0.11                       | 0.73                        | 0.87                        | 0.33                         | 1.00                    |
| $\chi^2/d.o.f$               | 8.5/8      |                             |                             |                             |                              |                         |

**Table 2:** Result of the full fit (see text) to  $Z$  pole data at NLO for  $\alpha_s(m_Z) = 0.1190$ .

In this equation,  $N_c^f = 1$  for leptons and  $N_c^f = 3$  for quarks,  $\Gamma_0 = (G_F m_Z^3)/(24\sqrt{2}\pi)$  and  $g_V^f, g_A^f$  are the effective EW vector and axial couplings, respectively. Note that, since within the expansion scheme of the LEET weak loops appear first at NNLO, we did not include any weak loop corrections in our NLO analysis (see the discussion on that point in section 3.2, too).

The hadronic pole cross section,  $\sigma_h^0$  and the total width  $\Gamma_Z$  of  $Z$  are rather sensitive to the value of  $\alpha_s$ . This allows to determine within the SM the value of  $\alpha_s(m_Z) = 0.1190(27)$  rather precisely [26]. In our case it turns out that the sensitivity of the fit to  $\alpha_s$  is considerably reduced due to the non-standard EW parameters. It is thus not possible to determine simultaneously  $\alpha_s$  and the additional EW parameters in a reliable way. In the following we use  $\alpha_s(m_Z) = 0.1190$ .

Let us first consider the LO results,  $\xi^2 \rho_L = \epsilon^i = \delta = 0$ .  $\tilde{s}^2 = s^2$  is fixed by the on-shell relation, see eq. (3.23) and we get  $(m_W)_{LO} = 79.97$  GeV, see the discussion in section 3.2. Figure 2 show the pulls

$$\frac{(|O^{meas} - O^{fit}|)}{\sigma^{meas}}, \quad (4.2)$$

where  $O^{meas/fit}$  is the measured/fitted value for a observable and  $\sigma^{meas}$  denotes the corresponding experimental error. Note that at LO all parameters are fixed and  $O^{fit}$  is determined from the calculation.<sup>7</sup> One obtains a good agreement except for  $\Gamma_Z$  and  $A_{FB}^{0,b}$  which are not well reproduced at this order.

Let us turn to the NLO calculation. Tables 1 and 2 give the values of our parameters for the restricted and the full fit, respectively.  $\tilde{s}^2$  is, together with  $\epsilon^e$ , severely constrained by the electron pseudo-observables due to the fact that the vector effective coupling of the electron  $g_V^e$  is very small. This coupling being well described already at LO,  $\tilde{s}^2$  is nearly unchanged at NLO and  $(\epsilon^e)_{\text{NLO}}$  is very small. All values for our parameters are nicely of the order expected from the LEET. Note that  $\epsilon_u \approx \epsilon_d$  and  $\delta \ll \epsilon_u, \epsilon_d$ , see the definitions, eqs. (3.15), (3.16). At this stage it is, however, too early to draw any conclusions on the size of the constants  $\eta, \xi$  and of the LECs.

<sup>7</sup>In principle, the value of  $\alpha_s$  can be varied for the LO fit. In order to better compare with the NLO result, we decided to keep  $\alpha_s(m_Z) = 0.1190$  fixed for the LO result, too. The value of  $\alpha_s$  has no influence on  $A_{FB}^{0,b}$ , whereas the agreement with  $\Gamma_Z$  can be slightly improved allowing  $\alpha_s$  to vary.



|                             | Measurement | Fit    | $\frac{( O^{meas} - O^{fit} )}{\sigma^{meas}}$ |
|-----------------------------|-------------|--------|--|
| $\Gamma_Z$ [GeV]            | 2.4952(23)  | 2.4842 |  |
| $\sigma_{had}$ [nb]         | 41.540(37)  | 41.507 |  |
| $R_e$                       | 20.767(25)  | 20.770 |  |
| $A_{FB}^l$                  | 0.0171(10)  | 0.0173 |  |
| $\mathcal{A}_l(P_\tau)$     | 0.1465(32)  | 0.1519 |  |
| $R_b$                       | 0.21629(66) | 0.2173 |  |
| $R_c$                       | 0.1721(30)  | 0.1719 |  |
| $A_{FB}^b$                  | 0.0992(16)  | 0.1066 |  |
| $A_{FB}^c$                  | 0.0707(35)  | 0.0763 |  |
| $\mathcal{A}_b$             | 0.923(20)   | 0.936  |  |
| $\mathcal{A}_c$             | 0.670(27)   | 0.670  |  |
| $\mathcal{A}_l(\text{SLD})$ | 0.1513(21)  | 0.1519 |  |
| $Br(W \rightarrow l\nu)$    | 0.1084(9)   | 0.1082 |  |

**Figure 2:** Pull for the  $Z$  pole observables at LO.

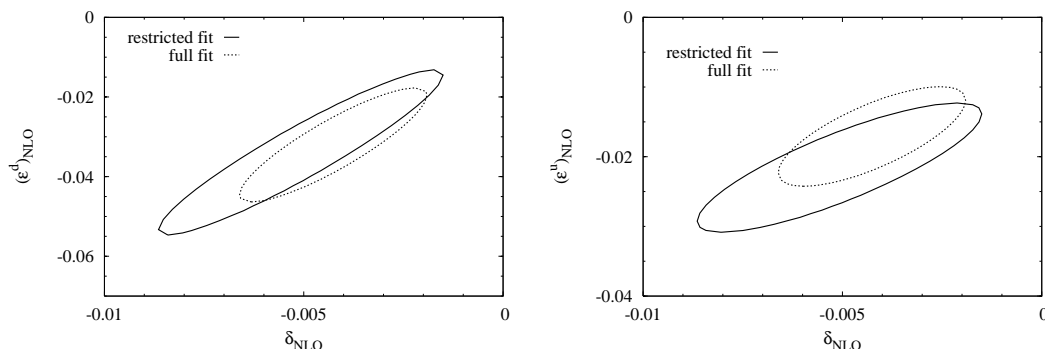


**Figure 3:**  $1\sigma$  contours for the parameters  $\epsilon^d$  (left panel) and  $\epsilon^u$  (right panel) versus  $\delta$  for the two different fits to  $Z$  pole data with  $\alpha_s(m_Z) = 0.1190$ , see table 1 and table 2.

Varying  $\alpha_s(m_Z)$  between 0.115 and 0.125, which should be reasonable values, we observe only very little effect on the fit result. For the restricted fit, for instance, the central value for the parameter  $\delta$ , which is the most sensitive to  $\alpha_s(m_Z)$ , varies between  $-0.005(4)$  and  $-0.006(4)$ . The  $\chi^2$  is not considerably modified, neither. It is  $3.0/5 d.o.f$  for  $\alpha_s(m_Z) = 0.125$  and  $3.2/5 d.o.f$  for  $\alpha_s(m_Z) = 0.115$ . It should be noted that the result for  $\delta$  is rather sensitive to the experimental value for the leptonic branching fraction of  $W$ . For the present fit we have taken the latter value from LEP data [27]. To illustrate the correlations between the different couplings we show the  $1\sigma$  ellipses for the most correlated combinations of parameters in figures 3, 4, 5, 6. The error thereby reflects only the experimental error. For the presented result  $\alpha_s(m_Z) = 0.1190$ .

The good agreement of our fit with the data can be seen from figures 7 and 8.  $\Gamma_Z$  and  $A_{FB}^{0,b}$  are much better reproduced at NLO compared with the LO result. Remarkably

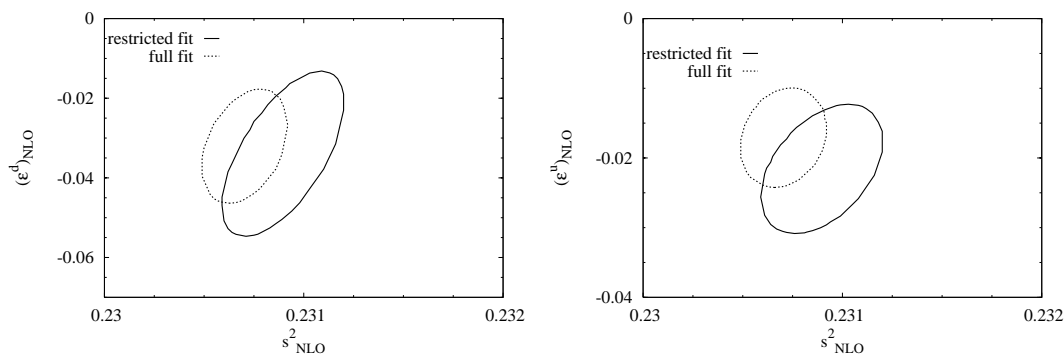


**Figure 4:**  $1\sigma$  contours for the parameters  $\epsilon^d$  (left panel) and  $\epsilon^u$  (right panel) versus  $\hat{s}^2$  for the two different fits to  $Z$  pole data with  $\alpha_s(m_Z) = 0.1190$ , see table 1 and table 2.

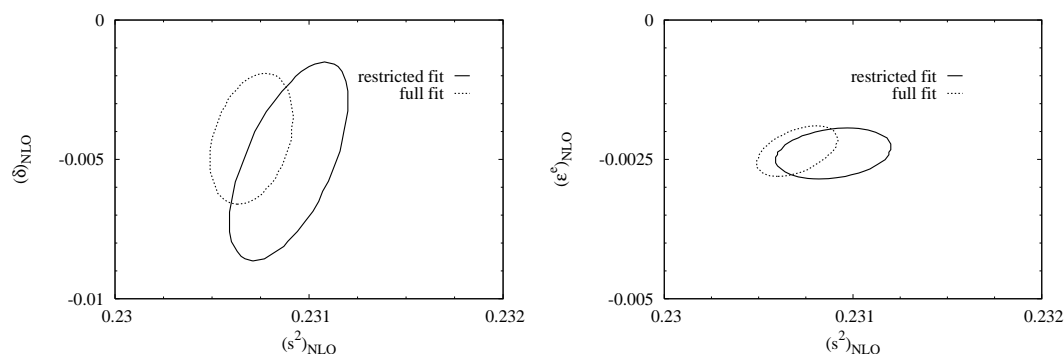


**Figure 5:**  $1\sigma$  contours for the parameters  $\delta$  (left panel) and  $\epsilon^e$  (right panel) versus  $\hat{s}^2$  for the two different fits to  $Z$  pole data with  $\alpha_s(m_Z) = 0.1190$ , see table 1 and table 2.

we can reproduce simultaneously the data for  $A_{FB}^{0,b}$  and  $R_b^0$  as well as  $A_{FB}^{0,c}$  and  $R_c^0$ . This is not straightforward. In the recent literature the “ $A_{FB}^b$  puzzle” has been intensively discussed and many models have been proposed providing solutions to this problem (see for instance [29]). Mostly, the proposed solution is based on a modification of the couplings of the third generation. Note that we do not need any non-universal couplings here to well reproduce the ratio  $R_b^0$  and the asymmetry. In our theory the effect is mainly due to (universal) non-standard right-handed couplings.

Clearly the values of our parameters will be modified at NNLO. Since we performed a fit they, in fact, implicitly contain at NLO higher order corrections. How big these are is hard to determine without doing the calculation. In our framework the Higgs particle is clearly absent from the loops and furthermore counter terms have to be added to the loop contributions. Indeed only the sum of loops plus counter terms is meaningful within our effective theory. However, if the expansion is convergent the higher order corrections should be small. Furthermore, from the fact that loops and our spurion contributions enter the observables in a similar way, we do not expect from a NNLO calculation a change in the

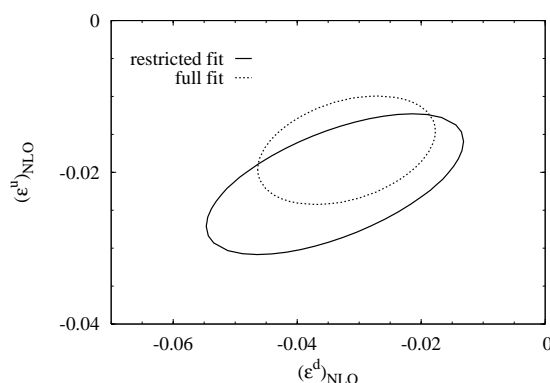


**Figure 6:**  $1\sigma$  contours for the parameters  $\epsilon^d$  versus  $\epsilon^u$  for the two different fits to  $Z$  pole data with  $\alpha_s(m_Z) = 0.1190$ , see table 1 and table 2.

|                             | Measurement | Fit     | $\frac{( O^{meas} - O^{fit} )}{\sigma^{meas}}$ |
|-----------------------------|-------------|---------|--|
|                             |             |         | 1 2 3 4 5                                      |
| $\Gamma_Z$ [GeV]            | 2.4952(23)  | 2.4942  |  |
| $\sigma_{had}$ [nb]         | 41.540(37)  | 41.568  |  |
| $R_e$                       | 20.767(25)  | 20.786  |  |
| $A_{FB}^l$                  | 0.0171(10)  | 0.0162  |  |
| $\mathcal{A}_l(P_\tau)$     | 0.1465(32)  | 0.1469  |  |
| $R_b$                       | 0.21629(66) | 0.21656 |  |
| $R_c$                       | 0.1721(30)  | 0.1729  |  |
| $A_{FB}^b$                  | 0.0992(16)  | 0.0999  |  |
| $A_{FB}^c$                  | 0.0707(35)  | 0.0689  |  |
| $\mathcal{A}_b$             | 0.923(20)   | 0.908   |  |
| $\mathcal{A}_c$             | 0.670(27)   | 0.627   |  |
| $\mathcal{A}_l(\text{SLD})$ | 0.1513(21)  | 0.1469  |  |
| $Br(W \rightarrow l\nu)$    | 0.1084(9)   | 0.1090  |  |

**Figure 7:** Pull for the  $Z$  pole observables in the restricted fit (see table 1). The pull for the quantities measured at SLD (which are not included in the fit) is shown in yellow (hatched light gray).

nice agreement between the calculated and experimental values of the pseudo-observables.

Having obtained the value of  $\tilde{s}^2$ ,  $m_W$  and  $\xi^2\rho_L$  can be determined from eqs. (3.21), (3.22). Since  $(\tilde{s}^2)_{\text{NLO}} \sim (\tilde{s}^2)_{\text{LO}}$  the difference between  $(m_W)_{\text{NLO}} = 79.97(11)$  GeV (restricted fit),  $(m_W)_{\text{NLO}} = 79.99(07)$  GeV (full fit), and  $(m_W)_{\text{LO}} = 79.97$  GeV is extremely small and  $(\xi^2\rho_L)_{\text{NLO}} = 0.000(18)$  (restricted fit),  $(\xi^2\rho_L)_{\text{NLO}} = 0.001(12)$  (full fit). This result contains the electromagnetic loop corrections in the spirit of our discussion of the way we do the expansion, see section 3.2. In this case the NLO corrections are thus extremely small. Clearly corrections at NNLO have to be evaluated. First,  $m_W$  does not receive direct corrections at NLO, it is only modified indirectly via the factor  $1 - \xi^2\rho_L$  from the redefinition of  $G_F$ , whereas at NNLO direct corrections to

|                             | Measurement | Fit     | $\frac{( O^{meas} - O^{fit} )}{\sigma^{meas}}$ |
|-----------------------------|-------------|---------|--|
|                             |             |         | 1 2 3 4 5                                      |
| $\Gamma_Z$ [GeV]            | 2.4952(23)  | 2.4943  |  |
| $\sigma_{had}$ [nb]         | 41.540(37)  | 41.569  |  |
| $R_e$                       | 20.767(25)  | 20.785  |  |
| $A_{FB}^l$                  | 0.0171(10)  | 0.0165  |  |
| $\mathcal{A}_l(P_\tau)$     | 0.1465(32)  | 0.1485  |  |
| $R_b$                       | 0.21629(66) | 0.21685 |  |
| $R_c$                       | 0.1721(30)  | 0.1725  |  |
| $A_{FB}^b$                  | 0.0992(16)  | 0.1012  |  |
| $A_{FB}^c$                  | 0.0707(35)  | 0.0707  |  |
| $\mathcal{A}_b$             | 0.923(20)   | 0.910   |  |
| $\mathcal{A}_c$             | 0.670(27)   | 0.636   |  |
| $\mathcal{A}_l(\text{SLD})$ | 0.1513(21)  | 0.1485  |  |
| $Br(W \rightarrow l\nu)$    | 0.1084(9)   | 0.1089  |  |

**Figure 8:** Pull for the  $Z$  pole observables in the full fit (see table 2).

$m_W$  will appear, too. Also, higher order corrections could be important due to numerically large factors of  $(m_t/m_W)^2$ . At NNLO the quantity  $\Delta r$  and the value of  $\tilde{s}^2$  will be modified. One can evaluate the value of  $\Delta r_w$ , the quantity which has to be added to  $\Delta r$  such that the physical mass of  $W$  is reproduced keeping  $\tilde{s}^2$  fixed. We obtain  $\Delta r_w = 0.046$  (where the subscript  $w$  means that they correspond to the weak contributions) of the size of the electromagnetic corrections  $\Delta\alpha = 0.059$ . In the standard model  $\Delta r_w = -0.0242$  and loop corrections to  $s_W$  are of the order of 0.04. Hence the value of 0.046 is of the expected size. We will see below another example of a quantity which is accidentally small at NLO.

## 4.2 Low energy observables

Several experiments provide data at energies below the  $Z$  pole. They could in principle give complementary information on the couplings. We did not include these observables into our fit for two reasons. First, in general the energies involved in these experiments are much smaller than  $m_Z$  such that the couplings involved are probed at a different energy scale. Second, in some cases the uncertainties are too large to detect non-standard effects on the percent level. Having fitted our parameters we can calculate some of these observables and compare with the experimental data.

### 4.2.1 Atomic parity violation

Measurements of atomic parity violation probe the coupling of electrons to the quarks inside the nucleus via the neutral current. The parity violating part of the amplitude has two contributions, one from an axial coupling to electrons and a vector coupling to quarks ( $A_e V_q$ ), and another one from a vector coupling to electrons and axial coupling to quarks ( $V_e A_q$ ). In order to keep hadronic uncertainties small, it is preferable to probe vector couplings for quarks. In this case, due to the conservation of the vector current, the hadronic matrix elements can be reliably predicted. The relevant part of the effective

four-fermion lepton/quark interaction Lagrangian is

$$\mathcal{L}_Z^{lq} = -\frac{G_F}{\sqrt{2}} 4g_A^e \bar{e} \gamma_\mu \gamma^5 e \left( g_V^u \bar{u} \gamma^\mu u + g_V^d \bar{d} \gamma^\mu d \right). \quad (4.3)$$

This allows to define the weak charge

$$Q_W = -4g_A^e \left( Z (2g_V^u + g_V^d) + N (g_V^u + 2g_V^d) \right), \quad (4.4)$$

where  $Z$  and  $N$  denote here the number of protons and neutrons in the nucleus, respectively. We kept here explicitly the dependence on the axial coupling of the electron since this makes it easier to distinguish non-standard quark and electron couplings, respectively. The usually defined effective four-fermion couplings are simply given by  $C_{1q} = 4g_V^q g_A^e$ . At NLO (see eqs. (A.3), (A.4) for the couplings) the weak charge is given by:

$$Q_W = (1 - \epsilon^e) \left( Z(1 - 4\tilde{s}^2 + \delta - \epsilon^d + 2\epsilon^u) - N(1 + \delta + 2\epsilon^d - \epsilon^u) \right). \quad (4.5)$$

Up to now the most precise measurements are those on  $^{133}\text{Cs}$  atoms [30]. Spin-dependent measurements allow to eliminate the small contribution from axial couplings to the nucleus, such that the result should be relatively reliable. Inserting the values for the parameters (cf. tables 1 and 2) discussed above into eq. (4.5), we obtain, respectively,  $(Q_W(^{133}\text{Cs}))_{\text{NLO}} = -70.72 \pm 3.72$  (restricted fit) and  $(Q_W(^{133}\text{Cs}))_{\text{NLO}} = -70.72 \pm 4.19$  (full fit),<sup>8</sup> in agreement with the relatively more precise experimental value,  $Q_W(^{133}\text{Cs}) = -72.71(49)$  [31]. Here again, we have to keep in mind that the already relatively large error of our NLO result is presumably subject to uncertainties related to NNLO corrections.

Interesting results on the weak charge of the proton are to be expected from the QWEAK experiment at Jefferson Lab. From our fit to  $Z$  pole data we predict  $Q_W^p = 0.062(17)$  (restricted fit) and  $Q_W^p = 0.062(22)$  (full fit) for the weak charge of the proton. Here, we have to stress that the accidental smallness of the NLO result (keep in mind that  $1 - 4\tilde{s}^2$  is very small), enhances the sensitivity of the result to sub-leading corrections, including loop corrections, too.

#### 4.2.2 Parity violation in $e^-e^-$ (Møller) scattering

Parity violation in  $e^-e^-$  scattering at low energies by the SLAC E158 collaboration provides another determination of the effective couplings of electrons [32]. The measured asymmetry can be written in terms of the weak charge for electrons,  $Q_W^e$ , probing the  $VA$  part of the purely electronic four-fermion interaction. It is defined in analogy with the nuclear weak charge defined above, see eq. (4.4),

$$Q_W^e = 4g_A^e g_V^e. \quad (4.6)$$

At NLO this reads

$$Q_W^e = 1 - 4\tilde{s}^2 (1 - \epsilon^e). \quad (4.7)$$

---

<sup>8</sup>These values contain the correlations listed in tables 1 and 2.

Inserting the values for  $\tilde{s}^2$  and  $\epsilon^e$  from the two fits to  $Z$  pole data into this equation, we obtain  $(Q_W^e)_{\text{NLO}} = 0.074(1)$ .<sup>9</sup> This is about six standard deviations away from the experimental result [32],  $Q_W^e = 0.041(5)$ . This represents another example where the NLO result is again accidentally small due to the fact that  $4\tilde{s}^2$  is close to one, such that sub-leading corrections can play an important role. We should therefore not be surprised that there is a discrepancy between our prediction at NLO and the data in this particular case.

## 5. Couplings of light quarks to $W$

Let us now discuss the modified couplings of quarks to  $W$  at NLO. We are faced in this case with the problem, how to disentangle QCD and non-standard electroweak effects. It is indeed most acute for the effective couplings to  $W$ ,  $\mathcal{V}_{eff}^{ij}$  and  $\mathcal{A}_{eff}^{ij}$ . Their measurement requires an independent knowledge of the involved QCD parameters like the decay constants  $F_\pi$ ,  $F_K$ ,  $F_D$ ,  $F_B$  or the transition form factors such as  $f_+^{K^0\pi^-}(0) \dots$ . The unfortunate circumstance is that the most accurate experimental information on QCD quantities mentioned above, in turn comes from semi-leptonic transitions of the type  $P \rightarrow l\nu$  and  $P' \rightarrow Pl\nu$  where  $P = \pi, K, D, B$  and, consequently, the result of their measurement depends on (a priori unknown) EW couplings.

The chiral generalisation of quark mixing and of CKM unitarity directly follows from the existence of couplings of right-handed quarks to  $W$ . It affects the meaning of the tests of the unitarity of the CKM matrix: The chiral matrices  $V_L$  and  $V_R$  have to be separately unitary, but the effective matrices  $\mathcal{V}_{eff}$  and  $\mathcal{A}_{eff}$ , eq. (3.18), which are more directly related to observables, can exhibit deviations from unitarity. The latter are expressible in terms of spurion parameters  $\delta$  and  $\epsilon$ . Even the unitarity triangles (“UT”) representing the off-diagonal elements of the unitarity condition might be but need not be affected. This gives a new motivation to the intense studies of UTs performed during the last years as a possible source of effects beyond the SM.

We will concentrate here on light quarks  $u$ ,  $d$ , and  $s$ . For them the SM loop effects inducing Right-Handed charged quark Currents (RHCs) are strongly suppressed by at least two powers of light quark masses. There are interesting tests in the heavy quark sector, too, which are certainly worth being studied, but since in the heavy quark sector additional quark mixing matrix elements become involved, we will postpone this investigation to future work.

### 5.1 Exclusive low-energy tests of couplings of right-handed quarks

#### 5.1.1 Chiral flavor mixing for light quarks

At NLO, the light quark effective couplings  $\mathcal{V}_{eff}^{ua}$ ,  $\mathcal{A}_{eff}^{ua}$ ,  $a = d, s$ , see eq. (3.18), can be expressed in terms of three non standard effective EW parameters: the spurion parameter  $\delta$ , eq. (3.15) and two RHCs parameters  $\epsilon_{ns}$  and  $\epsilon_s$  defined as (cf. eq. (3.16))

$$\epsilon_{ns} = \epsilon \operatorname{Re} \left( \frac{V_R^{ud}}{V_L^{ud}} \right), \quad \epsilon_s = \epsilon \operatorname{Re} \left( \frac{V_R^{us}}{V_L^{us}} \right). \quad (5.1)$$

---

<sup>9</sup>This value again contains the correlations, see tables 1 and 2.

We obtain

$$|\mathcal{V}_{eff}^{ud}|^2 = |V_L^{ud}|^2(1 + 2\delta + 2\epsilon_{ns}) \quad (5.2)$$

$$|\mathcal{A}_{eff}^{ud}|^2 = |V_L^{ud}|^2(1 + 2\delta - 2\epsilon_{ns}) \quad (5.3)$$

$$|\mathcal{V}_{eff}^{us}|^2 = |V_L^{us}|^2(1 + 2\delta + 2\epsilon_s) \quad (5.4)$$

$$|\mathcal{A}_{eff}^{us}|^2 = |V_L^{us}|^2(1 + 2\delta - 2\epsilon_s), \quad (5.5)$$

where  $V_L^{ud}$  and  $V_L^{us}$  are related by the unitarity condition of the left-handed mixing matrix. Neglecting  $V_L^{ub}$ , as suggested by the measurement of  $|\mathcal{V}_{eff}^{ub}|$  and  $|\mathcal{A}_{eff}^{ub}|$ , respectively, the unitarity condition can be written as follows,

$$|V_L^{ud}|^2 + |V_L^{us}|^2 = 1. \quad (5.6)$$

Let us discuss these equations.

- The only very precisely known quantity in this set of equations is  $|\mathcal{V}_{eff}^{ud}|$ . It is determined from nuclear  $0^+ \rightarrow 0^+$  transitions relying on the conservation of the vector current (CVC) and its value is [33]<sup>10</sup>

$$\mathcal{V}_{eff}^{ud} = 0.97377(26) \equiv \cos \hat{\theta}. \quad (5.7)$$

At LO, one recovers the unitarity of the CKM matrix in the SM, and  $\hat{\theta}$  corresponds to the Cabbibo angle. It is useful for the following discussions to rewrite the effective vector and axial couplings in terms of this quantity, using the relation between  $|V_L^{ud}|$  and  $|\mathcal{V}_{eff}^{ud}| = \cos \hat{\theta}$ , see eq. (5.2),

$$\begin{aligned} |\mathcal{V}_{eff}^{ud}|^2 &= \cos^2 \hat{\theta} \\ |\mathcal{A}_{eff}^{ud}|^2 &= \cos^2 \hat{\theta} (1 - 4\epsilon_{ns}) \\ |\mathcal{V}_{eff}^{us}|^2 &= \sin^2 \hat{\theta} \left( 1 + 2 \frac{\delta + \epsilon_{ns}}{\sin^2 \hat{\theta}} \right) (1 + 2\epsilon_s - 2\epsilon_{ns}) \\ |\mathcal{A}_{eff}^{us}|^2 &= \sin^2 \hat{\theta} \left( 1 + 2 \frac{\delta + \epsilon_{ns}}{\sin^2 \hat{\theta}} \right) (1 - 2\epsilon_s - 2\epsilon_{ns}), \end{aligned} \quad (5.8)$$

where we used the unitarity of the left-handed mixing matrix,  $V_L$ , eq. (5.6), in the last two equations. We only kept terms up to first order in the spurion parameters  $\delta, \epsilon_{ns}$ , and  $\epsilon_s$  except the term proportional to  $1/\sin^2 \hat{\theta}$ . For the latter the effect of spurions is enhanced due to the smallness of  $\sin \hat{\theta}$ .

- As already pointed out the genuine spurion parameters  $\delta$  and  $\epsilon$  are expected to be of the order 0.01. To obtain bounds on  $\epsilon_{ns}$  and  $\epsilon_s$  we can exploit the unitarity of the right-handed mixing matrix which gives the following condition:

$$|\epsilon_{ns}|^2 |V_L^{ud}|^2 + |\epsilon_s|^2 |V_L^{us}|^2 \leq \epsilon^2. \quad (5.9)$$

---

<sup>10</sup>Note that our phase convention is such that  $|\mathcal{V}_{eff}^{ud}| = \mathcal{V}_{eff}^{ud}$ . In this case  $V_L$  has not the same structure as the CKM matrix within the SM, but might have additional phases.

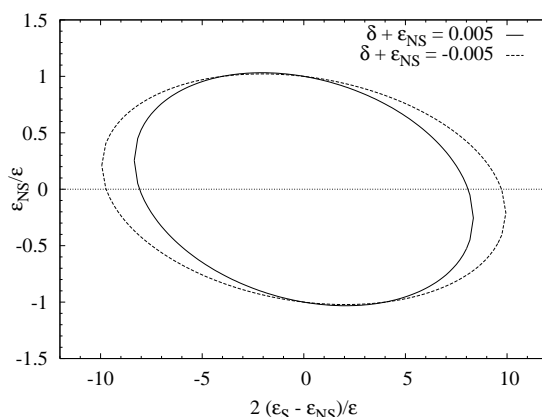


**Figure 9:** Maximum values of  $\epsilon_{\text{ns}}/\epsilon$  and  $(\epsilon_s - \epsilon_{\text{ns}})/\epsilon$  for two different values of  $\delta + \epsilon_{\text{ns}}$  compatible with the unitarity of  $V_{L,R}$ , cf. eq. (5.10).

Using the unitarity condition of the left-handed mixing matrix and the expression of  $V_L^{ud}$  in terms of  $\cos \hat{\theta}$  one obtains:

$$(|\epsilon_{\text{ns}}|^2 - |\epsilon_s|^2)(1 - 2(\delta + \epsilon_{\text{ns}})) \cos^2 \hat{\theta} + |\epsilon_s|^2 \leq \epsilon^2. \quad (5.10)$$

In the following we will see that all the observables can be written in terms of  $\delta + \epsilon_{\text{ns}}$ ,  $\epsilon_{\text{ns}}$  and  $\epsilon_s - \epsilon_{\text{ns}}$ . Fixing the value of  $\delta + \epsilon_{\text{ns}}$ , the above condition can be visualized as an ellipse in the plane  $\epsilon_{\text{ns}}/\epsilon, (\epsilon_s - \epsilon_{\text{ns}})/\epsilon$ . This is shown in figure 9 for two typical values of  $\delta + \epsilon_{\text{ns}}$ . It can be seen from figure 9 that, on the one hand  $|\epsilon_{\text{ns}}| \lesssim \epsilon$  is small. On the other hand,  $\epsilon_s$  can be enhanced to a few percent level:  $|\epsilon_s| \lesssim 4.5\epsilon$ . This enhancement of  $\epsilon_s$  is possible for example if the hierarchy in right-handed flavor mixing is inverted, i.e.  $|V_R^{ud}| < |V_R^{us}|$ .

As stressed above, in the presence of non-standard EW couplings, the effective mixing matrix  $\mathcal{V}_{\text{eff}}$  is not necessarily unitary. Wolfenstein [34] used this effect to find limits on the mixing of  $W_L$  and  $W_R$  in left-right symmetric models. Here, we can express the deviation from unitarity at NLO in terms of the EW parameters  $\delta, \epsilon_s, \epsilon_{\text{ns}}$ :

$$|\mathcal{V}_{\text{eff}}^{ud}|^2 + |\mathcal{V}_{\text{eff}}^{us}|^2 = 1 + 2(\delta + \epsilon_{\text{ns}}) + 2(\epsilon_s - \epsilon_{\text{ns}}) \sin^2 \hat{\theta}. \quad (5.11)$$

In this equation the only parameter,  $\epsilon_s$ , which can be significantly larger than  $\sim 0.01$  appears multiplied by  $\sin^2 \hat{\theta}$ . Since the possible enhancement of  $\epsilon_s$  is due to the mixing hierarchy of left-handed quarks proportional to  $1/|V_L^{us}| \approx 1/\sin \hat{\theta}$  the effect should be at most of the order  $\epsilon \sin \hat{\theta} \sim 0.002$ . The deviation from unitarity due to the spurionic parameters is thus at most of the order of the genuine spurion parameters  $\delta, \epsilon$ . It can, however, be much smaller. In addition, we cannot a priori say whether the r.h.s of eq. (5.11) should be smaller or larger than one.



### 5.1.2 Interface of effective electroweak and low-energy QCD couplings

As mentioned above, presently the most precise determinations of couplings of (light) quarks to  $W$  arise from semileptonic decay processes involving QCD parameters.

- From neutron life-time measurements and angular distributions we can extract the value of  $|g_A \mathcal{A}_{eff}^{ud}|/|g_V \mathcal{V}_{eff}^{ud}|$ ,
- from the decay rate  $\Gamma(\pi_{l2}(\gamma))$  we can infer  $|F_{\pi^+} \mathcal{A}_{eff}^{ud}|$ ,
- from the branching ratio  $\text{Br} \left( K_{l2}^+(\gamma)/\pi_{l2}^+(\gamma) \right)$  we can extract the value of  $|F_{K^+} \mathcal{A}_{eff}^{us}|/|F_{\pi^+} \mathcal{A}_{eff}^{ud}|$ ,
- and the  $K_{l3}^0$  decay rate allows to determine  $|f_+^{K^0\pi}(0) \mathcal{V}_{eff}^{us}|$ .

These decay processes involve hadronic matrix elements of vector/axial quark currents as for example the following exclusive matrix elements defining nucleon form factors

$$\langle p(k') | \bar{u} \gamma_\mu d | n(k) \rangle = g_V(q^2) \bar{u}_p(k') \gamma_\mu u_n(k) + \dots \quad (5.12)$$

$$\langle p(k') | \bar{u} \gamma_\mu \gamma_5 d | n(k) \rangle = g_A(q^2) \bar{u}_p(k') \gamma_\mu \gamma_5 u_n(k) + \dots, \quad (5.13)$$

with  $q^2 = (k' - k)^2$ , or the decay constants of pseudoscalar mesons

$$\langle 0 | \bar{u} \gamma_\mu \gamma_5 d(0) | \pi^+(p) \rangle = i\sqrt{2} F_\pi p_\mu, \quad \langle 0 | \bar{s} \gamma_\mu \gamma_5 u(0) | K^+(p) \rangle = i\sqrt{2} F_{K^+} p_\mu \quad (5.14)$$

as well as the hadronic matrix element describing the  $K_{\mu 3}^0$  decay. It can be written in terms of two form factors

$$\langle \pi^-(p') | \bar{s} \gamma_\mu u | K^0(p) \rangle = (p' + p)_\mu f_+^{K^0\pi^-}(t) + (p - p')_\mu f_-^{K^0\pi^-}(t), \quad (5.15)$$

where  $t = (p' - p)^2$ . Here the form factors and decay constants stand for radiatively corrected genuine QCD quantities. It is further understood that all isospin breaking effects due to  $m_d - m_u$  are included. These QCD quantities are subject to Chiral Perturbation Theory (ChPT) or lattice studies. Strictly speaking, without any theoretical input, none of them is experimentally accessible.

If the EW effective couplings of quarks to  $W$  are given by the SM, i.e.  $\delta = \epsilon_{\text{ns}} = \epsilon_s = 0$ , the above mentioned branching ratios and decay rates allow to determine the corresponding QCD quantities rather precisely since the EW effective couplings are all precisely determined by the value of  $\cos \hat{\theta}$ , see eq. (5.7). We will denote these QCD quantities extracted from semileptonic decay data assuming SM weak interactions with a hat. Their values are [24]

$$\begin{aligned} \hat{r}_A &= \left| \frac{g_A \mathcal{A}_{eff}^{ud}}{g_V \mathcal{V}_{eff}^{ud}} \right| = 1.2695(29), \\ \hat{F}_{\pi^+} &= 92.4(3) \text{ MeV}, \\ \hat{F}_{K^+}/\hat{F}_{\pi^+} &= 1.182(7), \\ \hat{f}_+^{K^0\pi^-}(0) &= 0.951(5). \end{aligned} \quad (5.16)$$

Here the errors merely reflect the experimental uncertainties in the measured branching ratios. Note that the value of  $\hat{F}_{K^+}/\hat{F}_{\pi^+} = 1.182(7)$  is significantly lower than the value largely used in ChPT studies,  $F_K/F_\pi = 1.22$  (cf. for instance [7, 35]).

In the presence of non-standard couplings of quarks to  $W$  the values of these QCD quantities extracted from semileptonic branching ratios are modified. Using eq. (5.8) the genuine QCD quantities can be written in terms of the corresponding quantities with a hat and the spurion parameters, e.g.:

$$\left(\frac{F_{K^+}}{F_{\pi^+}}\right)^2 = \left(\frac{\hat{F}_{K^+}}{\hat{F}_{\pi^+}}\right)^2 \frac{\sin^2 \hat{\theta} |\mathcal{A}_{eff}^{ud}|^2}{\cos^2 \hat{\theta} |\mathcal{A}_{eff}^{us}|^2} = \left(\frac{\hat{F}_{K^+}}{\hat{F}_{\pi^+}}\right)^2 \frac{1 + 2(\epsilon_s - \epsilon_{ns})}{1 + \frac{2}{\sin^2 \hat{\theta}}(\delta + \epsilon_{ns})}. \quad (5.17)$$

In a similar manner we can write

$$\begin{aligned} |r_A|^2 &= \hat{r}_A^2 (1 + 4\epsilon_{ns}) \\ |F_{\pi^+}|^2 &= \hat{F}_{\pi^+}^2 (1 + 4\epsilon_{ns}) \\ |f_+^{K^0\pi^-}(0)|^2 &= \left[\hat{f}_+^{K^0\pi^-}(0)\right]^2 \frac{1 - 2(\epsilon_s - \epsilon_{ns})}{1 + \frac{2}{\sin^2 \hat{\theta}}(\delta + \epsilon_{ns})}. \end{aligned} \quad (5.18)$$

To constrain the three NLO EW parameters  $\delta$ ,  $\epsilon_{ns}$  and  $\epsilon_s$  from the above relations, we need information on the QCD quantities like  $F_{\pi^+}$ ,  $F_{K^+}$ ,  $f_+^{K^0\pi^-}(0)$  which is independent of their extraction from semi-leptonic transitions. Such information could in principle originate from lattice simulations, from ChPT, or from short-distance constraints on QCD observables combined with purely strong/electromagnetic processes.

### 5.1.3 Neutron $\beta$ -decay and Adler-Weisberger sum rule

Let us illustrate the problem with two examples which historically played an important role in establishing the  $V-A$  character of the weak interaction. The first one is neutron  $\beta$ -decay. There exist precise measurements of various angular and spin correlations in the (polarized) neutron  $\beta$ -decay and more experimental results are expected (see e.g. [36]). These are often presented as accurate tests of the chirality of fermion couplings to  $W$ . Given the NLO minimal LEET expression of these couplings, eq. (3.12), one may ask what is the impact of these measurements on the RHCs parameter  $\epsilon_{ns}$  defined in eq. (5.1). Since at NLO the standard  $V-A$  couplings of *leptons* to  $W$  are not modified, any observable in neutron  $\beta$ -decay can be expressed in terms of the Fermi constant and two EW parameters concerning more particularly  $u$  and  $d$  quarks:  $|g_V \mathcal{V}_{eff}^{ud}|$  which normalizes the decay rate via the neutron lifetime and the relative parameter  $\hat{r}_A$ , see eq. (5.16). The compatibility of various extractions of  $\hat{r}_A$  from different measurements of independent correlations does, indeed, represent a valuable test of the  $V-A$  character of the coupling of leptons to  $W$ . These tests are so far compatible with a pure  $V-A$  leptonic coupling.

However, as precise they could possibly be, the neutron  $\beta$ -decay experiments alone say nothing about the quark RHCs unless one specifies the a priori unknown QCD quantity

$$r_A = g_A/g_V \quad (5.19)$$

which does not coincide with the experimentally known  $\hat{r}_A$  provided there exist right-handed  $\bar{u}d$  currents, i.e.,  $\epsilon_{\text{ns}} \neq 0$ . Actually, one has (cf. eq. (5.18))

$$r_A = \hat{r}_A(1 + 2\epsilon_{\text{ns}}). \quad (5.20)$$

Hence,  $\epsilon_{\text{ns}}$  could be determined if  $r_A$  was known.

Soon after the idea of universal  $V-A$  weak interactions has appeared [37], the issue of its tests for hadrons has been considered in the light of the current algebra charge relation  $[Q_5, Q_5^\dagger] = 2I_3$  which provides an absolute normalization of the axial current and gives a precise meaning to the ratio  $r_A$ . Combined with chiral symmetry, this relation yields the Adler-Weisberger sum rule [38], which may be written as

$$1 = r_A^2 + F_\pi^2 \frac{2}{\pi} \int dk \frac{k^2}{\omega^3(k)} [\sigma^{\pi^- p}(k) - \sigma^{\pi^+ p}(k)] + \mathcal{O}(m_\pi^2), \quad (5.21)$$

where  $k$  and  $\omega$  are pion laboratory momentum and energy, respectively. Since the charge current algebra, as well as chiral symmetry, are today integral parts of QCD and can be proven from first principles, the above relation is an exact QCD low-energy theorem which holds independently of the EW effective couplings  $\mathcal{V}_{\text{eff}}$  and  $\mathcal{A}_{\text{eff}}$ . Using the expressions (cf. eq. (5.18)) of  $r_A$  and  $F_\pi$  in terms of experimentally known quantities  $\hat{r}_A$  and  $\hat{F}_\pi$ , the Adler-Weisberger relation may be written as a sum rule for the RHCs parameter  $\epsilon_{\text{ns}}$ :

$$1 - 4\epsilon_{\text{ns}} = \hat{r}_A^2 + \hat{F}_\pi^2 \frac{2}{\pi} \int dk \frac{k^2}{\omega^3(k)} [\sigma^{\pi^- p}(k) - \sigma^{\pi^+ p}(k)] + \mathcal{O}(M_\pi^2). \quad (5.22)$$

Hence,  $\epsilon_{\text{ns}}$  can, in principle, be inferred from observable quantities under two conditions: (i) The chiral symmetry breaking corrections to the low-energy theorem, eq. (5.21), can be reliably estimated to high precision and (ii) the sum rule integral can be evaluated with a sufficient precision out of measured and radiatively corrected  $\pi N$  total cross sections (see for example ref. [39] and references therein).

Since  $\epsilon_{\text{ns}}$  is expected to reach at most the percent level, it does not appear realistic to control the sum rule, eq. (5.21), to this degree of precision. The previous discussion illustrates the typical problems one has to face extracting the spurion parameters  $\delta, \epsilon_{\text{ns}}$ , and  $\epsilon_s$  on the basis of chiral low-energy theorems.

An additional remark is in order: The Goldberger-Treiman low-energy theorem is insensitive to the modification of EW effective couplings considered here. The reason is that  $\epsilon_{\text{ns}}$  cancels in the ratio  $r_A/F_\pi = \hat{r}_A/\hat{F}_\pi$  reflecting the fact that QCD does not know about EW couplings.

#### 5.1.4 How to measure $F_\pi$ in non-EW processes?

(i)  $\pi^0 \rightarrow 2\gamma$

One possible determination of  $F_{\pi^+}$  comes from the  $\pi^0 \rightarrow 2\gamma$  partial width. This process has no interface with the EW couplings and it is independent of the standard determination based on the  $\pi_{l2}$  decay rate. It could thus provide a measurement of  $\epsilon_{\text{ns}}$  through eqs. (5.16) and (5.18). The process  $\pi^0 \rightarrow 2\gamma$  is governed by the anomaly

which exactly predicts the value of the amplitude in the chiral limit. Corrections up to  $\mathcal{O}(p^6, e^2 p^4)$  and to first order in  $m_d - m_u$  have recently been calculated [40, 41]. They are dominated by isospin breaking corrections and are of the order  $10^{-2}$ . For the moment we will not pursue this possibility further for an experimental and a theoretical reason.

- The experimental situation for the  $\pi^0$ -lifetime does not allow to determine the partial width  $\pi^0 \rightarrow 2\gamma$  better than with an error of 7.1% (current world average [24]). This induces an error of at least several percent on the determination of  $F_\pi$ . The upcoming result of the Primex experiment at Jefferson Lab will certainly improve on this situation aiming at a precision [42] of 1.5% for the partial width. Then in principle it becomes conceivable to look for effects of the order of percent relating eqs. (5.16) and (5.18).
- Upon relating the unknown  $\mathcal{O}(p^6)$  low-energy constants of the Wess-Zumino-Witten Lagrangian to the  $\eta$  decay width employing a three-flavor framework [40, 41], the dominant corrections to the chiral limit involve the isospin breaking quark mass ratio  $R = (m_s - \hat{m})/(m_d - m_u)$ . Thus from the theoretical side a sufficiently precise determination of  $F_\pi$  from the  $\pi^0 \rightarrow 2\gamma$  partial width requires a good knowledge of the isospin breaking parameter  $\epsilon^{(2)} = (\sqrt{3}/4) (1/R)$ . This can probably be achieved in the near future comparing the high statistics measurements of charged and neutral  $K_{l3}$  decays.

(ii)  $\pi\pi$  scattering.

In principle, another possibility to extract a value of  $F_\pi$  independently arises from  $\pi\pi$  scattering. In the low-energy domain the  $\pi\pi$  scattering amplitude is strongly constrained by chiral symmetry because of the Goldstone-boson character of the pions. Asking in addition for the amplitude to satisfy crossing symmetry and unitarity, it can be written in terms of six sub-threshold parameters [43], the pion mass and  $F_\pi$ . Matching the phenomenological description of the amplitude from the solution of Roy equations [44, 45] with the chiral representation, it should be possible to extract the value of  $F_\pi$ . Presently, however, the errors on the extracted sub-threshold parameters, assuming  $F_\pi = \hat{F}_\pi$  are at least of the order of one percent such that it seems difficult to reliably determine  $F_\pi$  with a precision of less than a percent.

## 5.2 The gold plated test: $K_{\mu 3}^L$ decays

In ref. [46] it has been shown that a stringent test involving the EW coupling  $\epsilon_s - \epsilon_{\text{ns}}$  can be devised in  $K_{\mu 3}^L$  decay. Indeed, combining the measurement of the scalar  $K\pi$  form factor in  $K_{\mu 3}^L$  decays with the Callan-Treiman low-energy theorem, it is possible to measure the ratio  $F_{K^+}/F_{\pi^+} f_+^{K^0\pi^+}(0)$  independently from the above mentioned semileptonic branching ratios and decay rates.

Let us briefly resume here the results of ref. [46]. We will concentrate on the normalized scalar form factor, see eq. (5.15)

$$f(t) = \frac{f_S^{K^0\pi^-}(t)}{f_+^{K^0\pi^-}(0)} = \frac{1}{f_+^{K^0\pi^-}(0)} \left( f_+^{K^0\pi^-}(t) + \frac{t}{\Delta_{K\pi}} f_-^{K^0\pi^-}(t) \right), \quad f(0) = 1. \quad (5.23)$$

The Callan-Treiman low-energy theorem (CT) [47] fixes the value of  $f(t)$  at the point  $t = \Delta_{K\pi} = m_{K^0}^2 - m_{\pi^+}^2$  in the  $SU(2) \times SU(2)$  chiral limit:

$$C \equiv f(\Delta_{K\pi}) = \frac{F_{K^+}}{F_{\pi^+}} \frac{1}{f_+^{K^0\pi^-}(0)} + \Delta_{CT}, \quad (5.24)$$

where the CT discrepancy  $\Delta_{CT}$  defined by eq. (5.24) is expected to be small and calculable in ChPT. It is proportional to  $m_u$  and/or  $m_d$ . In the limit  $m_d = m_u$  at NLO in ChPT one has  $\Delta_{CT}^{NLO} = -3.5 \times 10^{-3}$  [48]. We will focus the discussion on the neutral kaon mode since the analysis of the charged mode is subject to larger uncertainties related, in particular, to  $\pi^0\eta$  mixing [46] which could easily enhance the CT discrepancy by one order of magnitude.

In the physical region the form factor can be parameterized accurately in terms of only one parameter,  $\ln C$ , in a model independent way using the dispersive representation proposed in ref. [46]. This allows for a direct measurement of  $\ln C$  in  $K_{\mu 3}^L$  decays recently performed by the NA48 collaboration [49]. They obtain

$$\ln C_{exp} = 0.1438 \pm 0.0138. \quad (5.25)$$

This value can be combined with the determination from the branching ratios  $\text{Br } K_{l2(\gamma)}^+/\pi_{l2(\gamma)}^+$  [50], the inclusive decay rate  $K_{e3(\gamma)}^L$  [51], and the value of  $|\mathcal{V}_{eff}^{ud}|$  known from superallowed  $0^+ \rightarrow 0^+$  nuclear  $\beta$ -decays [33] as (see eqs. (5.17), (5.18))

$$C = B_{exp} r + \Delta_{CT}, \quad (5.26)$$

with

$$B_{exp} = \left| \frac{F_{K^+} \mathcal{A}_{eff}^{us}}{F_{\pi^+} \mathcal{A}_{eff}^{ud}} \right| \frac{1}{|f_+^{K^0\pi^-}(0) \mathcal{V}_{eff}^{us}|} |\mathcal{V}_{eff}^{ud}| \quad (5.27)$$

and

$$r = \left| \frac{\mathcal{A}_{eff}^{ud} \mathcal{V}_{eff}^{us}}{\mathcal{V}_{eff}^{ud} \mathcal{A}_{eff}^{us}} \right|. \quad (5.28)$$

This gives<sup>11</sup> to first order in  $\epsilon$ :

$$\ln C = 0.2182 \pm 0.0035 + \tilde{\Delta}_{CT} + 2(\epsilon_s - \epsilon_{ns}) = 0.2182 \pm 0.0035 + \Delta\epsilon \quad (5.29)$$

where  $\tilde{\Delta}_{CT} = \Delta_{CT}/B_{exp}$ . From the experimental result eqs. (5.25) one gets:

$$\Delta\epsilon = -0.074 \pm 0.014. \quad (5.30)$$

---

<sup>11</sup>There is a small difference between the value used in ref. [49] and the value given here because we use only the  $K_{e3}^L$  data to evaluate  $|f_+^{K^0\pi^-}(0) \mathcal{V}_{eff}^{us}|$ .

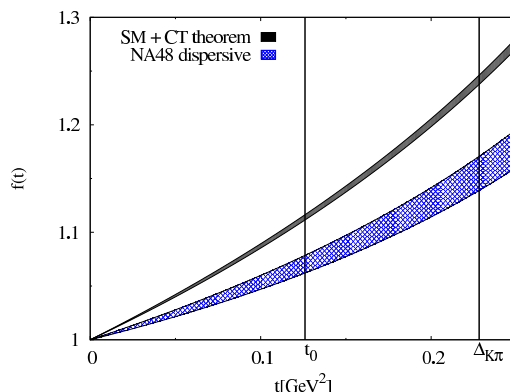


**Figure 10:** The normalized scalar  $K\pi$  form factor as a function of  $t$ .

This is an interesting result. Within our framework it suggests that  $\epsilon_s$  could be enhanced as a consequence of an inverted mixing hierarchy in the right-handed sector, see section 5.1.1. The strong deviation between the SM prediction and the measurement is clearly shown in figure 10 which display  $f(t)$ . The upper black curve corresponds to the SM prediction, i.e.  $\epsilon_s = \epsilon_{ns} = 0$ . The assigned error is purely experimental. The full blue curve correspond to the NA48 value using the dispersive representation. Of course, this result should be confirmed by other independent measurements of the scalar  $K\pi$  form factor based on the dispersive representation which are underway. For more discussion see refs. [46, 52].

### 5.3 Inclusive OPE based tests

In addition to the processes, where chiral dynamics controls the QCD part, we can investigate (semi-)inclusive processes where the QCD part is dominated by short-distance dynamics and can be evaluated applying operator product expansion techniques. We will discuss here three types of such processes: inelastic neutrino scattering,  $W$  boson (semi-) inclusive decays and hadronic tau decays.

#### 5.3.1 Inelastic neutrino scattering

The hadronic tensor contributing to the cross section for inelastic (anti-) neutrino-nucleon scattering is given by

$$W^{\mu\nu}(p, q) = \frac{1}{4\pi} \int d^4x \sum_{\sigma} e^{iqx} \langle p, \sigma | [J^{\nu}(x), (J^{\mu}(0))^{\dagger}] | p, \sigma \rangle, \quad (5.31)$$

where  $J^{\mu}$  is the EW hadronic current (see eq. 3.12)

$$J^{\mu} = (1 + \delta) \bar{U}_L V_L \gamma^{\mu} D_L + \epsilon \bar{U}_R V_R \gamma^{\mu} D_R \quad (5.32)$$

and  $\sigma$  indicates the sum over spins. The hadronic tensor can be splitted into contributions from different chiralities:

$$W^{\mu\nu} = (1 + \delta)^2 W_{LL}^{\mu\nu} + \epsilon (1 + \delta) W_{LR}^{\mu\nu} + \epsilon^2 W_{RR}^{\mu\nu}. \quad (5.33)$$

This decomposition makes obvious that we do not expect a sensitive test of the coupling of right-handed quarks to  $W$  from inelastic neutrino scattering. The only term linear in the spurion parameter  $\epsilon$ , the second term on the right-hand side of eq. (5.33), is proportional to  $W_{LR}^{\mu\nu}$  which, due to its chiral structure, does not contribute to the leading twist. Sizeable contributions could arise only from heavy quarks. These are, however, suppressed by the mixing hierarchy of left-handed quarks. The third term on the r.h.s of eq. (5.33), which contributes to the leading twist, is in turn suppressed by two powers of the spurion parameter  $\epsilon$ . According to the order of magnitude estimates from the LEET, this contribution should not be much larger than about  $10^{-4}$  and can therefore hardly be disentangled from higher twist left-handed contributions. The bound on the RHCs contribution in deep inelastic neutrino scattering obtained by the CDHS collaboration, later confirmed by CCFR [53] from the  $y$ -dependence of neutrino and antineutrino scattering cross sections is thus not very restrictive in the present case.

In conclusion, the parameter  $\delta$  is the only one which in principle can sensibly be extracted from inelastic neutrino scattering. To first order in the spurionic parameters, we can write

$$W^{\mu\nu} = (1 + 2\delta) \hat{W}^{\mu\nu}, \quad (5.34)$$

where  $\hat{W}^{\mu\nu}$  denotes the hadronic tensor assuming SM weak interactions. Hence the determination of the parameter  $\delta$  amounts to the precise knowledge of the absolute normalisation of the neutrino scattering cross section. As we discussed in section 4,  $\delta \lesssim 0.01$  and we would have to control the cross sections to a better accuracy. Note that currently the uncertainties in parton distribution functions (PDFs) (normalisation) do not reach this precision.

We would like to point out that there is a possibility to overcome this difficulty based on Adler's neutrino sum rule [54] which can be written as follows for the scattering on a proton target:

$$\int_0^\infty \left( W_2^{(\bar{\nu}p)}(q^2, \nu) - W_2^{(\nu p)}(q^2, \nu) \right) d\nu = 2(1 + 2\delta), \quad (5.35)$$

where the structure function  $W_2$  is defined via

$$W_{\mu\nu}^{(\nu)}(p, q) = \frac{p_\mu p_\nu}{m_N^2} \left( \theta(\nu) W_2^{(\bar{\nu}p)}(q^2, \nu) - \theta(-\nu) W_2^{(\nu p)}(q^2, -\nu) \right) + \text{independent tensor structures}. \quad (5.36)$$

$m_N$  is the nucleon mass and the integration variable is  $\nu = pq/m_N$ . Let us recall that the sum rule, eq. (5.35), is an exact QCD statement (not receiving any  $\alpha_s$  corrections), valid for fixed  $q^2 < 0$ . Hence, in principle, the Adler sum rule provides a test of EW couplings which is independent of high  $q^2$  approximations and/or precise knowledge of PDFs. In practice, it is however not easy to evaluate this sum rule precisely from existing data because not all values of  $\nu$  are equally well accessible and there are complications due to heavy quark thresholds. Notice further that the spurion parameter  $\delta$  enters the overall normalisation of the cross section, together with the factor  $(m_W^2/(-q^2 + m_W^2))^2$  from the propagator of the exchanged  $W$ -boson. This fact could be exploited to sharpen the combined EW and QCD analysis [55].

### 5.3.2 $W$ boson (semi-) inclusive decays

The non-standard charged currents couplings ( $\mathcal{V}_{eff}$  and  $\mathcal{A}_{eff}$ ) affect, among other things, the decay of  $W$  into hadrons. Consequently, these new couplings will appear in the description of the decay ratio and we can try to extract them from the corresponding data. The total hadronic decay width of  $W$  bosons can be obtained from the absorptive part of the corresponding two-point correlation function

$$\Pi^{\mu\nu}(q) = i \int d^4x e^{iqx} \langle 0 | T(J^\mu(x)(J^\nu(0))^\dagger | 0 \rangle . \quad (5.37)$$

The expression up to NLO within the LEET can be deduced from eq. (5.32). Considering only the effects of first order in  $\epsilon$  and  $\delta$ , we obtain:

$$\Gamma(W \mapsto h) = (1 + 2\delta) \hat{\Gamma}(W \mapsto h) , \quad (5.38)$$

where  $\hat{\Gamma}(W \mapsto h)$  is the hadronic  $W$  width extracted assuming SM interactions. Again, as in the case of inelastic neutrino scattering, only the parameter  $\delta$  appears. Perturbative QCD predicts the value of  $\hat{\Gamma}(W \rightarrow h)$  as a series in  $\alpha_s(m_W)$  [24]:

$$\hat{\Gamma}(W \rightarrow h) = \frac{G_F M_W^3}{6\sqrt{2}\pi} \left[ 6 R_W + \dots \right] , \quad (5.39)$$

where the factor

$$R_W = \left[ 1 + \frac{\alpha_S(m_W)}{\pi} + 1.409 \left( \frac{\alpha_S(m_W)}{\pi} \right)^2 - 12.77 \left( \frac{\alpha_S(m_W)}{\pi} \right)^3 \right] \quad (5.40)$$

arises from QCD corrections. For the total  $W$  decay width we obtain:

$$\Gamma_W = \frac{G_F M_W^3}{6\sqrt{2}\pi} \left[ 3 + 6 (1 + 2\delta) R_W \right] . \quad (5.41)$$

Let us recall that the leptonic contribution is not changed with respect to the SM because at NLO within the LEET, the universal modification of the couplings of left-handed leptons is absorbed into the definition of  $G_F$ . Right-handed charged leptonic currents are forbidden due to the additional  $Z_2$  symmetry for the neutrinos.

Hence, the measurements sensitive to the hadronic decay width of  $W$  should allow us to extract the parameter  $\delta$  that modifies the coupling of  $W$  to the left-handed fermions. This is a common feature to all inclusive charged current processes at high energies. This can be understood as follows. We are looking at a correction to the SM result where the charged current interaction is purely left-handed. The parameter  $\epsilon$  related to right-handed charged quark currents can therefore only appear to first order in connection with quark masses or other non-perturbative quantities inducing a  $LR$  structure, i.e. they are typically suppressed by a factor  $m_i m_j / m_W^2$ .

Let us now discuss the different measurements.



- There are direct and indirect experimental measurements of the total decay width of  $W$  available from LEP and Tevatron. At the moment, the direct measurements<sup>12</sup> are not precise enough to be sensitive to a value for  $\delta$  on the percent level. With the different data from [27, 56] we obtain roughly  $-0.03 < \delta < 0.03$ . In view of the experimental effort undertaken to improve on the precision for the  $W$  decay width, it will probably become possible to test the value of  $\delta$  more precisely from the decay width of  $W$  in the near future.
- Another possibility is to take the measured leptonic branching fraction  $\Gamma(W \rightarrow l\nu)/\Gamma_W$  which is known with high precision. We have included this quantity into the fit determining the spurionic parameters at NLO in the couplings to  $Z$ , since the same parameter  $\delta$  enters the couplings of left-handed quarks to  $Z$ . This fit has been discussed in detail in section 4. The resulting value is  $\delta = -0.006(4)$  at  $\alpha_s(m_Z) = 0.1190$ , taking the value for the leptonic branching fraction from LEP [27],  $\Gamma(W \rightarrow l\nu)/\Gamma_W = 0.1084(9)$ .
- If it was possible to measure precisely partial decay widths into hadrons, it would be conceivable to determine  $\delta$  and the corresponding matrix element of  $V_L$  simultaneously. Here again, the contributions from couplings of right-handed quarks to  $W$  are strongly suppressed since they appear only with powers of masses or other quantities with  $LR$  structure, divided by the  $W$  mass. For example, the partial width into  $c\bar{s}$  is given by

$$\Gamma(W \rightarrow c\bar{s}) = \frac{G_F M_W^3}{6\sqrt{2}\pi} (1 + 2\delta) |V_L^{cs}|^2 R_W. \quad (5.42)$$

Currently, although recently there has been some effort in order to measure partial widths, the assigned experimental errors [24, 57] are much too large to determine reliable  $\delta$  and/or the corresponding mixing matrix elements.

### 5.3.3 Hadronic tau decays

The hadronic tau decays are semileptonic decays involving the charged current. Even though the different analysis of these decays done so far [58] have not yet reported any evidence of physics beyond the standard model, it seems interesting to reconsider them in the light of our generalization of the electroweak charged current.

For our analysis we will consider the normalized total hadronic width given by the ratio

$$R_{\tau,c} = \frac{\Gamma(\tau^- \rightarrow \nu_\tau \text{hadrons}(\gamma))}{\Gamma(\tau^- \rightarrow \nu_\tau e^- \bar{\nu}_e)}, \quad (5.43)$$

where  $c$  can be  $V, A$  or  $S$  depending whether one considers the vector, axial or strange channel, respectively. Additional information is provided by the moments  $R_{\tau,c}^{(kl)}$  which

---

<sup>12</sup>We can only use the direct measurements because the indirect ones use some input from measurements at the  $Z$  pole, as for instance the value of the branching ratio  $Z \mapsto e^+e^-$ , which are extracted assuming the SM and which can get modified within the present framework.

explore the invariant mass distribution of final state hadrons,

$$R_{\tau,c}^{(kl)} = \int_0^{m_\tau^2} ds \left(1 - \frac{s}{m_\tau^2}\right)^k \left(\frac{s}{m_\tau^2}\right)^l \frac{dR_{\tau,c}}{ds}. \quad (5.44)$$

The two experimental collaborations ALEPH [59] and OPAL [60, 61] have presented precise results for the total ratio  $R_\tau = R_{\tau,V} + R_{\tau,A} + R_{\tau,S}$  as well as separate results for the vector, the axial, and the strange channel, respectively. In addition they give results for different measured moments. More precise data on tau decays are to be expected from the  $B$ -factories.

The inclusive character of these quantities allows for a theoretical description of the hadronic part in terms of the operator product expansion (OPE). This has triggered much work testing QCD — in particular quark masses and the value of  $\alpha_s$  — at the tau mass scale (for a recent review see [58]) assuming standard model weak interactions. We shall focus our discussion on the differences arising with respect to this standard analysis of inclusive hadronic decay rates due to non-standard charged current interactions. In particular, we will not discuss in detail the description of the hadronic part, but refer the reader to the comprehensive literature on that subject (for a recent review see [58]).

The ratios, eqs. (5.43) and (5.44), can be written as follows [62, 63]:

$$\begin{aligned} R_{\tau,V}^{(kl)} &= \frac{3}{2} S_{EW} |\mathcal{V}_{eff}^{ud}|^2 \left( r_{kl} + \delta^{(0),kl} + \delta'_{EW} + \sum_{D=2,4,\dots} \delta_{ud,V}^{(D),kl} \right) \\ R_{\tau,A}^{(kl)} &= \frac{3}{2} S_{EW} |\mathcal{A}_{eff}^{ud}|^2 \left( r_{kl} + \delta^{(0),kl} + \delta'_{EW} + \sum_{D=2,4,\dots} \delta_{ud,A}^{(D),kl} \right) \\ R_{\tau,S}^{(kl)} &= \frac{3}{2} S_{EW} \left( |\mathcal{V}_{eff}^{us}|^2 \left[ r_{kl} + \delta^{(0),kl} + \delta'_{EW} + \sum_{D=2,4,\dots} \delta_{us,V}^{(D),kl} \right] \right. \\ &\quad \left. + |\mathcal{A}_{eff}^{us}|^2 \left[ r_{kl} + \delta^{(0),kl} + \delta'_{EW} + \sum_{D=2,4,\dots} \delta_{us,A}^{(D),kl} \right] \right). \end{aligned} \quad (5.45)$$

$S_{EW} = 1.0198$  [58, 64] denotes a small electroweak radiative correction. The residual electroweak correction,  $\delta'_{EW} = 0.0010$  [65] will be neglected in what follows.  $r_{kl}$  is a normalization coefficient for the purely perturbative part. It determines the parton level prediction for the decay rates and moments. For  $k = l = 0$ ,  $r_{00} = 1$ . The other values are listed in appendix B. The quantities  $\delta_i^{(D),kl}$  are QCD corrections. They are functions of several QCD parameters:  $\alpha_s$ , quark masses and non-perturbative condensates.  $\delta^{(0),kl}$  describes the massless perturbative contribution, and  $\delta_i^{(2),kl}$  are corrections due to non-zero quark masses. The terms  $\delta^{(D),kl}$  for  $D \geq 4$  comprise non-perturbative contributions within the OPE expansion. In the following discussion we will be interested in the four quantities:

$$\begin{aligned} \Delta_{ui}^{+,kl} &= \frac{1}{r_{kl} + \delta^{(0),kl}} \frac{1}{2} \sum_{D=2,4,6,\dots} (\delta_{ui,V}^{(D),kl} + \delta_{ui,A}^{(D),kl}) \\ \Delta_{ui}^{-,kl} &= \frac{1}{r_{kl} + \delta^{(0),kl}} \frac{1}{2} \sum_{D=2,4,6,\dots} (\delta_{ui,V}^{(D),kl} - \delta_{ui,A}^{(D),kl}), \end{aligned} \quad (5.46)$$

with  $i = d$  or  $s$ .

**Spectral functions** Much effort has been devoted to obtain values for the non-perturbative condensates in the  $VV - AA$  channel employing different weighted sum rules based on the vector and axial hadronic spectral functions extracted from hadronic tau decay data (see e.g. [66–68]). In our case, this analysis would involve the parameter  $\epsilon_{\text{ns}}$ , too. In analogy with eq. (5.18) we can write the spectral functions in the  $VV - AA$  channel as:

$$v(s) = \hat{v}(s) \quad (5.47)$$

$$a(s) = (1 + 4 \epsilon_{\text{ns}}) \hat{a}(s) \quad (5.48)$$

$$v(s) - a(s) = (1 + 2 \epsilon_{\text{ns}})(\hat{v}(s) - \hat{a}(s)) - 2 \epsilon_{\text{ns}}(\hat{v}(s) + \hat{a}(s)), \quad (5.49)$$

where the quantities with a hat represent again the quantities extracted from experiment assuming SM electroweak interactions, i.e., under the assumption  $\mathcal{V}_{\text{eff}} = -\mathcal{A}_{\text{eff}}$ . It is clear from eq. (5.49) that, although the difference between the vector and the axial current is measured rather precisely, this is only of limited usefulness in our case since we cannot easily disentangle electroweak ( $\epsilon_{\text{ns}}$ ) and QCD quantities ( $v(s), a(s)$ ). We shall mention in particular one point. The function  $v(s) - a(s)$  should vanish for sufficiently large values of  $s$ , when the perturbative regime is reached. This does not necessarily imply that  $\hat{v}(s) - \hat{a}(s)$  should vanish: for a nonzero value of  $\epsilon_{\text{ns}}$ , this difference is proportional to  $\epsilon_{\text{ns}}(v(s) + a(s))$ . The expected values for  $\epsilon_{\text{ns}}$  are, however, much too small for this remark to be relevant for the discussion of quark-hadron duality violations at the tau mass scale from the ALEPH and OPAL data.

**Non-strange sector** Let us begin the discussion with the non-strange sector. The only parameter involved in that case is  $\epsilon_{\text{ns}}$ . Indeed since we are only considering tree-level charged current processes, the non-strange sector will not furnish us any information on the parameter  $\epsilon_s$  describing RHCs involving strange quarks. Furthermore, since  $|\mathcal{V}_{\text{eff}}^{ud}|^2$  can be determined rather precisely from superallowed beta decays, the parameter  $\delta$  does not appear, either, see eq. (3.15).

(i)  $VV + AA$ .

We will first discuss the  $VV + AA$  channel because the total non-strange rate  $R_{\tau, V+A}$  and the corresponding moments are more easily accessible experimentally than the separate quantities in the vector and the axial channel and it is generally assumed that in the  $VV + AA$  channel the non-perturbative contributions are extremely small, of the order of  $10^{-3}$ . This is based on the following theoretical consideration. Since in the non-strange sector the contributions proportional to light quark masses are negligible, the dominant non-perturbative contribution arises from  $D = 6$  condensates. In the large- $N_c$  limit, these condensates factorize.<sup>13</sup> In the  $VV + AA$  channel the large- $N_c$  result should be rather reliable, because it does not involve any order parameter of chiral symmetry breaking. In this case the contribution of the  $D = 6$  condensates in the  $VV + AA$  channel remains small due to a partial cancellation between the vector

---

<sup>13</sup>Employing the large  $N_c$  argument, the factorized expression in ref. [62] should be multiplied by a factor  $(N_c^2 - 1)/N_c^2 = 8/9$ .

and axial channel. A fit to the data presented by the ALEPH collaboration, seems to confirm the small value [59]. It should, however, be stressed that the theoretical argument is essentially based on prejudices and that the fit to the data has been done assuming SM weak interactions. We do not have any firm knowledge about the exact value of the non-perturbative contributions.

We can, of course, perform a combined fit to the data, trying to determine the QCD part and  $\epsilon_{\text{ns}}$  at the same time. Before discussing this option in more detail, it is instructive to have a closer look at the expression for the decay rate in the  $VV + AA$  channel. To first order in  $\epsilon_{\text{ns}}$  we obtain:

$$\begin{aligned} R_{\tau, V+A} &= 3 S_{EW} |\mathcal{V}_{eff}^{ud}|^2 \left(1 + \delta^{(0)}\right) \left(1 - 2\epsilon_{\text{ns}}\right) \left(1 + \Delta_{ud}^+\right) \\ &\approx 3 S_{EW} |\mathcal{V}_{eff}^{ud}|^2 \left(1 + \delta^{(0)}\right) \left(1 - 2\epsilon_{\text{ns}} + \Delta_{ud}^+\right), \end{aligned} \quad (5.50)$$

where we have neglected in the last line products of  $\epsilon_{\text{ns}}$  with the non-perturbative contributions  $\Delta_{ud}^{+,kl}$  which should be at most of the order of  $10^{-4}$ . In the absence of non-standard electroweak interactions, the above relation determines the value of  $\alpha_s(m_\tau)$  rather precisely since the non-perturbative contribution,  $\Delta_{ud}^+$ , is presumably very small. On the contrary, allowing for a coupling of right-handed quarks to  $W$ , we clearly see the strong correlation between the extracted value of  $\alpha_s(m_\tau)$  and  $\epsilon_{\text{ns}}$  (assuming that the non-perturbative part is indeed small). Similar conclusions can be drawn for the corresponding moments in the  $VV + AA$  channel, which can be written in essentially the same way as eq. (5.50).

(ii) Ratio of axial and vector channel.

Another possible way to extract the value of  $\epsilon_{\text{ns}}$  is to combine measured quantities in the vector and the axial channels. This is, however, less favorable than in the  $VV + AA$  channel for a theoretical and an experimental reason.

- Let us look at the ratio of the decay rate in the axial and in the vector channel which reads to first order in  $\epsilon_{\text{ns}}$ :

$$\frac{R_{\tau, A}}{R_{\tau, V}} = \frac{1 + \Delta_{ud}^+ - \Delta_{ud}^-}{1 + \Delta_{ud}^+ + \Delta_{ud}^-} (1 - 4\epsilon_{\text{ns}}) \approx (1 - 2\Delta_{ud}^- - 4\epsilon_{\text{ns}}). \quad (5.51)$$

We have again neglected products of  $\epsilon_{\text{ns}}$  with the non-perturbative contributions  $\Delta_{ud}^{+/-}$  which should be of the order of  $10^{-4}$ . Note that the purely perturbative contribution cancels in this ratio. It measures the combination  $4\epsilon_{\text{ns}} + 2\Delta_{ud}^-$ . The latter describes non-perturbative contributions in the  $VV - AA$  channel. Since the corresponding correlator represents an order parameter of chiral symmetry breaking, corrections to the large- $N_c$  limit are expected to be large [69, 70]. Present estimates give values of the order of  $\Delta_{ud}^- \approx 10^{-2}$ , thus of the same order as the expected effect of  $\epsilon_{\text{ns}}$ .  $\Delta_{ud}^-$  should therefore be known to a very high precision in order to extract the value of  $\epsilon_{\text{ns}}$ . The same argument applies to all

quantities involving separately the vector and the axial channel: the determination of  $\epsilon_{\text{ns}}$  from these quantities is strongly correlated with the determination of non-perturbative contributions in the  $VV - AA$  channel, in particular the  $D = 6$  condensates.

- Experimentally for some decay channels, in particular those involving kaons, it is not easy to disentangle vector and axial channel, such that the data are correlated [60, 61, 59] and subject to larger uncertainties.

(iii) Fits.

We can certainly try to infer the value of the non-perturbative contributions from a combined fit of these QCD quantities together with  $\epsilon_{\text{ns}}$  to tau decay data in the non-strange sector including  $R_{\tau,V}, R_{\tau,A}$  and the different measured spectral moments, see eq. (5.44). Of course, we cannot pretend to determine within these fits the QCD parameters reliably enough to be able to disentangle really quantitatively non-standard EW couplings of quarks to  $W$  of the order of percent. In addition, as already mentioned, the extracted value of  $\epsilon_{\text{ns}}$  will be strongly correlated with the QCD parameters. The analysis is nevertheless worth doing in order to show that no inconsistencies appear. We use the data provided by the OPAL collaboration for the total rate  $R_{\tau,V+A}$  and the spectral moments, see eq. (5.44),  $R_{\tau,V+A}^{ij}$  with  $(i, j) \in \{(1, 0), (1, 1), (1, 2), (1, 3), (2, 0), (2, 1), (3, 0), (4, 0)\}$  [60, 61] as well as the rates  $R_{\tau,V/A}$  and the spectral moments for axial and vector channel,  $R_{\tau,V/A}^{ij}$  with  $(i, j) \in \{(1, 0), (1, 1), (1, 2), (1, 3)\}$  [60]. A crosscheck with the ALEPH data is at the moment not possible because the experimental correlations between the vector and the axial channel necessary to perform the combined fit are at present not available. Our fits should thus primarily be seen as an illustration of the possibilities offered by the analysis of tau decay data, awaiting some details about the ALEPH data and more data from the B-factories.

Our assumptions for the theoretical description of the QCD part are as follows.

- To evaluate the purely perturbative part, we employ two different prescriptions, fixed order perturbation theory (FOPT) and contour improved perturbation theory (CIPT). We go up to the order  $\alpha_s^6$  [63, 58]. In the former case the series does not converge fast and it involves unknown coefficients already at order  $\alpha_s^4$ . We follow ref. [58] for the unknown coefficients of  $\mathcal{O}(\alpha_s^4)$ ,  $\mathcal{O}(\alpha_s^5)$ , and  $\mathcal{O}(\alpha_s^6)$  assuming a geometric growth for  $\mathcal{O}(\alpha_s^5, \alpha_s^6)$ , see appendix B. The latter method allows to partially resum higher order logarithmic contributions and it improves the convergence of the perturbative series. It should thus in principle be more reliable (see also the discussion in ref. [72]).
- In the non-strange channel, the  $D = 2$  contribution is completely negligible, since it is suppressed as  $m_{u/d}^2/M_\tau^2$ . For simplicity we therefore take  $m_u = m_d = 0$ . In this limit the  $D = 4$  contribution contains only terms proportional to  $m_s \langle \bar{s}s \rangle$  and to the gluon condensate,  $\langle \alpha_s / \pi G G \rangle$ . The contribution of the

latter to the total rate is very small, since it is suppressed as  $\alpha_s(m_\tau)^2$ , but for different moments, it enters with an  $\mathcal{O}(1)$  coefficient. The value of the quark condensate is fixed using the Gell-Mann-Oakes-Renner (GMOR) relation namely  $-m_s \langle \bar{s}s \rangle = F_K^2 m_K^2$ , whereas our theoretical knowledge about the value of the gluon condensate is rather poor. On the classical level it can be shown that it should be positive, but quantum corrections could obstruct this result. Since it is not protected by any symmetry, it is even not really well defined because of ambiguities arising from additive corrections. Present determinations from tau decay data give values of the order  $|\langle \alpha_s/\pi GG \rangle| \sim 0.01 \text{ GeV}^4$  or smaller with large errors [58, 60]. In particular, the determinations from the different channels do not always agree. Other phenomenological determinations, e.g. from different QCD sum rules (see for instance [73, 74]) give values of the same order, subject to large errors, too. Most determinations give  $\langle \frac{\alpha_s}{\pi} GG \rangle > 0$ . The most natural thing to do in this case is to include the gluon condensate as free parameter into the fit. But, this will induce large errors because due to the large correlations discussed above, the fits are not sensitive to many different non-perturbative parameters.

- Concerning the  $D = 6$  contribution, we have employed different prescriptions in the  $VV + AA$  and the  $VV - AA$  channel. For the former we take the factorized expression with  $\langle \bar{q}q \rangle = -(270 \text{ MeV})^3$ . The latter value can be motivated taking the GMOR relation and a reasonable value for the strange quark mass. As is clear from the above discussion, due to a partial cancellation between the vector and the axial part, the  $D = 6$  contribution remains small if we use the factorized expression, such that the precise value of the quark condensate is not important for our analysis in this case. In the  $VV - AA$  channel we parametrize the  $D = 6$  contribution with two parameters  $a_{6,V-A}$  and  $b_{6,V-A}$  (see for example ref. [66] for an explanation of the notation as well as for the relation between these parameters and the expectation values of the corresponding operators which are known for  $D = 6$ ). For  $D = 8, 10$  we include only two parameters  $a_{8,V+A}$ ,  $a_{8,V-A}$ , and  $a_{10,V+A}$ ,  $a_{10,V-A}$ . In the  $VV - AA$  channel different analysis employing sum rules based on the vector and axial spectral functions extracted from tau decay data show that non-perturbative contributions for  $D > 10$  can in principle be important (see e.g. ref. [66, 67]). We refrained from including higher order condensates, since, in particular in the  $VV + AA$  channel, with the given data, the sensitivity of the fits to these contributions is very low.

We obtain good fits to the data, and the results of all fits are compatible. In particular, the values for the non-perturbative parameters are perfectly compatible within errors between the  $V/A$  fits and the  $VV + AA$  fits. This is not the case for the fits assuming SM weak interactions presented by the experimental collaborations [59, 60]. But, as already anticipated, the fits are not sensitive to the many unknown non-perturbative coefficients. Especially the value of the gluon condensate induces a large error, which makes a really quantitative determination of  $\epsilon_{\text{ns}}$  difficult. This is

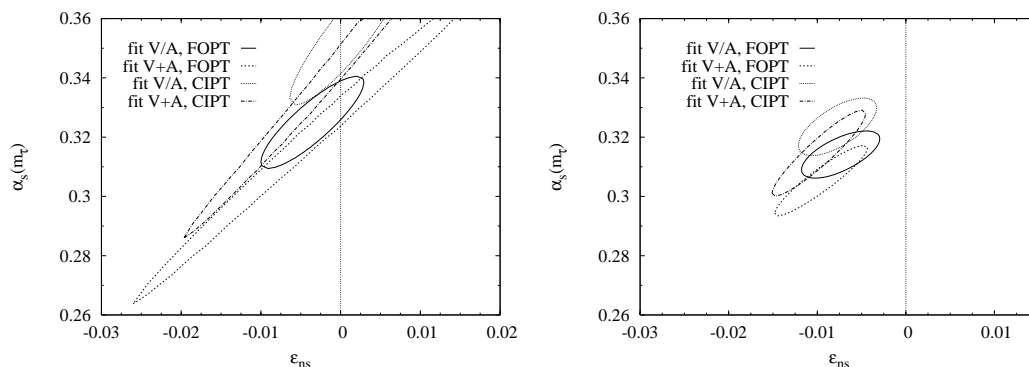


**Figure 11:** One-sigma contours for the extraction of  $\alpha_s(m_\tau)$  and  $\epsilon_{ns}$  from the  $VV + AA$  and  $V/A$  channel. Data are from the OPAL collaboration [60, 61]. Left: Result including the gluon condensate as fit parameter, right: fixing the value of the gluon condensate at  $\langle \frac{\alpha_s}{\pi} GG \rangle = 0$ .

reflected in the elongated  $1\sigma$  contours which we show as a function of  $\epsilon_{ns}$  and  $\alpha_s(m_\tau)$  in figure 11, left panel. Fixing the gluon condensate at some value, the result is much better determined, see figure 11, right panel, where we show as an example the result with  $\langle \frac{\alpha_s}{\pi} GG \rangle = 0$ . Increasing the value for  $\langle \frac{\alpha_s}{\pi} GG \rangle$  shifts the ellipses in direction of smaller values for  $\epsilon_{ns}$  and  $\alpha_s(m_\tau)$ , whereas upon decreasing the value of  $\langle \frac{\alpha_s}{\pi} GG \rangle$  shifts the ellipses towards higher values of  $\epsilon_{ns}$  and  $\alpha_s(m_\tau)$ . Another important effect already anticipated from the discussion of eq. (5.50) is obvious: the extracted value of  $\epsilon_{ns}$  is strongly correlated with that of  $\alpha_s(m_\tau)$ , see figure 11. Vice versa, this implies that the determination of  $\alpha_s(m_\tau)$  from hadronic  $\tau$  decay data depends on the assumptions made for the electroweak charged current interaction. It can be observed that the CIPT fits give slightly larger values of  $\alpha_s(m_\tau)$  than the FOPT fits. The same effect has already been seen in the determinations of  $\alpha_s(m_\tau)$  from hadronic tau decay data assuming SM weak interactions [58, 60]. In general, our values for  $\alpha_s(m_\tau)$  are smaller than those obtained assuming SM couplings of quarks to  $W$ , if  $\epsilon_{ns} < 0$  and larger if  $\epsilon_{ns} > 0$  in agreement with eq. (5.50).

Another source of uncertainty concerning these results should be mentioned. The quantitative outcome of our fits is rather sensitive to the treatment of the perturbative part. Assigning an error of 100% to the unknown perturbative coefficients of  $\mathcal{O}(\alpha_s^4)$ ,  $\mathcal{O}(\alpha_s^5)$ ,  $\mathcal{O}(\alpha_s^6)$  the central value of  $\alpha_s(m_\tau)$  changes by  $\sim 0.1$ . For the fits employing FOPT the change is even more pronounced if we cut the perturbative expansion at lower orders in  $\alpha_s$ . The ellipses are then shifted towards larger values for  $\epsilon_{ns}$  and  $\alpha_s(m_\tau)$ .

We should of course ask, can we improve on the precision, using input on the QCD parameters, for example  $\alpha_s(m_\tau)$ , from other sources? There are many different ways to determine the value of  $\alpha_s$  (cf. for example, ref. [75]). The most precise determinations, at the  $Z$ -pole and from tau decay data, depend on electroweak physics, see also section 4. There are determinations of  $\alpha_s$ , for instance from jet and event-shape

observables, which do not suffer from this drawback. Unfortunately, the precision reached, in particular for the determinations which do not depend on electroweak physics, is not high enough to further limit the range and increase the precision on  $\epsilon_{\text{ns}}$ .

Our conclusion is that presently the uncertainties are such that the analysis of tau decay data in the non-strange channel does not allow us to determine  $\epsilon_{\text{ns}}$  quantitatively. All that can be said is good fits are obtained for values of roughly  $-0.02 \lesssim \epsilon_{\text{ns}} \lesssim 0.02$ . These values are perfectly in agreement with the order of magnitude estimates from the LEET.

**Strange sector.** Recently a lot of work (see for instance refs. [76, 77]), assuming the absence of RHCs, has been devoted to the extraction of  $V_{us}$  and  $m_s$  from Cabbibo suppressed tau decays. The main quantity in this context is [78, 79]

$$\delta R_\tau = \frac{R_{\tau,V+A}}{|V_{ud}|^2} - \frac{R_{\tau,S}}{|V_{us}|^2} . \quad (5.52)$$

This quantity vanishes in the SU(3) flavor limit such that theoretical uncertainties are reduced. In the presence of RHCs,  $\delta R_\tau$  cannot be properly normalized since the couplings in the axial and vector channel are no longer the same and in the strange sector, the vector and axial parts cannot be separated experimentally. Instead, we will look at the ratio of the strange and the non-strange contribution. It can be written to first order in the spurionic parameters as:

$$\frac{R_{\tau,S}}{R_{\tau,V+A}} = \frac{\sin^2 \hat{\theta}}{\cos^2 \hat{\theta}} \left( 1 + 2 \frac{\epsilon_{\text{ns}} + \delta}{\sin^2 \hat{\theta}} \right) (1 + \Delta_{us}^+ - \Delta_{ud}^+) \quad (5.53)$$

where again we have neglected terms of the form  $\epsilon_{\text{ns}} \Delta_{ud}^-$  and  $\epsilon_s \Delta_{us}^-$ , which are of the order  $10^{-4}$ . Contrary to what one would naively expect, this ratio is in fact independent of  $\epsilon_s$  precisely due to the fact that this quantity only enters together with  $\Delta_{us}^-$ . Note that the hadronic part of this ratio contains the same SU(3) breaking quantity as  $\delta R_\tau$  within the SM.

The QCD corrections in this case are dominated by the mass corrections to  $\Delta_{us}^+$  which are proportional to  $m_s^2(m_\tau)/m_\tau^2$ . Unfortunately, the perturbative series for the Wilson coefficient of the  $D = 2$  term proportional to  $m_s^2(m_\tau)/m_\tau^2$  converges badly [80], such that there are large theoretical uncertainties concerning this coefficient. In the literature one can find different attempts to cure this problem. One possibility is to try to improve on the convergence of the series, for instance by employing contour improved perturbation theory instead of fixed order perturbation theory. More phenomenologically, one can replace the OPE by a direct integration of a (model dependent) parametrization of the hadronic spectral function [81, 82] to better determine the non-perturbative contributions in the strange sector (cf. the discussion in ref. [58]). Including sub-leading  $D = 4$  corrections [62] involving in particular terms proportional to  $m_s^4(m_\tau)/m_\tau^4$  and  $(m_s \langle \bar{s}s \rangle - m_d \langle \bar{d}d \rangle)/m_\tau^4$  values for  $\Delta_{us}^+$  in the literature are in the range  $-0.06$  to  $-0.15$  depending on the value of the strange quark mass. The range given here corresponds to varying  $m_s$  from 80 to 200 MeV.



Since  $r_s = R_{\tau,S}/R_{\tau,V+A} \cos^2 \hat{\theta} / \sin^2 \hat{\theta}$  is of the order one and the hadronic correction  $\Delta_{us}^+ - \Delta_{ud}^+$  is at most on the 10 percent level, the above equation is rather sensitive to  $\epsilon_{\text{ns}} + \delta$  (remember that  $1/\sin^2 \hat{\theta}$  is about 20). Let us now be more specific: what does eq. (5.53) tell us about the value of  $\epsilon_{\text{ns}} + \delta$ ? With the ALEPH data [59] we obtain  $r_s = 0.84 \pm 0.03$  and with the OPAL data [61]  $r_s = 0.89 \pm 0.01$ . This value has to be compared with the possible values of  $\epsilon_{\text{ns}} + \delta$  and the QCD corrections. We have seen previously that the latter are not well determined and that in addition, the strange quark mass is also not well known. Thus, a precise determination of  $\epsilon_{\text{ns}} + \delta$  is at present not possible. However we can have an estimation of its order of magnitude by comparing different prescriptions for the calculation of the  $D = 2$  Wilson coefficient and varying  $m_s(m_\tau)$  between 60 and 250 MeV. This should be a conservative estimate for possible values of the strange quark mass.

- The first observation is that with the present estimates of  $\Delta_{us}^-$  we need rather large values for the strange quark mass ( $m_s(m_\tau) \sim 150 - 200$  MeV) if we impose  $\delta + \epsilon_{\text{ns}} = 0$ , i.e. in the SM case. This is consistent with the finding that  $V_{us}$  should be somewhat smaller than the value obtained from unitarity with values of  $m_s$  of the order of 95 MeV (cf. for instance [82]).
- The second observation is that, for not too large values of the strange quark mass, the extracted value of  $\delta + \epsilon_{\text{ns}}$  lies between roughly -0.005 and 0.005 whatever method used. This indicates that  $\delta + \epsilon_{\text{ns}}$  should be below 1%.

In principle it is possible to exploit experimental information on the moments  $R_{\tau,S}^{kl}/R_{\tau,V+A}^{kl}$ . But without any further independent information on the QCD corrections, this will not determine  $\delta + \epsilon_{\text{ns}}$  more precisely.

## 6. Discussion

Let us now compare the different sources of information we have on the different parameters. One of our main results is that, apart from  $K_{\mu 3}^L$  decays, discussed in section 5.1.4, it is difficult to find any other clean manifestation of RHCs due to the parameter  $\epsilon_s$ , the only parameter which can be larger than the genuine spurion parameter  $\epsilon$ . In particular, the data on hadronic tau decays in the strange sector are not, in contrast to naive expectations, sensitive to  $\epsilon_s$ . The data by the NA48 collaboration [49] on  $K_{\mu 3}^L$  decays indicate indeed an enhancement of  $\epsilon_s$ , i.e. an inverted hierarchy for the flavor mixing of right-handed quarks.

One remark of caution is in order here: much of the numerology discussed within this section depends on the value of  $|\mathcal{V}_{eff}^{ud}| = \cos \hat{\theta}$ . We took the value (see eq. 5.7) from  $0^+ \rightarrow 0^+$  nuclear beta decays. This is by far the most precise one: the error is about one order of magnitude smaller than the error on the alternative determinations from pion and neutron beta decays (cf. for instance ref. [83]). We should nevertheless keep in mind that a change in the value of  $|\mathcal{V}_{eff}^{ud}|$  affects the numbers in particular for the hatted quantities.

The result for the value of  $\epsilon_s - \epsilon_{\text{ns}}$  discussed in section 5.1.4 has another interesting application. From eqs. (5.17), (5.18) we see that the two quantities  $f_+^{K^0\pi^-}(0)$  and  $F_{K^+}/F_{\pi^+}$  depend on the same two combinations of spurion parameters:  $\delta + \epsilon_{\text{ns}}$  and  $\epsilon_s - \epsilon_{\text{ns}}$ . Their

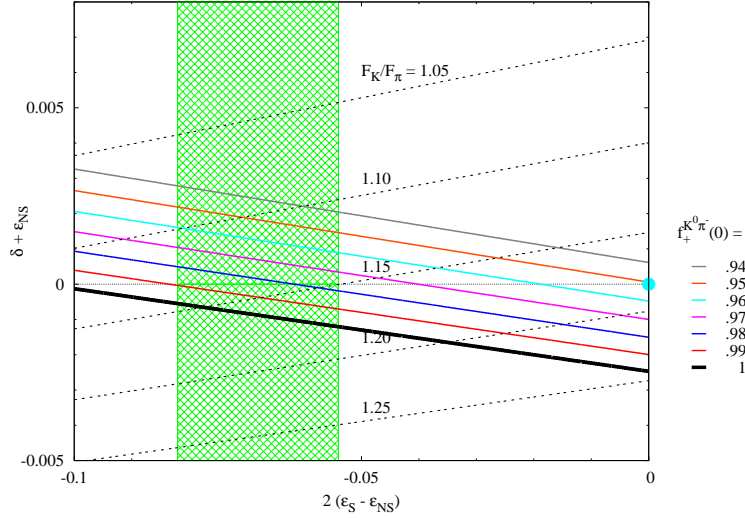


**Figure 12:** Lines of constant values for  $F_{K^+}/F_{\pi^+}$  and  $f_+^{K^0\pi}(0)$  in the plane  $\delta + \epsilon_{NS}$  and  $2(\epsilon_S - \epsilon_{NS})$  as resulting from eqs. (5.17), (5.18). The vertical band indicates the range for  $\Delta\epsilon - \Delta_{CT}^{NLO}$  from the NA48 data [49].

values are therefore related. In figure 12 we display lines of constant values for  $f_+^{K^0\pi}(0)$  and  $F_{K^+}/F_{\pi^+}$  in the plane  $\delta + \epsilon_{NS}$  and  $2(\epsilon_S - \epsilon_{NS})$ . Both,  $f_+^{K^0\pi}(0)$  and  $F_{K^+}/F_{\pi^+}$  decrease with increasing  $\delta + \epsilon_{NS}$ , i.e. from bottom to top. We have indicated  $f_+^{K^0\pi}(0) = 1$  with a thick line since we expect this value to represent an upper bound [84]. In the large  $N_c$ -limit this bound becomes exact.<sup>14</sup> The shaded region indicates the determination of  $2(\epsilon_S - \epsilon_{NS})$  from the NA48 data [49] assuming  $\Delta_{CT} = \Delta_{CT}^{NLO}$ . Taking the upper bound for  $f_+^{K^0\pi}(0)$  seriously, this imposes in turn an upper bound on  $F_{K^+}/F_{\pi^+} < 1.19$ . If we assume the recent determination of  $f_+(0) = 0.9680(16)$  from lattice simulations [85] we obtain an even smaller value,  $F_{K^+}/F_{\pi^+} = 1.12(2)$ . The isospin breaking corrections relating  $F_{K^+}/F_{\pi^+}$  to the value of  $F_K/F_\pi$  conventionally used in ChPT are presumably very small.

One interesting point should be mentioned. The ChPT prediction [7] for the slope of the scalar  $K\pi$  form factor depends strongly on the value of  $F_K/F_\pi$ . Taking the values for  $F_K/F_\pi$  discussed above, the ChPT prediction is in agreement with the values for the slope from NA48 [49] and KTeV [86], i.e., the ChPT prediction is in complete agreement with our findings.

Note that the effect of  $\delta + \epsilon_{NS}$  is enhanced in the relations, eqs. (5.17), (5.18), because of the factor  $1/\sin^2 \hat{\theta}$ . We therefore expect  $\delta + \epsilon_{NS}$  to remain well below 1%. This is consistent with the finding from the hadronic tau decays in the strange sector: for reasonable strange quark masses,  $\delta + \epsilon_{NS}$  does not exceed half a percent in this case, see section 5.3.3.

We have another indication that  $\delta + \epsilon_{NS}$  should be small. To that end let us look at the sum of the elements of the effective mixing matrix,  $\mathcal{V}_{eff}^{ud}$  and  $\mathcal{V}_{eff}^{us}$ , squared, see eq. (5.11).

<sup>14</sup>In the real world, a small violation of the large  $N_c$  bound  $f_+(0) < 1$  is conceivable due to light quark loops inducing exotic multi-meson contributions to the current algebra sum rule for  $f_+(0)$ .

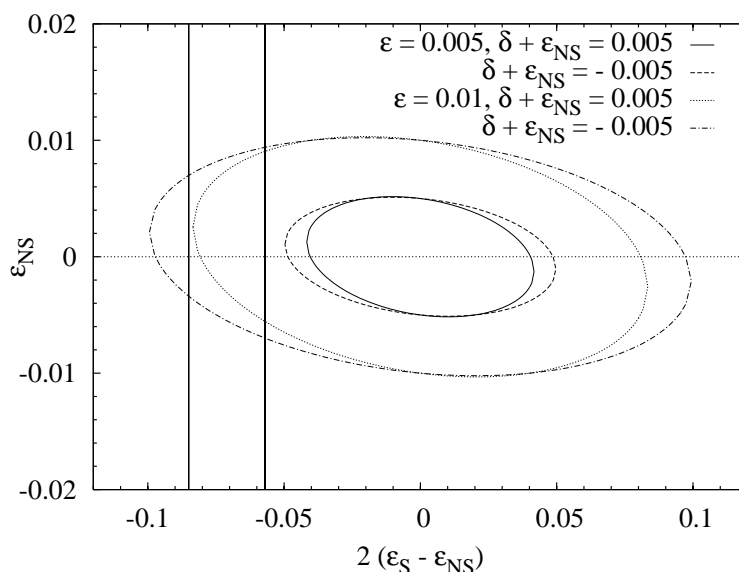


**Figure 13:** Maximum values of  $\epsilon_{\text{ns}}$  and  $\epsilon_s - \epsilon_{\text{ns}}$  compatible with the unitarity of  $V_{L,R}$ , cf. eq. (5.10), for two different values of  $\epsilon$  and  $\delta + \epsilon_{\text{ns}}$ . The vertical lines indicate the range for  $2(\epsilon_s - \epsilon_{\text{ns}})$  from the NA48 data [49] with  $\Delta_{\text{CT}} = \Delta_{\text{CT}}^{\text{NLO}}$ .

Inserting the NA48 value for  $\epsilon_s - \epsilon_{\text{ns}}$  with  $\Delta_{\text{CT}} = \Delta_{\text{CT}}^{\text{NLO}}$  into the second term of eq. (5.30), the latter equation can be rewritten as

$$|\mathcal{V}_{\text{eff}}^{ud}|^2 + |\mathcal{V}_{\text{eff}}^{us}|^2 = 1 - 0.0036(7) + 2(\delta + \epsilon_{\text{ns}}) . \quad (6.1)$$

We can now look at different instructive examples. If  $\mathcal{V}_{\text{eff}}$  was unitary, the left hand side of eq. (6.1) would be equal to one and  $(\delta + \epsilon_{\text{ns}}) = 0.0018(4)$ . Considering the recent theoretical evaluations of  $f_+^{K^0\pi^-}(0)$ , the left-hand side of eq. (6.1) is indeed very close to one. To be more precise, with the lattice result [85]  $f_+(0) = 0.9680(16)$  we have  $\delta + \epsilon_{\text{ns}} = 0.0008(5)$  and with the two-loop ChPT evaluation [87, 88],  $f_+^{K^0\pi^-}(0) = 0.984(12)$ , we obtain  $\delta + \epsilon_{\text{ns}} = 0. \pm 0.0007$ . This indeed indicates that  $\delta + \epsilon_{\text{ns}}$  is probably very small.

The determination of  $2(\epsilon_s - \epsilon_{\text{ns}})$  from  $K_{\mu 3}^L$  decays, see section 5.1.4, has an impact on the bounds on the spurion parameters we obtain from the unitarity condition of the mixing matrices  $V_{L,R}$ . In figure 13 we show the ellipses giving the maximum values for  $\epsilon_{\text{ns}}$  and  $\epsilon_s - \epsilon_{\text{ns}}$  compatible with unitarity of the mixing matrices, eq. (5.10) for two different values of  $\epsilon$  and  $\delta + \epsilon_{\text{ns}}$ . The vertical lines thereby indicate the range for  $2(\epsilon_s - \epsilon_{\text{ns}})$  from the NA48 data [49] with  $\Delta_{\text{CT}} = \Delta_{\text{CT}}^{\text{NLO}}$ . Note, that in contrast to figure 9, we show here absolute values choosing two values of  $\epsilon$ . Given a determination of  $\epsilon_s - \epsilon_{\text{ns}}$  we can thus obtain two informations. First, for too small values of  $\epsilon$ , there are no parameter values compatible with the unitarity of the mixing matrices and the range of allowed values for  $\epsilon_s - \epsilon_{\text{ns}}$  at the same time. Thus we obtain a lower bound on  $|\epsilon|$  which is for the NA48 data,  $\epsilon \gtrsim 0.006$ . Second, once  $\epsilon$  is fixed,  $\epsilon_{\text{ns}}$  is constrained. As an example, for  $\epsilon = 0.01$  the NA48 data indicate  $-0.007 \lesssim \epsilon_{\text{ns}} \lesssim 0.009$  for  $\delta + \epsilon_{\text{ns}} = -0.005$ . These values are perfectly

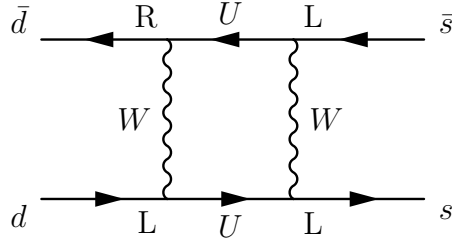


**Figure 14:** Box diagram contributing to the  $\Delta F = 2$  effective interaction with one insertion of a right-handed vertex.

compatible with the results from the analysis of tau decay data.

## 7. Other possible tests

Within this section we would like to discuss some other possible tests. A quantitative exploitation of these tests is beyond the scope of the present paper but should be considered as prospect for future work.

### 7.1 NLO analysis: hyperon decays and heavy quark sector

In the right-handed sector, in addition to the genuine spurion parameters, the quark mixing matrix elements have to be determined. For the moment, we have only considered the light quark sector. There, the parameter  $\epsilon_s$  can be enhanced, if  $V_R^{us}$  is enhanced with respect to  $V_L^{us}$ . We should therefore look for processes where  $\epsilon_s$  enters. In principle, we can have sizable effects due to  $\epsilon_s$  in hyperon decays. Recently an experimental effort has been undertaken to improve the precision on the data (cf. e.g. [89]). From the theoretical side, however, the SU(3) breaking effects are not yet under quantitative control. This constitutes a severe limitation to the precision attainable in the analysis of hyperon decays [90].

Evidently, we will have to explore the heavy quark sector looking for tests of  $V + A$  interactions. There exists already some work in this direction (cf. e.g. [91]), but for the moment the effective theories used in the heavy quark sector have not reached sufficient accuracy to determine the electroweak parameters precisely.

We should therefore look for processes where, as in  $K_{\mu 3}^L$  decays, the hadronic part is well controlled (by symmetry considerations). Since the Callan-Treiman theorem is based on  $SU(2) \times SU(2)$  chiral symmetry, it can be applied not only to the  $K\pi$  scalar form factor but to scalar form factors involving heavy quarks, too, for instance the  $D\pi$  scalar form factor. It could thus be measured in  $D_{\mu 3}$  decays. In this case the kinematics is very different: because  $m_D \gg m_\pi$ , the endpoint of the physical region,  $(m_D - m_\pi)^2 = 2.98 \text{ GeV}^2$ , the Callan-Treiman point,  $m_D^2 - m_\pi^2 = 3.46 \text{ GeV}^2$ , and the threshold for  $D\pi$  scattering,  $(m_D + m_\pi)^2 = 4.02 \text{ GeV}^2$  are very close together. At present, it does not seem very promising to exploit the Callan-Treiman theorem in  $D$  decays in the same way as we did in  $K$  decays because the actually available experimental data on  $D_{l3}$  decays are not as precise as for the  $K_{l3}$  decays. In addition, it is still not possible at the moment to extract  $D\pi$

phase shifts which are crucial to establish the dispersive representation of the form factor allowing to extrapolate the data in the physical region of  $D_{\mu 3}$  decays to the Callan-Treiman point.

The decay  $t \rightarrow Wb$  is a very promising process to directly access the chirality of the  $\bar{t}W$  coupling measuring the  $W$  polarisation. There has been a first pioneering attempt from Tevatron [92]. At present the uncertainties are too large to disentangle a small admixture of RHCs, but hopefully there will be more data from LHC, which will start to operate soon.

It has been further observed that a coupling of right-handed quarks to  $W$  would alter the chiral structure of the  $\mathcal{O}(p^2)$  tree-level effective weak Hamiltonian, and, in combination with soft-pion theorems, bounds on right-handed couplings can be derived, for example, from  $K \rightarrow \pi\pi$ ,  $K \rightarrow \pi\pi\pi$  decays [93]. Unfortunately,  $\mathcal{O}(p^4)$  chiral corrections, in particular long distance loop corrections and final state interaction can be rather important and can upset small  $\mathcal{O}(p^2)$  effects.

Note that at the present order no significant modifications of the muon ( $g - 2$ ) arise. First, no additional contributions arise within the LEET at this order since charged right-handed currents in the lepton sector are absent. Second, the Higgs contribution within the SM is several orders of magnitude smaller than the dominant contributions, such that the absence of this contribution in the LEET does not change the conclusions.

## 7.2 Loop effects: flavor changing neutral current processes and CP violation

Flavor changing neutral current (FCNC) processes can give stringent limits on new physics contributions because the SM contributions are generally very small due to the GIM mechanism. Constraints arising on couplings of right-handed quarks to  $W$  have been considered in this context already for a long time within left-right symmetric models. The strongest constraint in this case comes from  $K^0 - \bar{K}^0$  mixing [94]. Interesting constraints can come from the (rare)  $B$  meson decay processes, too, for which recently a large amount of new data has become available from the B-factories. A very prominent example is here the radiative decay  $b \rightarrow s\gamma$  [95].

It is clear that a comprehensive analysis of FCNC processes within the LEET merits to be performed, but is beyond the scope of the present paper. Here we only want to stress what the systematic power counting of the LEET tells us about the different contributions to FCNC processes and their respective suppression. Let us consider the box diagram contribution to  $\bar{s}d \rightarrow \bar{d}s$  shown in figure 14. Following the generalized Weinberg power counting, see eqs. (2.5), (2.55), the dominant SM contribution counts as  $d^* = 4$ , because there is one loop with only  $\mathcal{O}(p^2)$  vertices without any spurions. The diagrams with one insertion of a vertex  $\mathcal{O}(p^2 \xi^2)$  or  $\mathcal{O}(p^2 \eta^2)$  consequently count as  $d^* = 5$  and with two vertices  $\mathcal{O}(p^2 \xi^2)$  or  $\mathcal{O}(p^2 \eta^2)$  as  $d^* = 6$ . That means that contributions with one right-handed vertex, as shown in figure 14, have dimension  $d^* = 5$  and with two right-handed vertices they have dimension  $d^* = 6$ . At  $d^* = 6$  there are in addition contributions from diagrams with one vertex of dimension  $d_v = 4$  which is clearly beyond NLO, see eqs. (3.11), (3.12). In contrast to left-right symmetric models, where the dominant non-standard contribution arises from a  $W_R$ -boson exchange, we expect the dominant non-standard effect in the LEET

to show up at order  $d^* = 5$ , i.e., with only one insertion of a “non-standard” vertex. In addition, we have to keep in mind, that at each order new counter terms will arise<sup>15</sup> which have to be included in a quantitative analysis.

The non-standard contribution of order  $d^* = 5$ , which should a priori be the most important one, merits a further comment. In general, we expect that unusual operators, not considered in the SM and its extensions so far, appear in the effective four-fermion interaction. Let us consider as an example the box diagram shown in figure 14 which contributes to  $H_W^{\Delta S=2}$ , i.e., to  $K^0\text{-}\bar{K}^0$  mixing. Inserting the vertices from the Lagrangian at NLO, eq. (3.12), the leading contribution from this diagram is clearly of dimension  $d^* = 5$  since we have three (left-handed)  $\mathcal{O}(p^2)$  vertices and one (right-handed)  $\mathcal{O}(p^2 \eta^2)$  vertex. We find, for instance, the following type of four-fermion operator

$$i\epsilon \frac{m_{u_i}}{m_W^2} \bar{s}_R \sigma^{\alpha\tau} d_L \bar{s}_L \gamma_\tau \partial_\alpha d_L \quad (7.1)$$

and the corresponding permutations. The factor  $\epsilon$  reflects the spurion suppression. Note that there is an additional suppression from the derivative which appears because of Lorentz invariance. Apart from the power counting arguments, inherent to the LEET, we can at present give no more quantitative estimate of the actual numerical value of the non-standard contributions to FCNC processes.

Our analysis concerns only the real part of the mixing matrix elements in the light quark sector. The constraints on the phases, for example from the electric dipole moment of the neutron, have to be considered separately.

## 8. Summary and conclusion

An effective theory framework is a very elegant and efficient way to treat effects beyond the SM without relying on a specific model. The basis of the present work is a “not-quite decoupling” alternative to the usually applied decoupling effective theory framework. Within the not-quite decoupling LEET, the heavy particles adherent to an extended symmetry  $S_{nat} \supset S_{ew} = \text{SU}(2)_L \times \text{U}(1)_Y$  at high energies decouple, but the symmetry becomes partly non-linearly realised at low energies and constrains the effective interactions at low energies. The classification of the different operators is thereby based on infrared power counting. The symmetry  $S_{nat}$  can be inferred within this “bottom-up” approach from the requirement that at lowest order we want to recover the (higgsless) vertices of the SM and nothing else. We have worked with the minimal version of  $S_{nat} = [\text{SU}(2)]^4 \times \text{U}(1)^{B-L}$  fulfilling this requirement, which has been constructed in ref. [9–11].

This LEET predicts that a priori the most important effects beyond the SM are (universal) non-standard couplings of fermions to the gauge bosons  $W$  and  $Z$  appearing at NLO. From general arguments (see the discussion on that point in ref. [11]) these non-standard couplings are expected to be of the order of percent. The aim of this paper was

---

<sup>15</sup>In principle, four-fermion operators contributing to FCNC processes can be written at  $\mathcal{O}(p^2)$ . They are, however, dimensionally suppressed by a factor  $\Lambda^{-2}$ , where  $\Lambda \gg \Lambda_W$  is an energy scale exterior to the LEET, see the discussion in (v), section 2. Here we will limit the discussion to the operators generated within the LEET.

to perform a phenomenological analysis of these non-standard couplings. Let us summarize our results

- In the neutral current sector we obtain a good agreement with the  $Z$ -pole data. In particular, we can solve the long-standing  $A_{FB}^b$  puzzle without introducing non-universal effects in the couplings. The important point here is the NLO modification of the right-handed couplings. Also low-energy data such as atomic parity violation are well reproduced. There are only exceptional cases, when the LO + NLO contribution is accidentally small, where we fail to reproduce the data. One such example is the  $e^-e^-$  Møller scattering. For these cases it is particularly important to extend the analysis to higher orders.
- The most striking NLO effect is probably the direct coupling of right-handed quarks to  $W$ . We should emphasize here that due to an additional (discrete) symmetry in the lepton sector, intended to suppress the neutrino Dirac mass, there are no lepton right-handed charged currents. That means that many of the stringent tests on a right-handed  $W_R$  boson present in left-right symmetric extensions of the SM do not apply in our case. Due to quark confinement it is very difficult to establish a stringent test of quark couplings. We always face the problem that it is not easy to disentangle QCD from electroweak effects. This is most obvious in semileptonic decays. To determine the axial and vector effective EW couplings, one has to know the QCD parameters like decay constants and form factors and vice versa. The presence of right-handed charged quark currents implies that quark mixing is modified: we have to consider two (a priori independent) unitary mixing matrices,  $V_L$  and  $V_R$ . This means in particular that axial and vector couplings have to be considered independently.

We have focused on the light quark sector. There, one stringent test is conceivable. The Callan-Treiman low energy theorem allows for a very precise prediction for the value of the scalar  $K\pi$  form factor at the Callan-Treiman point with only a small hadronic correction,  $\Delta_{CT}$ . The first direct measurement of the form factor in  $K_{\mu 3}^L$  decays by the NA48 collaboration [49] indicates a  $5\sigma$  deviation with the SM prediction. It is hard to imagine that this deviation could be explained entirely as the deviation from the Callan-Treiman theorem. In this case the  $\mathcal{O}(p^4)$  ChPT calculation of  $\Delta_{CT}$  would have to be wrong by a factor of 20, i.e., there should be anomalously large higher order corrections. This deviation, can however, be explained by a direct coupling of right-handed quarks to  $W$  with a (partially) inverted mixing hierarchy in the right-handed sector. Within the LEET considered here, this explanation is unique. Before drawing any firm conclusion, this effect needs additional experimental verification.

The extracted values for the decay constants  $F_\pi$  and  $F_K/F_\pi$  from the decay rate  $\Gamma(\pi_{l2}(\gamma))$  and the branching ratio  $\text{Br}(K_{l2}(\gamma)/\pi_{l2}(\gamma))$ , which are needed as input for many ChPT calculations, are modified in the presence of RHCs. For instance, the value for  $F_K/F_\pi$  could be as low as  $\approx 1.12$  if we take the RHCs parameters from the scalar  $K\pi$  form factor. We should mention in this context, that the ChPT prediction

for the slope of the scalar  $K\pi$  form factor is in perfect agreement with the value from the NA48 measurement if the value of  $F_K/F_\pi$  is changed accordingly.

At the present order there are hardly any other sensitive tests. The analysis of hadronic tau decay data in the non-strange channel, for example, only indicates that the non-standard couplings stay on the percent level. A more precise determination seems not possible for the moment. In the strange channel the contribution from non-standard couplings is enforced due to the mixing hierarchy in the left-handed sector. Here, new data from the B-factories and an improved treatment of the QCD part in the near future can give interesting new results.

- Another consequence of the correlation between the values for the QCD and the EW parameters extracted from experiment, is that the sensitivity to  $\alpha_s$  is lost in the two processes furnishing up to now the most precise determination of the strong coupling constant: In the analysis of  $Z$ -pole data as well as in the analysis of hadronic tau decays, the additional EW parameters make a sensible extraction of the value of  $\alpha_s$  difficult.

To conclude, for the moment our analysis at NLO does not show any sign for an inconsistency of experimental data with the order by order LEET estimates. The values we obtained for the parameters are of the order of magnitude expected from the LEET. Of course, the higher order contributions should be investigated with care, especially in the charged current sector where stringent constraints on the coupling of right-handed quarks can arise from processes at NNLO.

## Acknowledgments

We would like to thank M. Antonelli, A. Ceccucci, M. Davier, S. Descotes-Genon, A. Djouadi, P. Franzini, J. Hirn, M. Knecht, H. Leutwyler, U.-G. Meißner, B. Moussallam, A. Pich, J. J. Sanz Cillero, M. Veltri, and R. Wanke for their interest, suggestions and help. We are grateful to D. Plane and S. Menke (OPAL collaboration) for providing us with the precise correlation matrix concerning the OPAL hadronic tau decay data. This work has been partially supported by EU contract MRTN-CT-2006-035482 (“Flavianet”) and the EU Integrated Infrastructure Initiative Hadron Physics (RH3-CT-2004-506078).

## A. Expressions for the $Z$ -pole observables

We will list here the expressions for the  $Z$ -pole observables in terms of the effective couplings up to NLO. The couplings discussed in section 3.1 can be rewritten in terms of effective couplings of left-handed fermions to  $Z$ ,

$$g_L^u = \frac{1+\delta}{2} - \frac{2}{3}\tilde{s}^2 \quad g_L^d = -\frac{1+\delta}{2} + \frac{1}{3}\tilde{s}^2 \quad g_L^e = -\frac{1}{2} + \tilde{s}^2 \quad g_L^\nu = \frac{1}{2}, \quad (\text{A.1})$$

and effective couplings of right-handed fermions to  $Z$

$$g_R^u = -\frac{2}{3}\tilde{s}^2 + \frac{\epsilon^u}{2} \quad g_R^d = \frac{1}{3}\tilde{s}^2 - \frac{\epsilon^d}{2} \quad g_R^e = \tilde{s}^2 - \frac{\epsilon^e}{2} \quad g_R^\nu = \frac{\epsilon^\nu}{2}. \quad (\text{A.2})$$



The corresponding effective couplings for vector and axial channel are obtained from  $g_A^f = g_L^f - g_R^f, g_V^f = g_L^f + g_R^f$ . This gives

$$g_V^u = \frac{1+\delta}{2} - \frac{4}{3}\tilde{s}^2 + \frac{\epsilon^u}{2} \quad g_V^d = -\frac{1+\delta}{2} + \frac{2}{3}\tilde{s}^2 - \frac{\epsilon^d}{2} \quad g_V^e = -\frac{1}{2} + 2\tilde{s}^2 - \frac{\epsilon^e}{2} \quad g_V^\nu = \frac{1}{2} + \frac{\epsilon^\nu}{2}, \quad (\text{A.3})$$

and

$$g_A^u = \frac{1+\delta}{2} - \frac{\epsilon^u}{2} \quad g_A^d = -\frac{1+\delta}{2} + \frac{\epsilon^d}{2} \quad g_A^e = -\frac{1}{2} + \frac{\epsilon^e}{2} \quad g_A^\nu = \frac{1}{2} - \frac{\epsilon^\nu}{2}. \quad (\text{A.4})$$

The asymmetries can be written as

$$A_{FB}^f = \frac{3}{4} \frac{(g_L^e)^2 - (g_R^e)^2}{(g_L^e)^2 + (g_R^e)^2} \frac{(g_L^f)^2 - (g_R^f)^2}{(g_L^f)^2 + (g_R^f)^2}, \quad (\text{A.5})$$

and

$$\mathcal{A}_f = \frac{(g_L^f)^2 - (g_R^f)^2}{(g_L^f)^2 + (g_R^f)^2}, \quad (\text{A.6})$$

where we did not explicitly write the expressions up to first order in the spurionic parameters although this is a straight forward manipulation because the expression then becomes somewhat cumbersome.

The ratios  $R_q^0$  are defined as

$$R_q^0 = \frac{\Gamma_q}{\Gamma_h}, \quad (\text{A.7})$$

where we have calculated the corresponding partial widths according to eq. (4.1). For the ratio  $R_l^0$  we have

$$R_q^0 = \frac{\Gamma_h}{\Gamma_l}. \quad (\text{A.8})$$

The total width is obtained from the sum over all partial widths

$$\Gamma_Z = \sum_f \Gamma_f. \quad (\text{A.9})$$

The hadronic pole cross section is defined as

$$\sigma_h^0 = \frac{12\pi}{m_Z^2} \frac{\Gamma_e \Gamma_h}{\Gamma_Z^2}. \quad (\text{A.10})$$

## B. Hadronic tau decays: description of the perturbative part

In this appendix we will mention some details concerning the different prescriptions employed to describe the purely perturbative part for the total tau hadronic decay rate and the related moments. It can be written as [58, 62, 63]

$$\delta^{(0),kl} = \sum_{n=1}^{\infty} \tilde{K}_n(\zeta) A^{(n,kl)}(a_s), \quad (\text{B.1})$$

| $k$ | $l$ | $g_2$ | $g_3$  | $g_4$   | $g_5$                | $g_6$   |
|-----|-----|-------|--------|---------|----------------------|---|
| 0   | 0   | 3.56  | 19.995 | 78.00   | 14.25 $K_4$ -391.54  | 17.81 $K_5$ + 45.11 $K_4$ + 1.58 $\beta_4$ - 8062.  |
| 1   | 0   | 4.17  | 28.35  | 161.06  | 225.58 + 16.69 $K_4$ | -5424. + 1.85 $\beta_4$ + 102.1 $K_4$ + 20.87 $K_5$ |
| 1   | 1   | 2.59  | 5.16   | -90.59  | -1932. +10.35 $K_4$  | -18683. + 1.15 $\beta_4$ -60.88 $K_4$ +12.94 $K_5$  |
| 1   | 2   | 1.94  | -2.03  | -135.98 | -1875. + 7.76 $K_4$  | -12337. + 0.862 $\beta_4$ -104.6 $K_4$ +9.70 $K_5$  |
| 1   | 3   | 1.57  | -5.60  | -151.4  | -1730.+6.27 $K_4$    | -8394. + 0.697 $\beta_4$ -124.1 $K_4$ +7.84 $K_5$   |
| 2   | 0   | 4.67  | 35.59  | 239.7   | 899.7 + 18.68 $K_4$  | -1281. + 2.10 $\beta_4$ + 153.0 $K_4$ + 23.34 $K_5$ |
| 2   | 1   | 2.97  | 9.40   | -63.77  | -1965. + 11.88 $K_4$ | -22433. + 1.32 $\beta_4$ - 35.06 $K_4$ +14.85 $K_5$ |
| 3   | 0   | 5.08  | 41.99  | 313.9   | 1600. + 20.34 $K_4$  | 3889. + 2.26 $\beta_4$ + 199.0 $K_4$ + 25.42 $K_5$  |
| 4   | 0   | 5.44  | 47.73  | 383.9   | 2310. + 21.76 $K_4$  | 9781. + 2.42 $\beta_4$ + 240.9 $K_4$ + 27.20 $K_5$  |

**Table 3:** Coefficients for the FOPT expansion

| $k$ | $l$ | $r_{kl}$ |
|-----|-----|----------|
| 0   | 0   | 1        |
| 1   | 0   | 7/10     |
| 1   | 1   | 1/6      |
| 1   | 2   | 13/210   |
| 1   | 3   | 1/35     |
| 2   | 0   | 8/15     |
| 2   | 1   | 11/105   |
| 3   | 0   | 3/7      |
| 4   | 0   | 5/14     |

**Table 4:** Normalization coefficients determining the parton level predictions.

with  $a_s = \alpha_s/\pi$ . The functions  $\tilde{K}_n(\zeta)$  contain the perturbative coefficients  $K_n$ . The dependence on the renormalization scale parameter  $\zeta$  is determined by the condition that physical quantities are independent of  $\zeta$ . The values of the perturbative coefficients can be inferred from the calculation of the  $e^+e^-$  inclusive cross section.  $K_0 = K_1 = 1$  are universal, whereas the remaining coefficients depend on the renormalization scheme used. They have been calculated up to  $n = 3$ . In the  $\overline{\text{MS}}$  scheme they are given by (for three flavors)  $K_2 = 1.640$  and  $K_3 = 6.317$ . The functions  $A^{(n,kl)}$  are defined as

$$A^{(n,kl)} = \frac{1}{2\pi i} \oint_{|s|=m_\tau^2} \frac{ds}{s} \left( 2\Gamma(3+k) \left( \frac{\Gamma(1+l)}{\Gamma(4+k+l)} + 2 \frac{\Gamma(2+l)}{\Gamma(5+k+l)} \right) \right. \\ \left. - 2 I\left(\frac{s}{s_0}, 1+l, 3+k\right) - 4 I\left(\frac{s}{s_0}, 2+l, 3+k\right) \right) a_s^n(-\zeta s), \quad (\text{B.2})$$

with  $I(x, a, b) = \int_0^x t^{a-1} (1-t)^{b-1} dt$ .  $\alpha_s(s)$  is given by the solution of the renormalization group equation,

$$\frac{da_s}{ds} = -a_s^2 \sum_n \beta_n a_s^n, \quad (\text{B.3})$$

where the coefficients are known up to  $n = 3$  [96]:  $\beta_0 = 9/4, \beta_1 = 4, \beta_2^{\overline{\text{MS}}} = 10.0599, \beta_3^{\overline{\text{MS}}} = 47.2306$ . For FOPT one integrates eq. (B.2) inserting a Taylor expansion for the running of  $\alpha_s(s)$  around some reference point  $s_0$  which we chose  $s_0 = m_\tau^2$ . This gives

$$\delta^{(0),kl} = r_{kl} \sum_{n=1}^6 (K_n + g_n^{kl}) a_s^n(m_\tau) . \quad (\text{B.4})$$

We have  $g_1^{kl} = 0$ . The numerical values of the other functions  $g_n^{kl}$  are listed in table 3 up to  $g_6^{kl}$ .

In table 4 we list the parton level predictions for the different moments. For CIPT, one numerically integrates the RGE equation for the running of  $\alpha_s$  on the contour to evaluate the function  $A^{(n,kl)}$ . Following the discussion in ref. [58] we took  $K_4 = 25$ ,  $K_5 = 98$  and  $K_6 = 384$ , and  $\beta_4 = 222$  for our calculations.

## References

- [1] R.W. Schnee, *Status of direct searches for WIMP dark matter*, *AIP Conf. Proc.* **903** (2007) 8; B.C. Allanach et al., *Les Houches 'Physics at TeV colliders 2005' beyond the standard model working group: summary report*, [hep-ph/0602198](#).
- [2] S. Weinberg, *Implications of dynamical symmetry breaking: an addendum*, *Phys. Rev. D* **19** (1979) 1277;  
S. Dimopoulos and L. Susskind, *Mass without scalars*, *Nucl. Phys. B* **155** (1979) 237;  
L. Susskind, *Dynamics of spontaneous symmetry breaking in the Weinberg- Salam theory*, *Phys. Rev. D* **20** (1979) 2619;  
E. Eichten and K.D. Lane, *Dynamical breaking of weak interaction symmetries*, *Phys. Lett. B* **90** (1980) 125.
- [3] N. Arkani-Hamed, A.G. Cohen and H. Georgi, *Electroweak symmetry breaking from dimensional deconstruction*, *Phys. Lett. B* **513** (2001) 232 [[hep-ph/0105239](#)];  
N. Arkani-Hamed, A.G. Cohen, T. Gregoire and J.G. Wacker, *Phenomenology of electroweak symmetry breaking from theory space*, *JHEP* **08** (2002) 020 [[hep-ph/0202089](#)];  
N. Arkani-Hamed et al., *The minimal moose for a little Higgs*, *JHEP* **08** (2002) 021 [[hep-ph/0206020](#)];  
N. Arkani-Hamed, A.G. Cohen, E. Katz and A.E. Nelson, *The littlest Higgs*, *JHEP* **07** (2002) 034 [[hep-ph/0206021](#)];  
I. Low, W. Skiba and D. Smith, *Little higgses from an antisymmetric condensate*, *Phys. Rev. D* **66** (2002) 072001 [[hep-ph/0207243](#)].
- [4] I. Antoniadis, *A possible new dimension at a few TeV*, *Phys. Lett. B* **246** (1990) 377;  
N. Arkani-Hamed, S. Dimopoulos and G.R. Dvali, *The hierarchy problem and new dimensions at a millimeter*, *Phys. Lett. B* **429** (1998) 263 [[hep-ph/9803315](#)];  
C. Csáki, C. Grojean, L. Pilo and J. Terning, *Towards a realistic model of higgsless electroweak symmetry breaking*, *Phys. Rev. Lett.* **92** (2004) 101802 [[hep-ph/0308038](#)].
- [5] S. Weinberg, *Phenomenological lagrangians*, *Physica A* **96** (1979) 327.
- [6] J. Gasser and H. Leutwyler, *Chiral perturbation theory to one loop*, *Ann. Phys. (NY)* **158** (1984) 142.

- [7] J. Gasser and H. Leutwyler, *Chiral perturbation theory: expansions in the mass of the strange quark*, *Nucl. Phys. B* **250** (1985) 465.
- [8] U.G. Meissner, *Recent developments in chiral perturbation theory*, *Rev. Mod. Phys.* **56** (1993) 903 [[hep-ph/9302247](#)];  
G. Ecker, *Chiral perturbation theory*, *Prog. Part. Nucl. Phys.* **35** (1995) 1 [[hep-ph/9501357](#)];  
A. Pich, *Chiral perturbation theory*, *Rev. Mod. Phys.* **58** (1995) 563 [[hep-ph/9502366](#)];  
S. Scherer, *Introduction to chiral perturbation theory*, *Adv. Nucl. Phys.* **27** (2003) 277 [[hep-ph/0210398](#)];  
V. Bernard and U.-G. Meissner, *Chiral perturbation theory*, *Ann. Rev. Nucl. Part. Sci.* **57** (2007) 33 [[hep-ph/0611231](#)].
- [9] J. Hirn and J. Stern, *The role of spurions in Higgs-less electroweak effective theories*, *Eur. Phys. J. C* **34** (2004) 447 [[hep-ph/0401032](#)].
- [10] J. Hirn and J. Stern, *Anomaly-matching and Higgs-less effective theories*, *JHEP* **09** (2004) 058 [[hep-ph/0403017](#)].
- [11] J. Hirn and J. Stern, *Lepton-number violation and right-handed neutrinos in Higgs-less effective theories*, *Phys. Rev. D* **73** (2006) 056001 [[hep-ph/0504277](#)].
- [12] J. Stern, *Chiral dynamics beyond the standard model*, *Nucl. Phys. B* **174** (Proc. Suppl.) (2007) 109 [[hep-ph/0611127](#)].
- [13] J. Wudka, *Electroweak effective lagrangians*, *Int. J. Mod. Phys. A* **9** (1994) 2301 [[hep-ph/9406205](#)].
- [14] A. Nyffeler and A. Schenk, *The electroweak chiral lagrangian reanalyzed*, *Phys. Rev. D* **62** (2000) 113006 [[hep-ph/9907294](#)].
- [15] R. Urech, *Virtual photons in chiral perturbation theory*, *Nucl. Phys. B* **433** (1995) 234 [[hep-ph/9405341](#)].
- [16] P. Sikivie, L. Susskind, M.B. Voloshin and V.I. Zakharov, *Isospin breaking in technicolor models*, *Nucl. Phys. B* **173** (1980) 189.
- [17] A.C. Longhitano, *Heavy Higgs bosons in the Weinberg-Salam model*, *Phys. Rev. D* **22** (1980) 1166.
- [18] R.N. Mohapatra and J.C. Pati, *A natural left-right symmetry*, *Phys. Rev. D* **11** (1975) 2558;  
G. Senjanovic and R.N. Mohapatra, *Exact left-right symmetry and spontaneous violation of parity*, *Phys. Rev. D* **12** (1975) 1502.
- [19] R.N. Mohapatra, *Left-right symmetric models of weak interactions: a review*, PRINT-84-0012 (MARYLAND), based on lecture given at *NATO summer school on particle physics*, Munich, Germany, 5-16 September (1983).
- [20] H. Georgi, *A tool kit for builders of composite models*, *Nucl. Phys. B* **266** (1986) 274;  
N. Arkani-Hamed, A.G. Cohen and H. Georgi, *(De)Constructing dimensions*, *Phys. Rev. Lett.* **86** (2001) 4757 [[hep-th/0104005](#)].
- [21] W. Buchmuller and D. Wyler, *Effective lagrangian analysis of new interactions and flavor conservation*, *Nucl. Phys. B* **268** (1986) 621.
- [22] C.D. Froggatt and H.B. Nielsen, *Hierarchy of quark masses, Cabibbo angles and CP-violation*, *Nucl. Phys. B* **147** (1979) 277.

- [23] G. D'Ambrosio, G.F. Giudice, G. Isidori and A. Strumia, *Minimal flavour violation: an effective field theory approach*, *Nucl. Phys. B* **645** (2002) 155 [[hep-ph/0207036](#)].
- [24] PARTICLE DATA GROUP collaboration, W.M. Yao et al., *Review of particle physics*, *J. Phys. G* **33** (2006) 1.
- [25] P. Langacker and S. Uma Sankar, *Bounds on the mass of  $W(R)$  and the  $W(L)$ - $W(R)$  mixing angle  $\xi$  in general  $SU(2)_L \times SU(2)_R \times U(1)$  models*, *Phys. Rev. D* **40** (1989) 1569.
- [26] ALEPH collaboration, *Precision electroweak measurements on the  $Z$  resonance*, *Phys. Rept.* **427** (2006) 257 [[hep-ex/0509008](#)].
- [27] ALEPH collaboration, J. Alcaraz et al., *A combination of preliminary electroweak measurements and constraints on the standard model*, [hep-ex/0612034](#).
- [28] D.Y. Bardin et al., *Electroweak working group report*, [hep-ph/9709229](#).
- [29] A. Djouadi, G. Moreau and F. Richard, *Resolving the  $A(FB)(b)$  puzzle in an extra dimensional model with an extended gauge structure*, *Nucl. Phys. B* **773** (2007) 43 [[hep-ph/0610173](#)];  
K. Agashe, R. Contino, L. Da Rold and A. Pomarol, *A custodial symmetry for  $ZB\bar{B}$* , *Phys. Lett. B* **641** (2006) 62 [[hep-ph/0605341](#)].
- [30] S.C. Bennett and C.E. Wieman, *Measurement of the  $6S \rightarrow 7S$  transition polarizability in atomic cesium and an improved test of the standard model*, *Phys. Rev. Lett.* **82** (1999) 2484 [[hep-ex/9903022](#)];  
C.S. Wood et al., *Measurement of parity nonconservation and an anapole moment in cesium*, *Science* **275** (1997) 1759.
- [31] J. Guena, M. Lintz and M.A. Bouchiat, *Atomic parity violation: principles, recent results, present motivations*, *Mod. Phys. Lett. A* **20** (2005) 375 [[physics/0503143](#)].
- [32] SLAC E158 collaboration, P.L. Anthony et al., *Precision measurement of the weak mixing angle in moeller scattering*, *Phys. Rev. Lett.* **95** (2005) 081601 [[hep-ex/0504049](#)].
- [33] W.J. Marciano and A. Sirlin, *Improved calculation of electroweak radiative corrections and the value of  $V(ud)$* , *Phys. Rev. Lett.* **96** (2006) 032002 [[hep-ph/0510099](#)].
- [34] L. Wolfenstein, *A limit on  $W(L)W(R)$  mixing in the  $SU(2)_L \times SU(2)_R$  model*, *Phys. Rev. D* **29** (1984) 2130.
- [35] G. Amoros, J. Bijnens and P. Talavera, *QCD isospin breaking in meson masses, decay constants and quark mass ratios*, *Nucl. Phys. B* **602** (2001) 87 [[hep-ph/0101127](#)].
- [36] T.M. Ito, *Neutron beta decay: status and future of the asymmetry measurement*, [arXiv:0704.2365](#).
- [37] R.P. Feynman and M. Gell-Mann, *Theory of the Fermi interaction*, *Phys. Rev.* **109** (1958) 193.
- [38] S.L. Adler, *Calculation of the axial vector coupling constant renormalization in beta decay*, *Phys. Rev. Lett.* **14** (1965) 1051;  
W.I. Weisberger, *Renormalization of the weak axial vector coupling constant*, *Phys. Rev. Lett.* **14** (1965) 1047.
- [39] V.V. Abaev, P. Metsa and M.E. Sainio, *The Goldberger-Miyazawa-Oehme sum rule revisited*, *Eur. Phys. J. A* **23** (2007) 321 [[arXiv:0704.3167](#)].

- [40] B. Ananthanarayan and B. Moussallam, *Electromagnetic corrections in the anomaly sector*, *JHEP* **05** (2002) 052 [[hep-ph/0205232](#)].
- [41] J.L. Goity, A.M. Bernstein and B.R. Holstein, *The decay  $\pi^0 \rightarrow \gamma\gamma$  to next to leading order in chiral perturbation theory*, *Phys. Rev. D* **66** (2002) 076014 [[hep-ph/0206007](#)].
- [42] PRIMEX collaboration, D.S. Dale, *Measuring the transition form factors of pseudoscalar mesons at low  $Q^2$* , *Fizika* **B13** (2004) 365;  
see also <http://meetings.aps.org/link/BAPS.2007.APR.B2.1>.
- [43] J. Stern, H. Sazdjian and N.H. Fuchs, *What  $\pi$ - $\pi$  scattering tells us about chiral perturbation theory*, *Phys. Rev. D* **47** (1993) 3814 [[hep-ph/9301244](#)];  
M. Knecht, B. Moussallam, J. Stern and N.H. Fuchs, *The low-energy  $\pi\pi$  amplitude to one and two loops*, *Nucl. Phys. B* **457** (1995) 513 [[hep-ph/9507319](#)].
- [44] S. Descotes-Genon, N.H. Fuchs, L. Girlanda and J. Stern, *Analysis and interpretation of new low-energy  $\pi\pi$  scattering data*, *Eur. Phys. J. C* **24** (2002) 469 [[hep-ph/0112088](#)].
- [45] B. Ananthanarayan, G. Colangelo, J. Gasser and H. Leutwyler, *Roy equation analysis of  $\pi\pi$  scattering*, *Phys. Rept.* **353** (2001) 207 [[hep-ph/0005297](#)].
- [46] V. Bernard, M. Oertel, E. Passemar and J. Stern,  *$K(L)(\mu_3)$  decay: a stringent test of right-handed quark currents*, *Phys. Lett. B* **638** (2006) 480 [[hep-ph/0603202](#)].
- [47] R.F. Dashen and M. Weinstein, *Theorem on the form-factors in  $K$ - $L$ -3 decay*, *Phys. Rev. Lett.* **22** (1969) 1337.
- [48] J. Gasser and H. Leutwyler, *Low-energy expansion of meson form-factors*, *Nucl. Phys. B* **250** (1985) 517.
- [49] NA48 collaboration, A. Lai et al., *Measurement of  $k_{\mu 3}^0$  form factors*, *Phys. Lett. B* **647** (2007) 341 [[hep-ex/0703002](#)].
- [50] E. Blucher and W. Marciano in ref. [24].
- [51] KTeV collaboration, T. Alexopoulos et al., *A determination of the CKM parameter  $|V(us)|$* , *Phys. Rev. Lett.* **93** (2004) 181802 [[hep-ex/0406001](#)];  
KLOE collaboration, F. Ambrosino et al., *Measurements of the absolute branching ratios for the dominant  $K_L$  decays, the  $K_L$  lifetime and  $V(us)$  with the KLOE detector*, *Phys. Lett. B* **632** (2006) 43 [[hep-ex/0508027](#)];  
NA48 collaboration, A. Lai et al., *Measurement of the branching ratio of the decay  $K_L \rightarrow \pi^\pm e^\mp \nu$  and extraction of the CKM parameter  $|V(us)|$* , *Phys. Lett. B* **602** (2004) 41 [[hep-ex/0410059](#)].
- [52] V. Bernard, M. Oertel, E. Passemar and J. Stern, in preparation.
- [53] H. Abramowicz et al., *Limit on right-handed weak coupling parameters from inelastic neutrino interactions*, *Z. Physik C* **12** (1982) 225;  
S.R. Mishra et al., *Search for right-handed coupling in neutrino  $n$  scattering*, *Phys. Rev. Lett.* **68** (1992) 3499.
- [54] S.L. Adler, *Sum rules giving tests of local current commutation relations in high-energy neutrino reactions*, *Phys. Rev.* **143** (1966) 1144.
- [55] H1 collaboration, A. Aktas et al., *A determination of electroweak parameters at HERA*, *Phys. Lett. B* **632** (2006) 35 [[hep-ex/0507080](#)].

- [56] TEVATRON ELECTROWEAK WORKING GROUP collaboration, B. Ashmanskas et al., *Combination of CDF and D0 results on the  $w$ -boson width*, [hep-ex/0510077](#).
- [57] OPAL collaboration, G. Abbiendi et al., *Measurement of the  $e^+e^- \rightarrow W^+W^-$  cross section and  $W$  decay branching fractions at LEP*, [arXiv:0708.1311](#).
- [58] M. Davier, A. Hocker and Z. Zhang, *The physics of hadronic  $\tau$  decays*, *Rev. Mod. Phys.* **78** (2006) 1043 [[hep-ph/0507078](#)].
- [59] ALEPH collaboration, S. Schael et al., *Branching ratios and spectral functions of tau decays: final ALEPH measurements and physics implications*, *Phys. Rept.* **421** (2005) 191 [[hep-ex/0506072](#)].
- [60] OPAL collaboration, K. Ackerstaff et al., *Measurement of the strong coupling constant  $\alpha_s$  and the vector and axial-vector spectral functions in hadronic  $\tau$  decays*, *Eur. Phys. J. C* **7** (1999) 571 [[hep-ex/9808019](#)].
- [61] OPAL collaboration, G. Abbiendi et al., *Measurement of the strange spectral function in hadronic  $\tau$  decays*, *Eur. Phys. J. C* **35** (2004) 437 [[hep-ex/0406007](#)].
- [62] E. Braaten, S. Narison and A. Pich, *QCD analysis of the tau hadronic width*, *Nucl. Phys. B* **373** (1992) 581.
- [63] F. Le Diberder and A. Pich, *Testing QCD with  $\tau$  decays*, *Phys. Lett. B* **289** (1992) 165.
- [64] M. Davier, S. Eidelman, A. Hocker and Z. Zhang, *Confronting spectral functions from  $e^+e^-$  annihilation and tau decays: consequences for the muon magnetic moment*, *Eur. Phys. J. C* **27** (2003) 497 [[hep-ph/0208177](#)].
- [65] E. Braaten and C.-S. Li, *Electroweak radiative corrections to the semihadronic decay rate of the  $\tau$  lepton*, *Phys. Rev. D* **42** (1990) 3888.
- [66] V. Cirigliano, E. Golowich and K. Maltman, *QCD condensates for the light quark  $V$ - $A$  correlator*, *Phys. Rev. D* **68** (2003) 054013 [[hep-ph/0305118](#)].
- [67] S. Narison,  *$V$ - $A$  hadronic  $\tau$  decays: a laboratory for the QCD vacuum*, *Phys. Lett. B* **624** (2005) 223 [[hep-ph/0412152](#)].
- [68] A.A. Almasy, K. Schilcher and H. Spiesberger, *QCD condensates of dimension  $D = 6$  and  $D = 8$  from hadronic  $\tau$  decays*, *Phys. Lett. B* **650** (2007) 179 [[hep-ph/0612304](#)].
- [69] S. Descotes-Genon, L. Girlanda and J. Stern, *Paramagnetic effect of light quark loops on chiral symmetry breaking*, *JHEP* **01** (2000) 041 [[hep-ph/9910537](#)].
- [70] J. Stern, *Two alternatives of spontaneous chiral symmetry breaking in QCD*, [hep-ph/9801282](#).
- [71] F. Le Diberder and A. Pich, *The perturbative QCD prediction to  $R(\tau)$  revisited*, *Phys. Lett. B* **286** (1992) 147;  
A.A. Pivovarov, *Renormalization group summation of perturbative series in timelike momentum region*, *Nuovo Cim.* **A105** (1992) 813; *Renormalization group analysis of the tau-lepton decay within QCD*, *Z. Physik C* **53** (1992) 461 [*Sov. J. Nucl. Phys.* **54** (1991) 676] [[hep-ph/0302003](#)].
- [72] M. Jamin, *Contour-improved versus fixed-order perturbation theory in hadronic  $\tau$  decays*, *JHEP* **09** (2005) 058 [[hep-ph/0509001](#)].

- [73] F.J. Yndurain, *Gluon condensate from superconvergent QCD sum rule*, *Phys. Rept.* **320** (1999) 287 [[hep-ph/9903457](#)].
- [74] B.L. Ioffe and K.N. Zyablyuk, *Gluon condensate in charmonium sum rules with 3-loop corrections*, *Eur. Phys. J. C* **27** (2003) 229 [[hep-ph/0207183](#)].
- [75] S. Bethke, *Experimental tests of asymptotic freedom*, [hep-ex/0606035](#).
- [76] K. Maltman and C.E. Wolfe, *The joint extraction of  $M_s$  and  $V_{us}$  from hadronic tau decay data*, [hep-ph/0611180](#).
- [77] E. Gamiz, M. Jamin, A. Pich, J. Prades and F. Schwab,  *$|V(us)|$  from strange hadronic  $\tau$  data*, [hep-ph/0610246](#).
- [78] ALEPH collaboration, R. Barate et al., *Study of  $\tau$  decays involving kaons, spectral functions and determination of the strange quark mass*, *Eur. Phys. J. C* **11** (1999) 599 [[hep-ex/9903015](#)].
- [79] A. Pich and J. Prades, *Strange quark mass determination from Cabibbo-suppressed tau decays*, *JHEP* **10** (1999) 004 [[hep-ph/9909244](#)].
- [80] A. Pich and J. Prades, *Perturbative quark mass corrections to the  $\tau$  hadronic width*, *JHEP* **06** (1998) 013 [[hep-ph/9804462](#)].
- [81] E. Gamiz, M. Jamin, A. Pich, J. Prades and F. Schwab, *Determination of  $M(s)$  and  $|V(us)|$  from hadronic tau decays*, *JHEP* **01** (2003) 060 [[hep-ph/0212230](#)].
- [82] E. Gamiz, M. Jamin, A. Pich, J. Prades and F. Schwab,  *$V(us)$  and  $M(s)$  from hadronic  $\tau$  decays*, *Phys. Rev. Lett.* **94** (2005) 011803 [[hep-ph/0408044](#)].
- [83] J.C. Hardy, *The status of  $V(ud)$* , [hep-ph/0703165](#).
- [84] H. Leutwyler and M. Roos, *Determination of the elements  $V(us)$  and  $V(ud)$  of the Kobayashi-Maskawa matrix*, *Z. Physik C* **25** (1984) 91.
- [85] D.J. Antonio et al.,  *$K \rightarrow \pi l \nu$  form factor with  $N(f) = 2 + 1$  dynamical domain wall fermions*, *PoS(LAT2006)* 101 [[hep-lat/0610080](#)].
- [86] KTeV collaboration, T. Alexopoulos et al., *Measurements of semileptonic  $K(L)$  decay form factors*, *Phys. Rev. D* **70** (2004) 092007 [[hep-ex/0406003](#)].
- [87] J. Bijnens and P. Talavera,  *$K(l3)$  decays in chiral perturbation theory*, *Nucl. Phys. B* **669** (2003) 341 [[hep-ph/0303103](#)].
- [88] V. Cirigliano et al., *The Green function and SU(3) breaking in  $K(l3)$  decays*, *JHEP* **04** (2005) 006 [[hep-ph/0503108](#)].
- [89] NA48/I collaboration, J.R. Batley et al., *Measurement of the branching ratios of the decays  $\Xi_0 \rightarrow \sigma^+ e^- \bar{\nu}_e$  and  $\bar{\Xi}_0 \rightarrow \bar{\sigma}^+ e^+ \nu_e$* , *Phys. Lett. B* **645** (2007) 36 [[hep-ex/0612043](#)].
- [90] V. Mateu and A. Pich,  *$V(us)$  determination from hyperon semileptonic decays*, *JHEP* **10** (2005) 041 [[hep-ph/0509045](#)];  
G. Villadoro, *Chiral corrections to the hyperon vector form factors*, *Phys. Rev. D* **74** (2006) 014018 [[hep-ph/0603226](#)];  
A. Lacour, B. Kubis and U.-G. Meissner, *Hyperon decay form factors in chiral perturbation theory*, *JHEP* **10** (2007) 083 [[arXiv:0708.3957](#)].
- [91] B.M. Dassinger, R. Feger and T. Mannel, *Testing the left-handedness of the  $B \rightarrow C$  transition*, *Phys. Rev. D* **75** (2007) 095007 [[hep-ph/0701054](#)].



- [92] D0 collaboration, V.M. Abazov et al., *Measurement of the  $W$  boson helicity in top quark decays*, *Phys. Rev. D* **72** (2005) 011104 [[hep-ex/0505031](#)]; *Measurement of the  $w$  boson helicity in top quark decay at  $D0$* , *Phys. Rev. D* **75** (2007) 031102 [[hep-ex/0609045](#)]; CDF collaboration, A.A. Affolder et al., *Measurement of the helicity of  $W$  bosons in top quark decays*, *Phys. Rev. Lett.* **84** (2000) 216 [[hep-ex/9909042](#)].
- [93] J.F. Donoghue and B.R. Holstein, *Strong bounds on weak couplings*, *Phys. Lett. B* **113** (1982) 382.
- [94] G. Beall, M. Bander and A. Soni, *Constraint on the mass scale of a left-right symmetric electroweak theory from the  $K(L)$   $K(S)$  mass difference*, *Phys. Rev. Lett.* **48** (1982) 848.
- [95] P.L. Cho and M. Misiak,  *$B \rightarrow S\gamma$  decay in  $SU(2)_L \times SU(2)_R \times U(1)$  extensions of the standard model*, *Phys. Rev. D* **49** (1994) 5894 [[hep-ph/9310332](#)].
- [96] T. van Ritbergen, J.A.M. Vermaseren and S.A. Larin, *The four-loop  $\beta$ -function in quantum chromodynamics*, *Phys. Lett. B* **400** (1997) 379 [[hep-ph/9701390](#)].